



TECHNISCHE  
UNIVERSITÄT  
WIEN  
Vienna University of Technology

## Dissertation

# Exploration of procedures translating batch synthesis into flow for the synthesis of bioactive small molecules

ausgeführt zum Zwecke der Erlangung des akademischen Grades eines  
Doktors der technischen Wissenschaften unter der Leitung von

Prof. Dr. Marko D. Mihovilovic

Assist. Prof. Dr. Michael Schnürch

Institut für Angewandte Synthesechemie, E163

eingereicht an der Technischen Universität Wien

Fakultät für Technische Chemie

von

MSc Maria Christakakou

Wiedner Hauptstrasse 118/31

1050, Vienna

Wien, **13 May 2015**

*“Learn from yesterday,  
live for today,  
hope for tomorrow.  
The important thing is to  
not stop questioning.”*

*Albert Einstein*

## Acknowledgements

I am using this opportunity to express my gratitude to everyone who supported me throughout the course of this PhD Thesis.

First and foremost, I would like to thank my supervisor Prof. Marko D. Mihovilovic for giving me the opportunity to work in his group and to further develop my knowledge of chemistry in a research based environment. I would like to express my gratitude to my co-supervisor Assist. Prof. Michael Schnürch whose contribution in stimulating suggestions and encouragement helped me to proceed with my project, overcoming all the arising issues. I am sincerely thankful to both for their aspiring guidance, invaluable constructive criticism and friendly advice during my Thesis. Their truthful and illuminating views on a number of issues helped for the completion of this work.

I would also like to thank my colleague Dipl.-Ing. Max Haider who always had a good experimental advise to give me, Dr. Michael Schön for his help in flow related issues and MSc Yago Magan Montoto, for his contribution in the “Neurodazine” part of this Thesis. I am also thankful to all NMR and HPLC operators who measured for me loads of samples.

I am gratefully acknowledge the Austrian Science Fund (FWF, projects P21202-N17 and S107) and the Vienna University of Technology Doctorate Program “Catalysis Materials and Technology-CatMat” for financial support.

At the end, I would like to take the opportunity to thank my parents Yiannis and Stavroula, my sisters Kelly and Elisabeth, my grandparents Kuriakos and Stavroula and my aunt Evdokia for their endless love, care and support. Their belief on my skills had boosted my efforts and encourage me to chase my dreams, knowing that they are always there for me whenever I need them. I would also like to express my gratitude to my husband’s parents George and Zili who have played a special role with their love and support in my academic development. I am also thankful to my friends with whom we had countless relaxing/happy moments all these years of my studies. I would especially like to thank my dear friends: Nicola Stephanou-Rieser and Fabian Rieser for the German translation of the Abstract of this Thesis. Last but not least, I would like to thank my

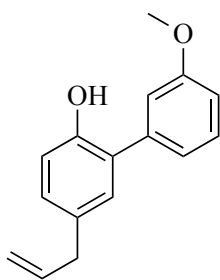
beloved husband Dr. Pascal Anastasopoulos for his never-ending love, encouragement and support. During this Thesis, he stood by my side, not only as a supporting partner who believed in me but also as a scientist who always had the time and wiliness to give me his feedback for my presentations and papers and to help me with the drawing of figures. His inspiring words were always priceless in times where the stress and tiredness seemed overwhelming. Furthermore, I would like to thank him for working by my side for countless hours in the very demanding work of transferring the whole Thesis from Microsoft Word to LaTeX.

## Abstract

The objective of this thesis was to explore cross coupling and C-H activation reactions, especially their possible translation into a flow system.

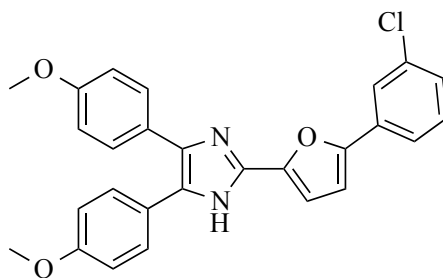
In particular, the following research topics were explored:

- Optimization of batch reaction conditions for the synthesis of a bioactive Magnolol/Honokiol derivative was investigated in order to be applicable for a flow process and exploration of the possible translation into flow.



Magnolol/Honokiol derivative

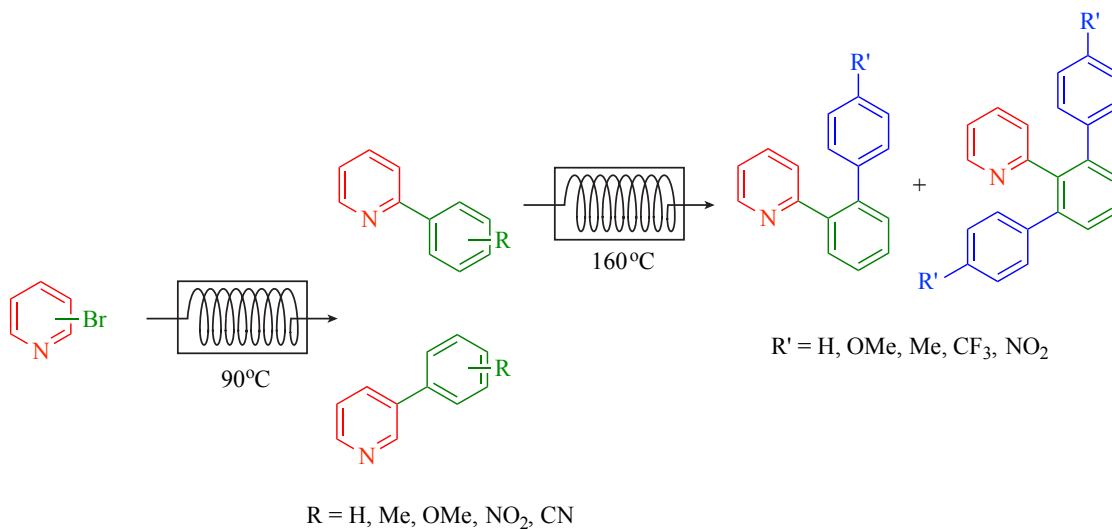
- Development of batch reaction conditions for the synthesis of Neurodazine, a bioactive small molecule, which is considered to be promising for the treatment of neurodegenerative diseases. The possibility to translate the batch protocol in flow was also investigated.



Neurodazine

- The synthesis of several arylated phenyl pyridines and their further decoration via C-H activation chemistry taking advantage of an in-house developed continuous-flow

reactor system. Although there were contributions known in literature concerning the first part of the synthesis, the second part, an intermolecular direct arylation reaction, was presented herein for the first time under continuous-flow conditions [1].



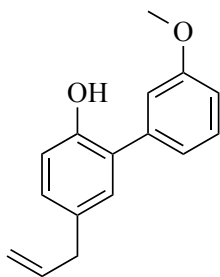
Flow synthesis of substituted aryl pyridines.

## Kurzfassung

Das Ziel dieser Doktorarbeit war die Untersuchung von Kreuzkupplungsreaktionen und C-H Aktivierungsreaktionen und besonders deren mögliche Anwendung in Flow-Prozessen.

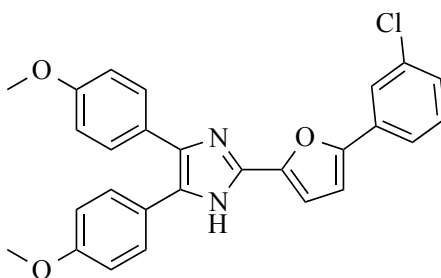
Im speziellen wurden folgende Forschungsbereiche untersucht:

- Die Optimierung der Synthese von bioaktiven Magnolol/Honokiol Derivaten unter diskontinuierlichen Reaktionsbedingungen, um sie für kontinuierliche Durchflussprozesse anwendbar zu machen und die Untersuchung der möglichen Umsetzung unter flow-chemischen Bedingungen.



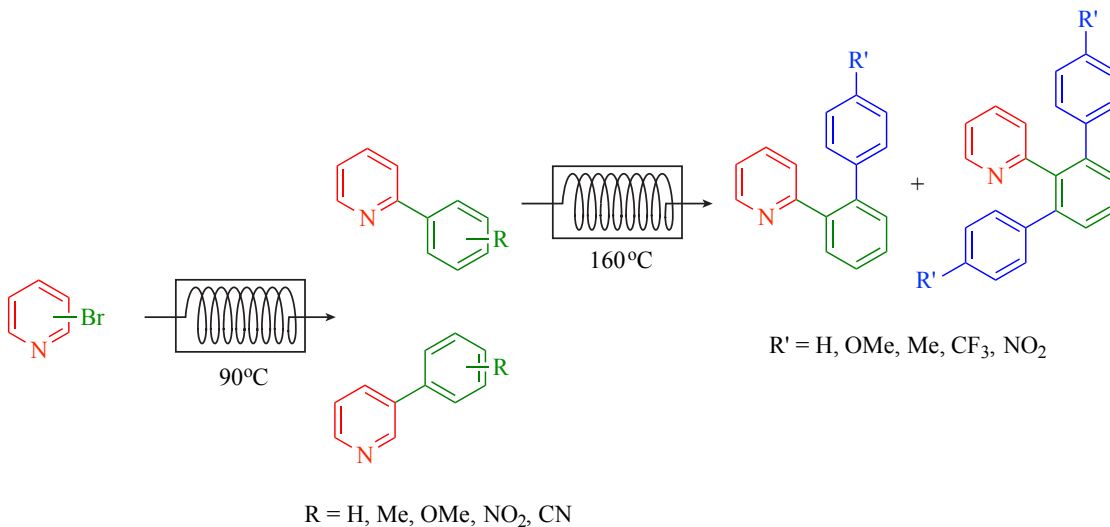
Magnolol/Honokiol Derivat

- Entwicklung von diskontinuierliche Reaktionsbedingungen für die Synthese von Neurodazin, einem bioaktiven Molekül, welches als vielversprechend gilt bei der Behandlung von neurodegenerativen Krankheiten. Optionen zur Übertragung auf einen kontinuierlichen Prozess wurden studiert.



Neurodazine

- Neben der Synthese von verschiedenen arylierten Phenylpyridinen und deren weitere Funktionalisierung über C-H Aktivierung, unter Nutzung eines selbst entwickelte Durchflussreaktor-Systems. Obwohl es in der Literatur über den ersten Teil der Synthese Beiträge gibt, wurde der zweite Teil, eine intermolekulare direkte Arylierungsreaktion, hier das erste Mal unter kontinuierlichen Durchflussbedingungen präsentiert [1].



Kontinuierliche Durchflusssynthese vom substituierten Arylpyridinen.



# Contents

<b>1</b>	<b>Introduction</b>	<b>25</b>
1.1	Flow Chemistry . . . . .	25
1.1.1	Definition and Advantages . . . . .	25
1.1.2	Factors important to interpret a Continuous-Flow Process . . . . .	32
1.2	Metal Catalyzed C-C Bond Forming Reactions . . . . .	33
1.2.1	Cross Coupling Reactions . . . . .	33
1.2.2	Suzuki-Miyaura cross-coupling reaction . . . . .	35
1.2.3	C-H Functionalization . . . . .	39
1.3	Catalysts in organic reactions . . . . .	44
1.3.1	Heterogeneous catalysts in cross coupling reactions . . . . .	44
1.3.2	Homogeneous catalysts in cross coupling reactions . . . . .	45
<b>2</b>	<b>Results and Discussion</b>	<b>46</b>
2.1	Towards the synthesis of biologically active Magnolol and Honokiol derivatives in flow . . . . .	46
2.1.1	Objective . . . . .	46
2.1.2	Magnolol and Honokiol properties . . . . .	46
2.1.3	Exploration of appropriate conditions to translate the batch process into flow . . . . .	47
2.1.4	Summary/Conclusions . . . . .	66
2.2	Towards streamlining Neurodazine synthesis . . . . .	68
2.2.1	State of art . . . . .	68
2.2.2	Objective . . . . .	70
2.2.3	Synthetic strategy towards Neurodazine . . . . .	70

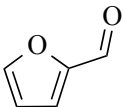
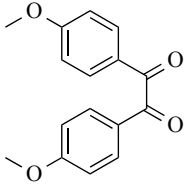
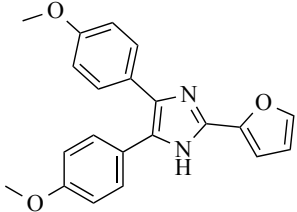
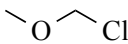
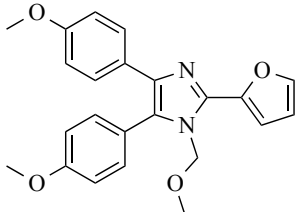
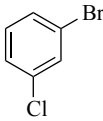
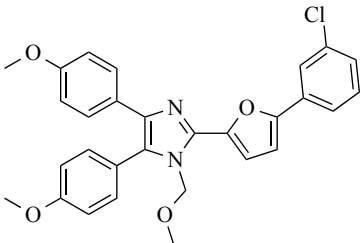
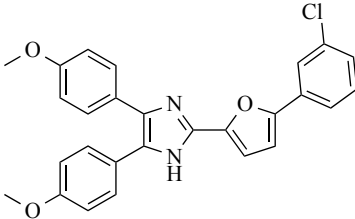
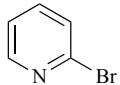
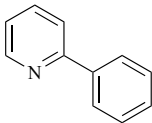
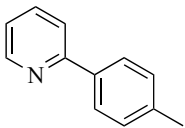
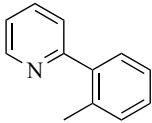
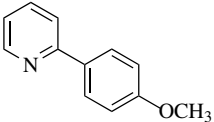
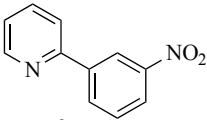
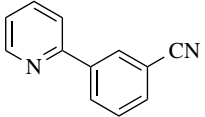
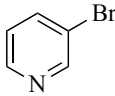
2.2.4	Synthesis of Neurodazine / optimization of reaction conditions in batch . . . . .	74
2.2.5	Summary/Conclusions . . . . .	87
2.3	Arylation of Pyridines via Suzuki-Miyaura Cross-Coupling and Pyridine-Directed C-H Activation Using a Continuous-Flow Approach . . . . .	90
2.3.1	Objective . . . . .	90
2.3.2	Synthesis of 2- and 3-phenylpyridines via Suzuki-Miyaura Cross-Coupling . . . . .	90
2.3.3	Pyridine properties and reactivity . . . . .	90
2.3.4	Optimization of reaction conditions . . . . .	91
2.3.5	Arylation of 2-phenylpyridine via C-H activation in flow . . . . .	104
2.3.6	Optimization of reaction conditions . . . . .	105
2.3.7	Summary/Conclusions . . . . .	120
<b>3</b>	<b>Experimental Section</b>	<b>125</b>
3.1	General notes . . . . .	125
3.2	Towards streamlining Neurodazine synthesis . . . . .	127
3.2.1	Synthesis of 2-(furan-2-yl)-4,5-bis(4-methoxyphenyl)-1 <i>H</i> -imidazole ( <b>3</b> ) . . . . .	127
3.2.2	Synthesis of 2-(furan-2-yl)-1-(methoxymethyl)-4,5-bis(4-methoxyphenyl)-1 <i>H</i> -imidazole ( <b>5</b> ) . . . . .	129
3.2.3	Synthesis of 2-(5-(3-chlorophenyl)furan-2-yl)-1-(methoxymethyl)-4,5-bis(4-methoxyphenyl)-1 <i>H</i> -imidazole ( <b>7</b> ) . . . . .	131
3.2.4	Synthesis of 2-(5-(3-chlorophenyl)furan-2-yl)-4,5-bis(4-methoxyphenyl)-1 <i>H</i> -imidazole ( <b>8</b> ) . . . . .	133
3.3	Flow Synthesis of 2-arylpyridine and 3-arylpyridine derivatives and subsequent ortho-arylation towards their 2-phenylpyridine derivatives . . . . .	135

3.3.1	Synthesis of 2-arylpyridine and 3-arylpyridine derivatives [1] . . . . .	135
3.3.2	Synthesis of ortho-arylated 2-phenylpyridine derivatives [1] . . . . .	137
3.3.3	Synthesis of 2-phenylpyridine ( <b>10</b> ) . . . . .	139
3.3.4	Synthesis of 2-(p-tolyl)pyridine ( <b>11</b> ) . . . . .	140
3.3.5	Synthesis of 2-(o-tolyl)pyridine ( <b>12</b> ) . . . . .	141
3.3.6	Synthesis of 2-(4-methoxyphenyl)pyridine ( <b>13</b> ) . . . . .	142
3.3.7	Synthesis of 2-(3-nitrophenyl)pyridine ( <b>14</b> ) . . . . .	143
3.3.8	Synthesis of 3-(pyridine-2-yl)benzotrile ( <b>15</b> ) . . . . .	144
3.3.9	Synthesis of 3-phenylpyridine ( <b>17</b> ) . . . . .	145
3.3.10	Synthesis of 3-(p-tolyl)pyridine ( <b>18</b> ) . . . . .	146
3.3.11	Synthesis of 3-(o-tolyl)pyridine ( <b>19</b> ) . . . . .	147
3.3.12	Synthesis of 3-(4-methoxyphenyl)pyridine ( <b>20</b> ) . . . . .	148
3.3.13	Synthesis of 2-(3-nitrophenyl)pyridine ( <b>21</b> ) . . . . .	149
3.3.14	Synthesis of 3-(pyridine-3-yl)benzotrile ( <b>22</b> ) . . . . .	150
3.3.15	Synthesis of 2-([1,1'-biphenyl]-2'-yl)pyridine ( <b>23</b> ) . . . . .	151
3.3.16	Synthesis of 2-([1,1':3',1''-terphenyl]-2'-yl)pyridine ( <b>24</b> ) . . . . .	152
3.3.17	Synthesis of 2-(4'-methoxy-[1,1'-biphenyl]-2'-yl)pyridine ( <b>25</b> ) . . . . .	153
3.3.18	Synthesis of 2-(4'-methyl-[1,1'-biphenyl]-2-yl)pyridine ( <b>26</b> ) + 2-(4,4''- dimethyl-[1,1':3,1''-terphenyl]-2'-yl)pyridine ( <b>27</b> ) . . . . .	154
3.3.19	Synthesis of 2-(4'-trifluoromethyl-[1,1'-biphenyl]-2-yl)pyridine ( <b>28</b> )	156
3.3.20	Synthesis of 2-(4,4''-bis(trifluoromethyl)-[1,1':3',1''-terphenyl]-2'-yl)pyridine ( <b>29</b> ) . . . . .	157
3.3.21	Synthesis of 2-(4-methoxy-[1,1':3',1''-terphenyl]-2'-yl)pyridine ( <b>30</b> )	158

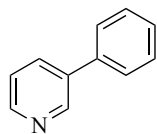
**B Bibliography 162**

**C Curriculum Vitae 174**

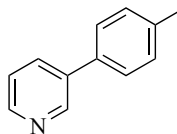
## List of compounds presented in the Results and Discussion/Experimental Section of the Thesis

No	Compound	No	Compound
1		2	
3		4	
5		6	
7		8	
9		10	
11		12	
13		14	
15		16	

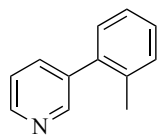
17



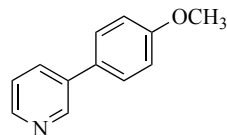
18



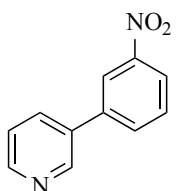
19



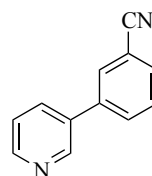
20



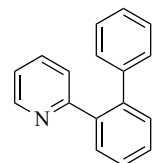
21



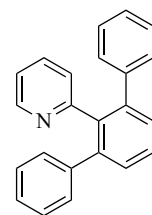
22



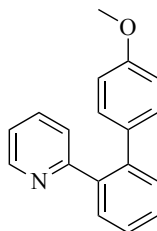
23



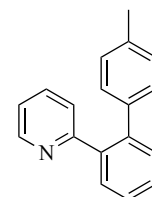
24



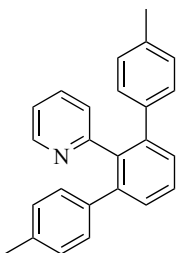
25



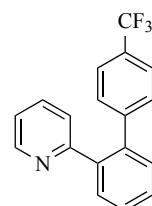
26



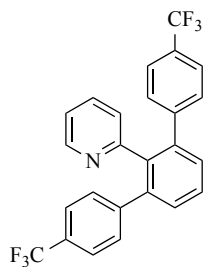
27



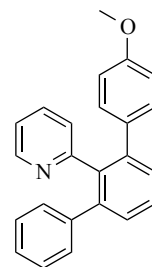
28



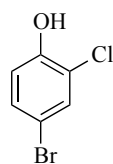
29



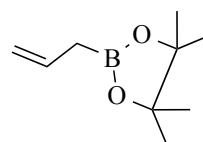
30

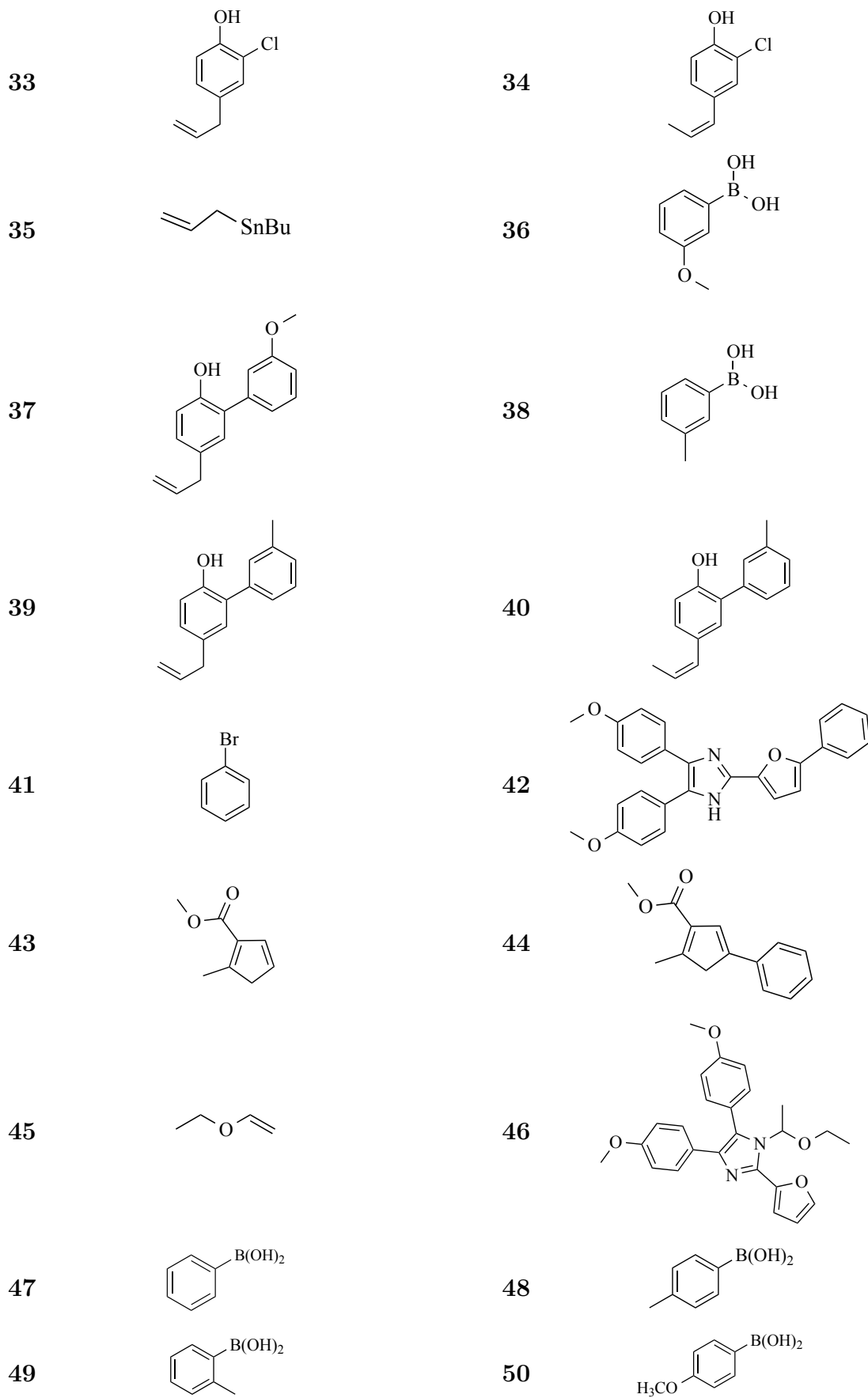


31

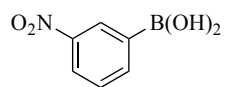


32

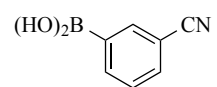




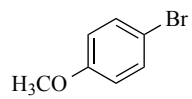
51



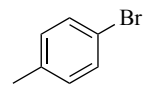
52



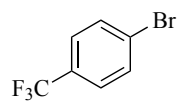
53



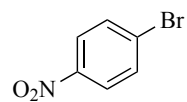
54



55

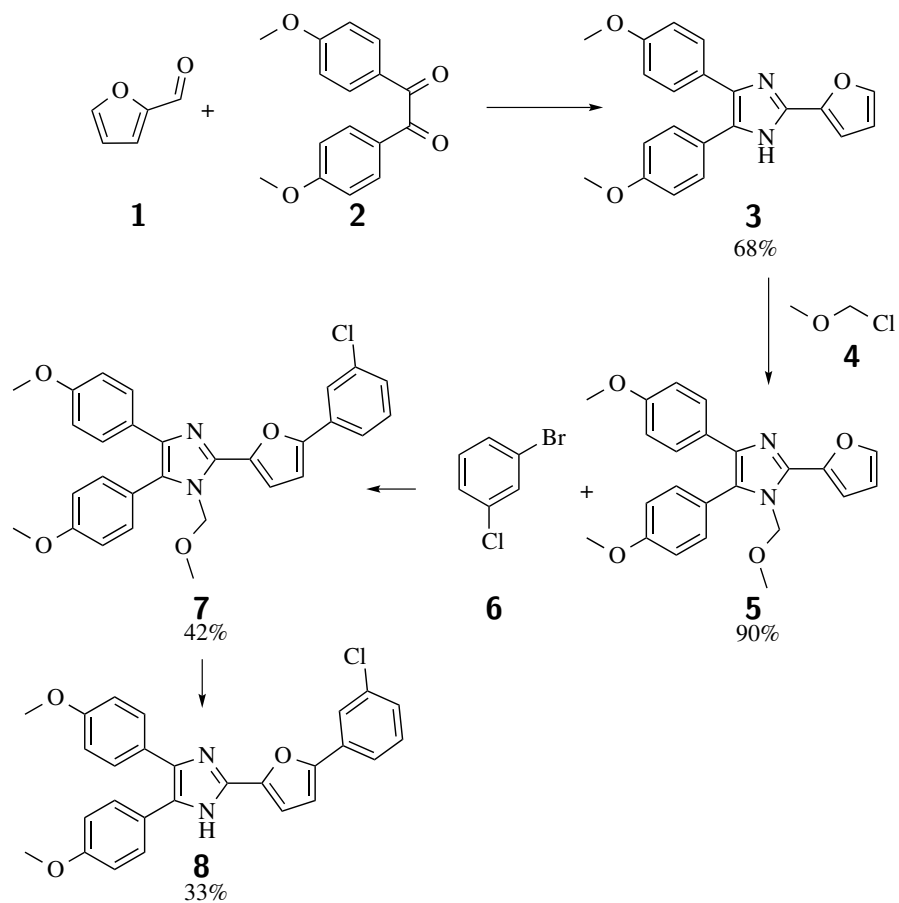


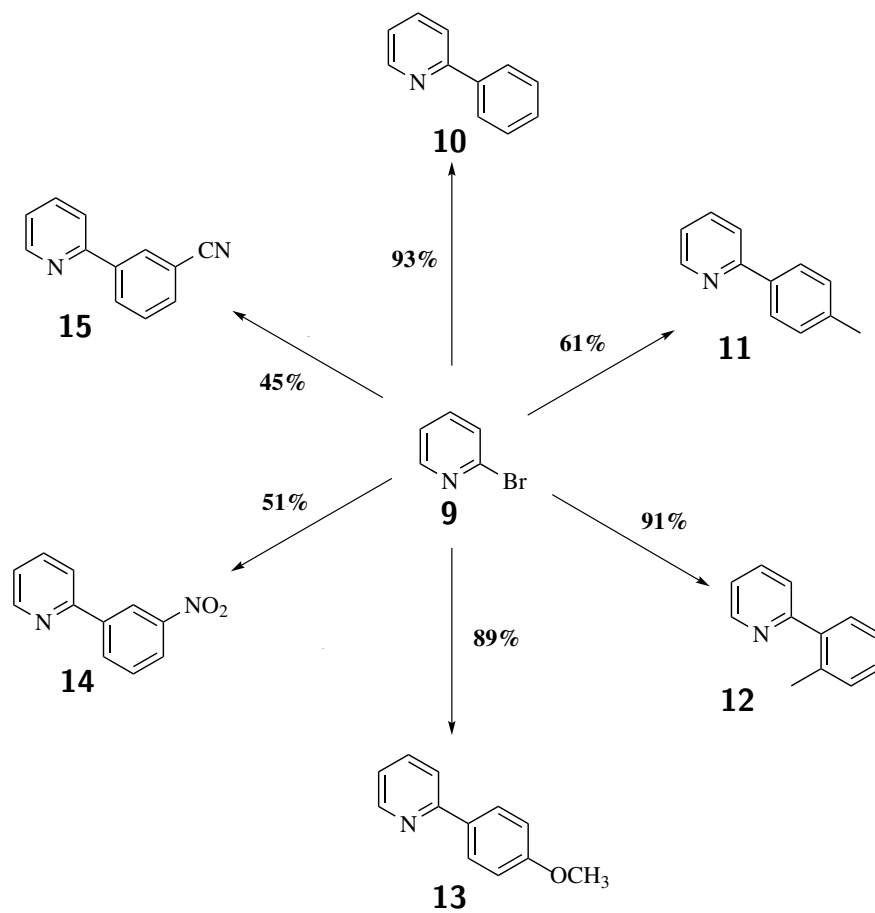
56

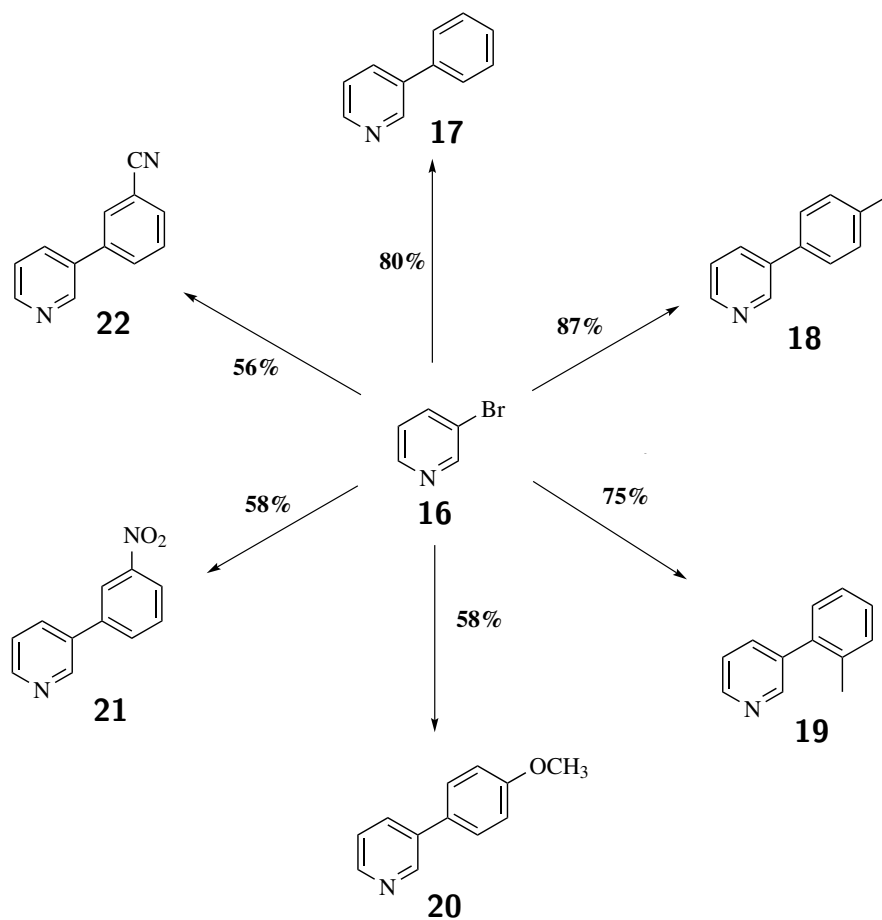




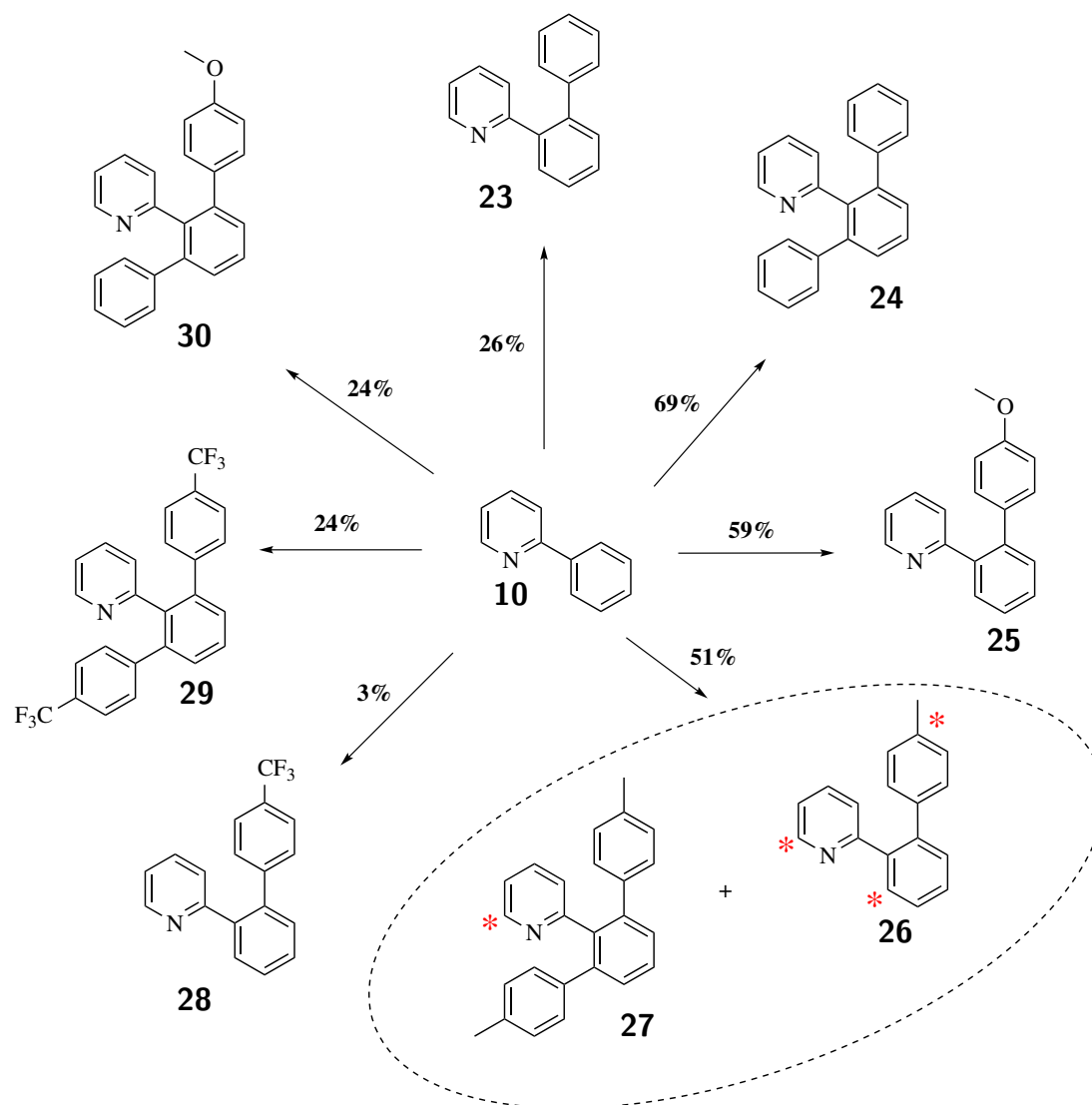
## Synthetic schemes







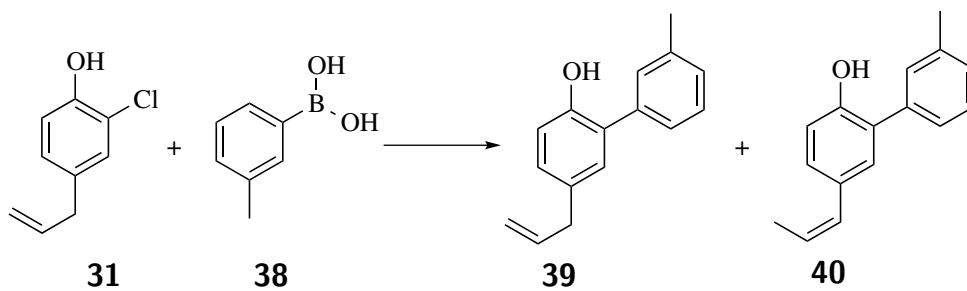
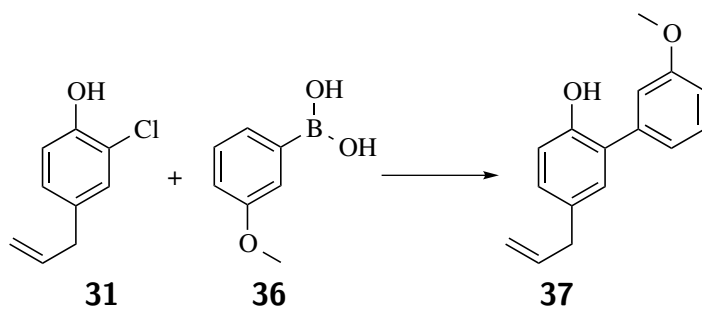
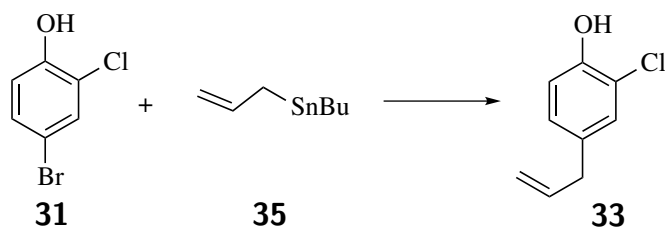
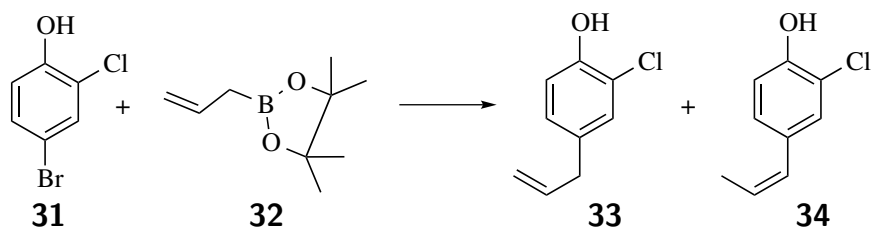
Aryl boronic acids which were used for the coupling reactions with 2- and 3-bromopyridine:  
47, 48, 49, 50, 51, 52.

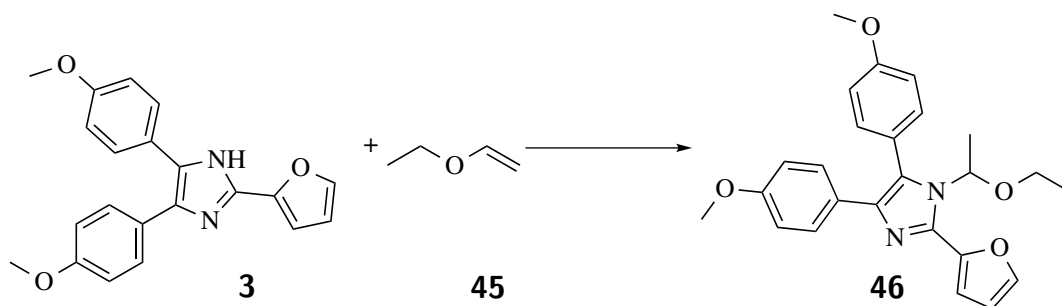
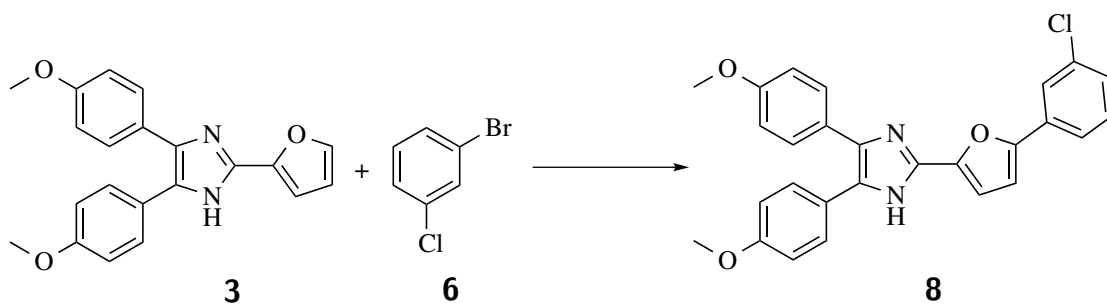
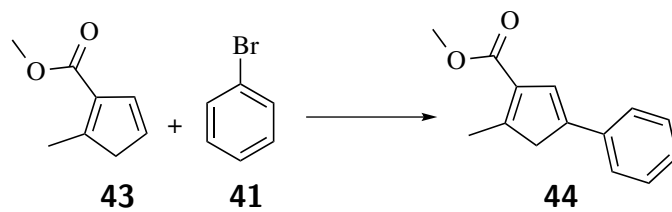
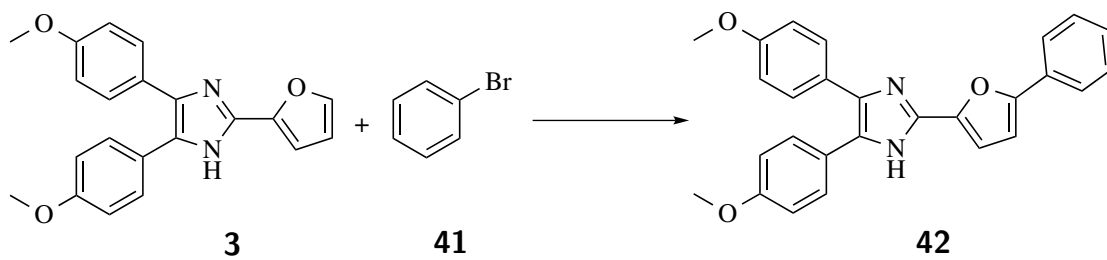


\* : The asterisk indicates the signals of protons which they have been used for NMR quantification of the inseparable mixture between compounds **26** and **27**.

Substituted bromobenzenes which were used for the arylation reactions with 2-phenylpyridine: **41**, **53**, **54**, **55**, **56**.

## Screening reactions





## Abbreviations

abs.	Absolute
aq.	Aqueous
AFRICA	Automated Flow Reaction, Incubation, Control Apparatus
Ac <sub>2</sub> O	Acetic anhydride
Bn	Benzyl
BPR	Back Pressure Regulator
BQ	Benzoquinone
Cat. load.	Catalyst Loading
CF	Continuous Flow system
CFR	Continuous Flow Reactor
C-H activation	Carbon Hydrogen bond activation
Conv.	Conversion
diox.	Dioxane
DBU	1,8-Diazabicycloundec-7-ene
DCM	Dichloromethane
DMAc	<i>N,N</i> -Dimethylacetamide
dppf	1,1'-Bis(diphenylphosphino)ferrocene
eq.	Equivalent
EnCat	Encapsulated
EtOAc	Ethyl Acetate
f.r.	Flow rate
FG	Functional Group
GC	Gas Chromatography
GCMS	Gas Chromatography-Mass Spectrometry
het.	Heterogeneous
hom.	Homogeneous
IS	Internal Standard
HPLC	High Performance Liquid Chromatography
M	Molecular weight

---

MODDE	Software for design of experiments
MOMCl	Chloromethyl Methyl Ether
MPLC	Medium Pressure Liquid Chromatography
MW	Microwave irradiation
n.c.	No conversion
n.h.	Not homogeneous
NMP	1-Methyl-2-pyrrolidinone
NMR	Nuclear Magnetic Resonance
P	Product
PG	Protecting group
PEG-400	Polyethylene glycol 400
PdEnCat30 / PdEnCat40	Palladium acetate, Encapsulated in polyurea matrix
PIFA	[Bis(trifluoroacetoxy)iodo]benzene
PFA	PerFluoroAlkoxy
prep. TLC	Preparative Thin Layer Chromatography
R.T.	Residence Time
r.t.	Room temperature
sat.	Saturated
SEM	[2-(Trimethylsilyl)ethoxy]methyl acetal
SM	Starting Material/reaction reagent
t	Time
TFA	Trifluoroacetic acid
THF	Tetrahydrofuran
TLC	Thin Layer Chromatography
X-Cube	Flow reactor system from Thales Nano (see Appendix A)



# 1 Introduction

## 1.1 Flow Chemistry

### 1.1.1 Definition and Advantages

In the past decades efforts have been made to develop techniques that would enable researchers to perform reactions in an automated way. An ideal reaction procedure would lead to highly pure compounds, in an economic and safe way, in 100% yield and with the minimum attention from the researcher's side, employing automation. One of the most promising technologies, in this regard, is flow chemistry.

The principle on which every flow system is based on, is very simple. The reagents are forced with the aid of a pump through tubing into a heated reactor and after the reaction zone the product is collected, e.g. into a vial of choice (Figure 1). In flow set ups it is possible to perform reactions exceeding the boiling point of the solvent or reactions that are involving gas formation, since pressure regulators can control the pressure rise. Those regulators can modulate themselves to keep pressure at a set point and consequently to keep the mass flow through the system constant.

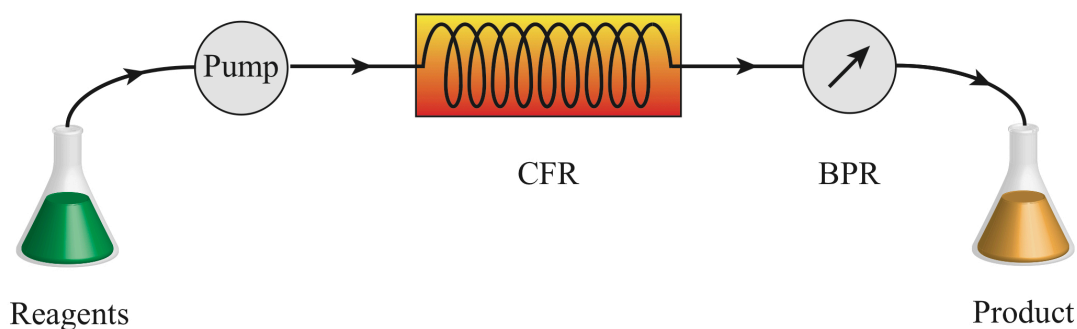


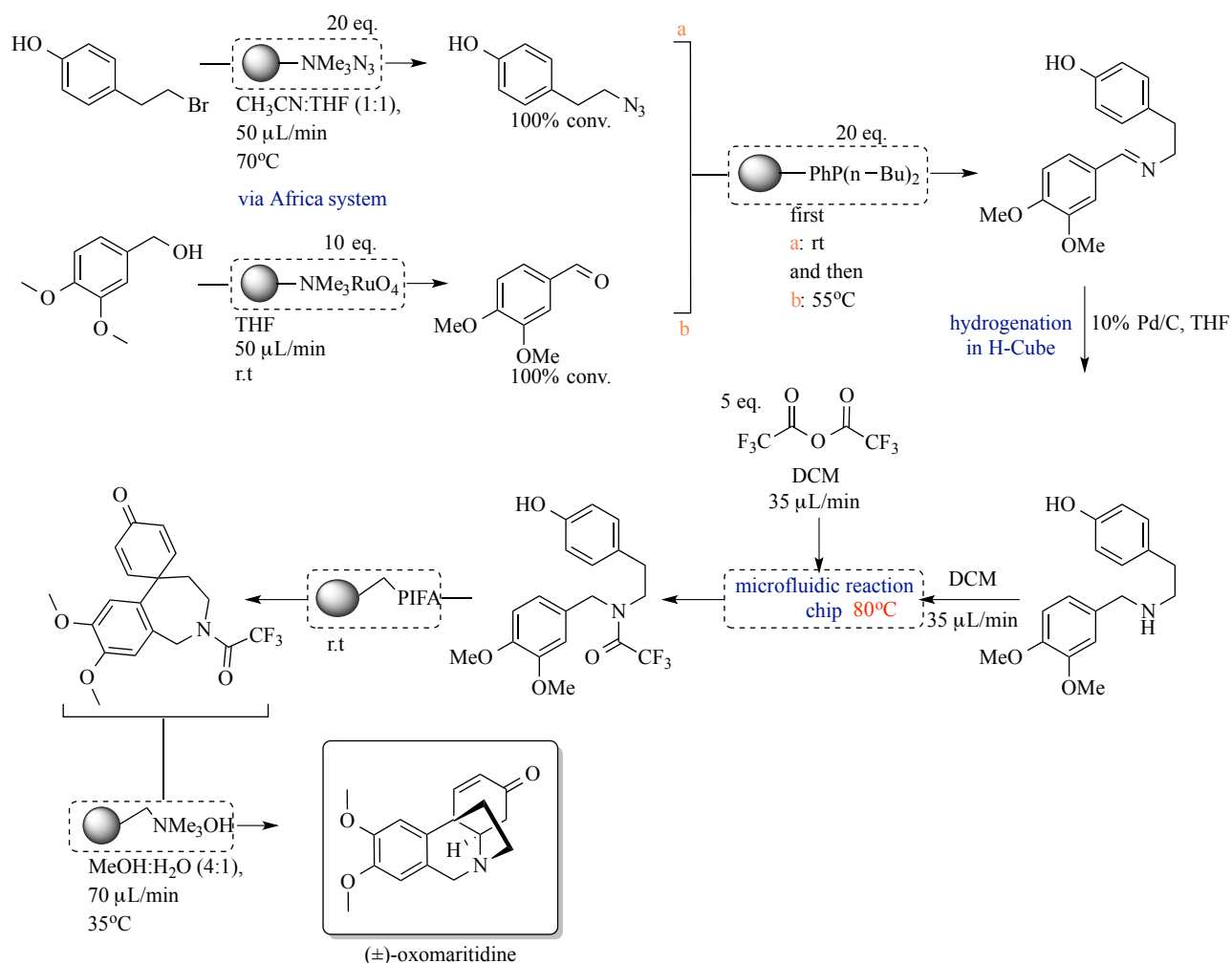
Figure 1: Illustrated Flow step.

Due to its operational simplicity and the possibility of potential automation, along with other advantages, flow chemistry has gained increased interest from both academia and industry [2,3]. In the following, a more detailed look on the benefits that this technology

offers is provided.

One of the most promising features of flow chemistry is that it can potentially lead to the target compound without the need of intermediate work-up steps or column chromatography, taking advantage of the automation feature. This is especially useful in a multistep synthesis where work-up has to be performed for each individual step.

Ley, one of the pioneer scientists in this field, and his group presented in 2006 an efficient way to achieve such synthesis for the alkaloid natural product oxomaritidine. This was the first contribution concerning a natural product synthesis via a continuous flow process [4]. To achieve such synthesis they employed two automated flow systems: The AFRICA system from Syrris and the H-Cube from Thales Nano and they paired them with glass columns packed with reagents and catalysts in series, achieving the synthesis of the target compound in high efficiency, as shown in Scheme 1. Reaction conditions were controlled precisely with the aid of those two systems. Initially AFRICA was used to pump a solution of 4-(2-bromoethyl)phenol through a column packed with an azide exchange resin to convert it to the alkyl azide (stream a) while within another stream the aldehyde coupling partner was prepared via oxidation from 3,4-dimethoxybenzyl alcohol after passing through a pre-packed column containing tetra-*N*-alkylammonium per-ruthenate (stream b). Then both streams were connected and passed through a column containing the immobilized aza-Wittig intermediate resulting in the corresponding imine. Afterwards, a solution of this imine in THF underwent hydrogenation in the H-Cube, under catalysis of 10% Pd/C, which was packed in a cartridge. The intermediate product was collected online and the solvent was evaporated with the aid of Vapourtec V-10<sup>®</sup> and then replaced by DCM. Then it was reacted in a microfluidic reaction chip whilst also a DCM solution of trifluoroacetic acid anhydride (TFAA) was pumped through. Then the resultant trifluoroacetylated amide was pumped through a scavenging column which was packed with a silica supported primary amine to catch any excess of TFAA or TFA. Next, the reaction solution passed through a column containing polymer-supported [Bis(trifluoroacetoxy)iodo]benzene (PIFA) and after oxidative phenolic coupling had taken place, it resulted in a seven-membered tricyclic compound. Finally the latter was passed through a column containing a polymer-supported base which resulted in the cleavage of



Scheme 1: Flow synthesis of (±)-oxomaritidine.

the amide bond and allowed 1,4-conjugate addition to take place affording the desired product: (±)-oxomaritidine. This was indeed a very impressive synthesis, which was cost effective since work-up procedures and column chromatography were avoided, moreover it was also user friendly since the scientist had to interfere with the whole process only by planning the synthetic route and by programming the devices to perform the task.

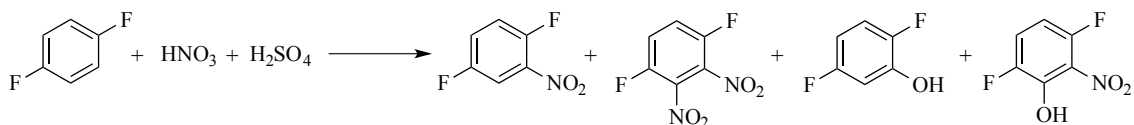
Another advantage of flow chemistry is that the optimization of the reaction conditions can be done faster and more economically. The automation ability of a flow system, allows the programming of various experiments ahead e.g for screening purposes and in each of them, the parameters of interest can be varied (e.g temperature, concentration, flow rate). Since the required amount of material is minimal, the optimized conditions

can be identified in a more efficient manner, without having to waste grams of substrate. Jensen *et al* installed in a microfluidic system consisting of syringe pumps, a microreactor and a micromixer as well as an inline HPLC monitoring system that allowed live time analysis with the aid of algorithms [5]. Via this method it was possible to tune the reaction parameters adjusting them to achieve the best results regarding reaction yield. The same group presented the possibility for multi-step synthesis, introducing this time, in the microreactor setup, a liquid-liquid microseparator to perform in-line work-up [6]. In this way, the reaction time was minimized since there was no need for isolating the intermediates before proceeding to the next reaction step.

The automation potential of flow reactors facilitates also the synthesis of compound libraries to be submitted for structure activity relationship studies (SAR), minimizing the reaction time that would be required for the corresponding batch protocol if it had to be applied for each individual compound. This is especially useful for preclinical drug discovery. Moreover Selway *et al*, went a step further integrating the flow microreactor technology with the SAR technique, achieving the automated synthesis of various compounds and in the same time identifying novel Abl kinase inhibitors. This was achieved by using computational activity prediction methodology to identify the candidate compounds and then by employing flow chemistry principals for synthesis and purification of the compounds along with integrated LC-MS analysis of the candidates [7].

Flow chemistry can also facilitate reaction scale up, minimizing the up-scaling issue that is one of the major problems in batch processes. This is done by ensuring efficient mixing through the reaction zone, keeping constant the heating of the reaction mixture and adjusting either the reactor's volume and flow rate to the preferred production or by combining many microreactors at the same time or just by letting the system pump for prolonged time. To evaluate the productivity of a flow process, the amount of product produced per hour per reactor volume, the so called: space time yield, is measured [2].

Recently Yu *et al*, reported the synthesis of heterogeneous nitration of p-difluorobenzene (Scheme 2) in flow [8]. The translation of this reaction in flow minimized the side products (dinitro and phenol) allowing for a selective and very effective synthesis. In terms of yield a 98% yield with 99% purity (crude product) was achieved, when a 4mm tube was used



Scheme 2: Nitration of p-difluorobenzene.

with a 167 mL/min flow rate. In terms of greener reaction procedures, they recycled the waste sulfuric acid by assuming 100% conversion and adding 1 eq. of nitric acid to it after each run. Then they collected the H<sub>2</sub>SO<sub>4</sub>, H<sub>2</sub>O and HNO<sub>3</sub> which was produced by the nitration. In Table 3, a comparison of the results, from the flow and the batch process is given.

Table 3: Comparison of batch to flow results.

Entry	Yield [%]	Purity [%]	t (min)	Production
batch	80	99.5 (after distillation)	Slow addition of the nitric acid which was followed by 1h stirring	Dependent on the reaction scale
flow	98	99 (crude product)	2.3 min	6.25kg/h

Until now there are also a few examples, where this technology has been successfully employed to the up-scaling of more challenging procedures as for example biotransformations, which usually require long residence times and multiphase media. For example Gasparini *et al* presented the up-scaling of the oxidase of the DL-amino acid in flow employing a Coflore reactor and then they compared the batch results with the flow showing the superiority of the continuous process (reaction rate, conversion, oxygen consumption) [9]. Furthermore, amongst others, the up-scaling of reactions involving gaseous reaction partners [10,11] and photochemical reactions [12,13], as well as high temperature cyclizations and de-protections [14], have been reported in flow.

Continuous flow processing allows also for reaction control through efficient heat trans-

fer. Due to the high surface to volume ratio and the fast diffusion mixing, it is possible to perform reactions that include highly reactive, explosive, hazardous or toxic chemicals but also to achieve excellent compound selectivity and eventually even higher product yields [15, 16]. Reactions that require an autoclave or high-pressure devices to be performed, can be done much more safely in flow without taking any special precaution [17]. For example, hydrogenations are usually done by binding the supported catalyst in a disposable cartridge and the generation of hydrogen takes place *in situ*, which makes it much safer in comparison to its corresponding batch reaction [16, 18–20]. Another approach enhancing safety in flow was made by Ley et.al with the development of a device capable to evaporate, concentrate and switch solvents during a flow process as well as in a batch mode [21]. This device was then used to remove an explosive reagent, nitromethane, which is used in large excess in the Henry reaction for the synthesis of nitro alkanes via the condensation of nitromethane to aldehydes.

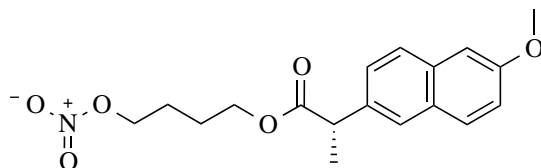


Figure 2: Naproxcinod.

A noteworthy industrial application of flow chemistry was made with the Naproxcinod (Figure 2) synthesis in flow. This compound is used as an arthritis drug and constitutes a derivative of naproxen, a nonsteroidal anti-inflammatory drug. DSM, a global science-based company located in Linz made possible the production of several hundred tons of this compound per year, effortlessly and cost efficiently, by combining several identical reactors in parallel. This configuration promotes a smooth process even if one or more of the reactors break down during the pumping, since there are several others which could still work properly. In batch synthesis a failure in the heating system for example, would be of vital importance, because it would immediately lead to termination of the whole procedure. Another parameter that DSM took in account while designing the flow system was the possible formation of explosive side-products, since the synthesis of the target compound is based on nitration. Employing microreactor technology gives the

advantage that the reaction mixture travels through channels which have a few millimeter-diameter and consequently even if formation of unstable materials take place, the short residence time will make the whole process safe, being in a better control in comparison to a batch synthesis. The latter would have to involve highly dilute and biphasic conditions in specialized equipment to ensure safety.

Another advantage of flow chemistry is that it provides the researcher with a greener process since the solvents or reagents, which are removed can be recycled and reused. This is especially useful in a multi step process in which usually the solvents differ from one step to the other.

Additionally, reproducibility of results can be assured due to the precise control of the reaction conditions.

With flow chemistry we can also achieve high reaction rates which is of particular interest to the pharmaceutical industry since it enables accelerated synthesis of diverse compound libraries leading to more time-efficient structure-activity relationship studies [22]. In particular, increased reaction rates of several orders of magnitude could be achieved in cases of heterogeneous reactions, due to the high catalyst to reagents ratio. In other words, when the reaction mixture travels through the particles of catalyst located e.g in a cartridge or a fixed bed reactor, it comes in a continuous contact with them, reacting in a faster and more facile way in comparison to batch processes.

However, despite the many benefits which flow chemistry has to offer, there also some drawbacks associated with it. In batch the homogeneity of the reaction mixture does not play a pronounced role in the reaction performance. However, in flow, sustainable homogeneity through the reaction zone is a crucial factor for a smooth pumping. Any possible precipitation will lead to blockage of the system and consequently will lead to termination of the process. Also in flow chemistry, purchase of special equipment is required in order to perform the reactions and this factor increase significantly the cost of the process in comparison to the standard batch equipment. Furthermore, the translation of a batch process in flow is usually time consuming since many parameters (e.g developing a method, suitable instrumentation, homogeneity) have to be taken in account.

### 1.1.2 Factors important to interpret a Continuous-Flow Process

There are some differences between a flow process and a batch process, which have to be taken in account in order to translate a batch protocol to a flow one.

For instance, the reaction time in batch is defined as the time, which is required for a reaction mixture reacting in a specific temperature to reach completion by the full conversion of the starting materials. In contrast, in a flow procedure we define the reaction time using the term residence time, which in this case is determined by the flow rate and the reactor's volume.

Since a flow system can be used for large-scale reactions in industry, chemists have introduced a term to describe quantitatively, such productions. It is called space time yield and is defined as the amount of product produced per hour per reactor volume.

The ideal outcome of a flow process can be achieved using the highest flow rate which naturally leads to the lowest residence time ( $\text{flow rate (mL/min)} = \text{volume (mL)} / \text{residence time (min)}$ ) in a given system. Another difference between the two processes is that in flow, the stoichiometry of the reaction is defined by the concentration of the reagents and the ratio of their flow rates instead of their volumetric ratio, which applies in the batch processes [23].



## 1.2 Metal Catalyzed C-C Bond Forming Reactions

### 1.2.1 Cross Coupling Reactions

Cross-Coupling reactions constitute a very robust methodology towards C-C and C-heteroatom (=H, N, O, S, P, metal) bond formation. The transformation usually takes place between an electrophile (halide or pseudohalide) and an organometallic reagent or an unsaturated compound (alkene or alkyne with the aid of a transition-metal catalyst, usually palladium (Figure 3)) [24–28].

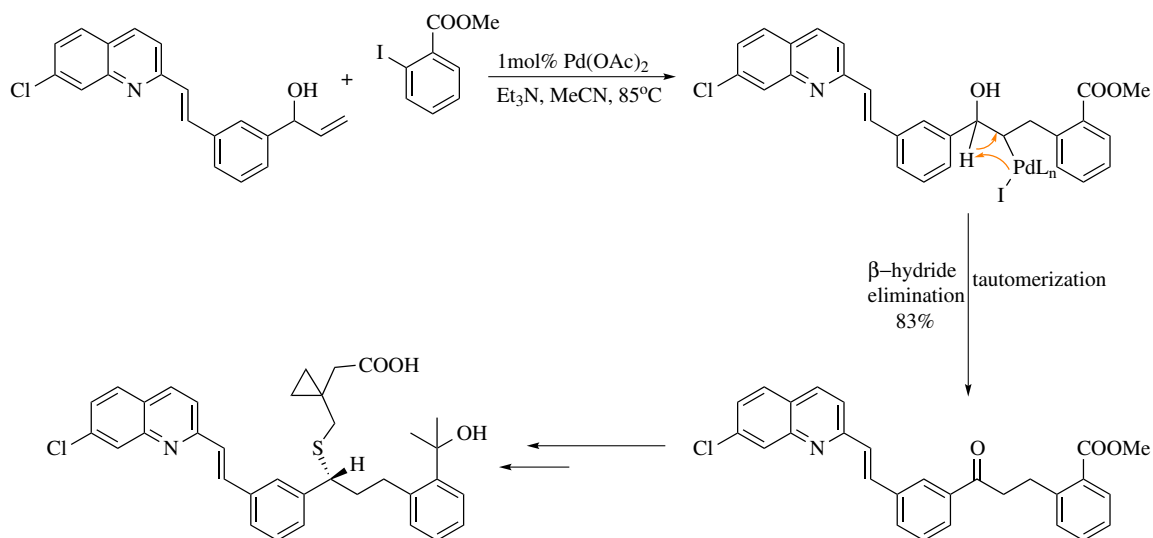


Figure 3: C-C bond formation via “classical” metal assisted transformations.

Depending on the nature of the nucleophile, each coupling reaction bears a different name dedicated to the researcher who has discovered it. Some of the most well known protocols are given in the following: Heck (alkene) [29], Sonogashira (terminal alkyne) [30], Suzuki-Miyaura (boronic acid) [31], Negishi (organozinc, organoaluminum or organozirconium compound) [32], Stille (organotin compound) [33], Himaya (organosilanes) [34], Kumada-Corriu-Tamao (Grignard reagent) [35,36]. In fact, Akira Suzuki, Ei-ichi Negishi and Richard F. Heck were awarded the Nobel Prize in chemistry in 2010 for their contributions in palladium catalyzed cross-coupling reactions in organic chemistry. These methods are of immense importance, which is reflected by their wide application as for example in the total synthesis of natural product or many pharmaceutical compounds [37].

An outstanding synthesis concerning a pharmaceutical product taking advantage of cross coupling strategy was the one of Singulair (Scheme 3) [38–40], a drug which is used to prevent asthma attacks and allergies. Its functional properties are based on the inhibition of leukotrienes. The synthesis starts with an intermolecular Heck coupling between the allylic alcohol and the aromatic iodide shown in Scheme 3 with the aid of a small amount of  $\text{Pd}(\text{OAc})_2$  and  $\text{Et}_3\text{N}$  in acetonitrile. The alkyl palladium(II) intermediate which is formed, undergoes  $\beta$ -hydride elimination and tautomerization to the corresponding ketone which

with a simple recrystallisation leads to the target molecule.



Scheme 3: Singulair synthesis.

It is worth mentioning that the nature of the electrophile can influence the rate-determining step of a cross-coupling reaction. Other factors which can play a role in this are the following: the nature of the nucleophile, the ligands on the metal center, the presence of additives and the nature of the solvent [41]. To date, the Suzuki-Miyaura and Sonogashira reactions have been most extensively studied in terms of their mechanistic understanding, heterogeneous catalysis, separation of the catalyst and catalyst re-use [42].

However, as we will not go in details for each different palladium cross-coupling reaction, a general mechanism involves the following steps: oxidative addition, transmetalation and reductive elimination (Figure 4) [43]. The oxidative addition refers to the addition of the halide or pseudo-halide (e.g. triflate) to Pd(0) and the subsequent formation of a Pd(II) species (I). In the transmetalation step, the organic residue of the organometal species is transferred to palladium and concomitantly the halide or triflate binds to the metal part. In case of the Heck reaction in which the coupling partner is an olefin there are two steps substituting transmetalation: the syn-addition and β-hydride elimination. Finally, the Pd(II) complex (II) undergoes reductive elimination to give the coupled product and regenerate the Pd(0) catalyst for a new cycle.

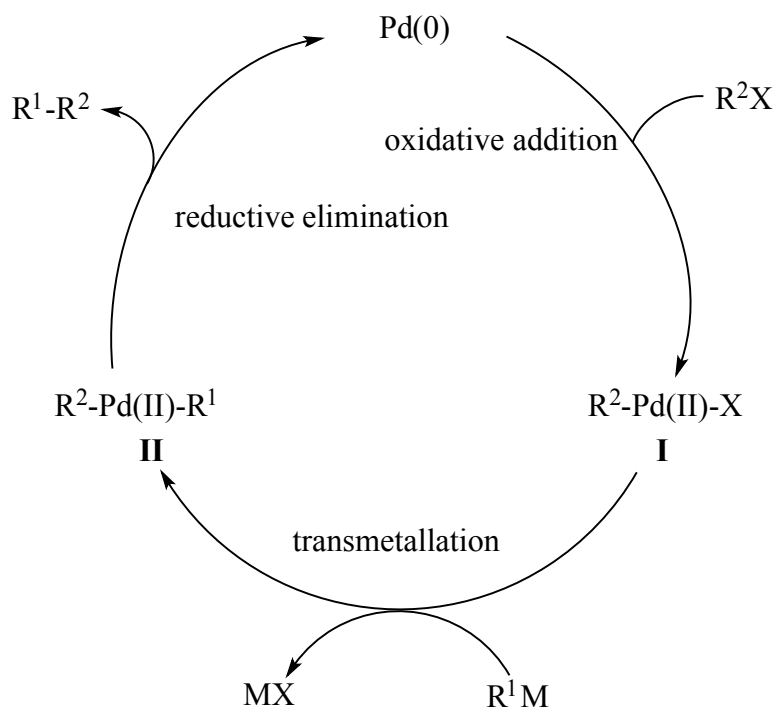
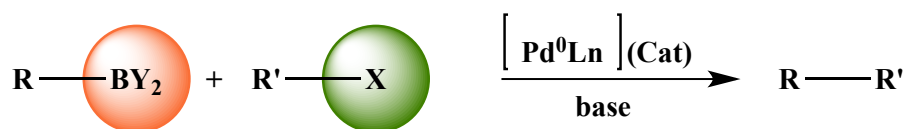


Figure 4: Mechanism for Pd catalyzed cross-coupling reactions.

Since, cross coupling reactions are widely used for the synthesis of important organic and organometallic compounds [28], a technique as flow chemistry was embraced from the research community as highly attractive. Many reactions of this type have been reported in continuous flow to date [1, 23, 44–50]. However, as the focus of this thesis was on the Suzuki-Miyaura cross-coupling reaction a more detailed discussion about it and its translation in flow is given in the following.

### 1.2.2 Suzuki-Miyaura cross-coupling reaction

The formation of arylated heterocycles is a process of great importance due to their presence in molecules with interesting biological activities or interesting properties in material science [51–57]. To synthesize such compounds, the Suzuki-Miyaura cross-coupling reaction is a very successful method and is considered as a general, versatile and mild protocol for the formation of C-C bonds [37, 58–65]. It is a palladium-catalyzed cross-coupling reaction between organoboron compounds and organic halides (Figure 5) [28, 31, 66].



*R*: alkyl, alkynyl, aryl, vinyl, *R'*: aryl, alkynyl, aryl, benzyl, vinyl, *Y*: OH, OR etc  
*X*: Cl, Br, I, OTf, OTs, OP(=O)(OR)<sub>2</sub>

Figure 5: Suzuki-Miyaura reaction.

The commercial availability of the reagents contributes to its popularity in comparison with other cross-coupling protocols [67]. Beneficial features are the stability of the boronic acids [68] towards moisture and air as well as the comparatively low toxicity of byproducts and the easy handling and removal which makes it also an “industry friendly process” [66, 67]. It also tolerates many functional groups and often proceeds regio- and stereoselectively [66]. The reaction also tolerates a large variety of solvents.

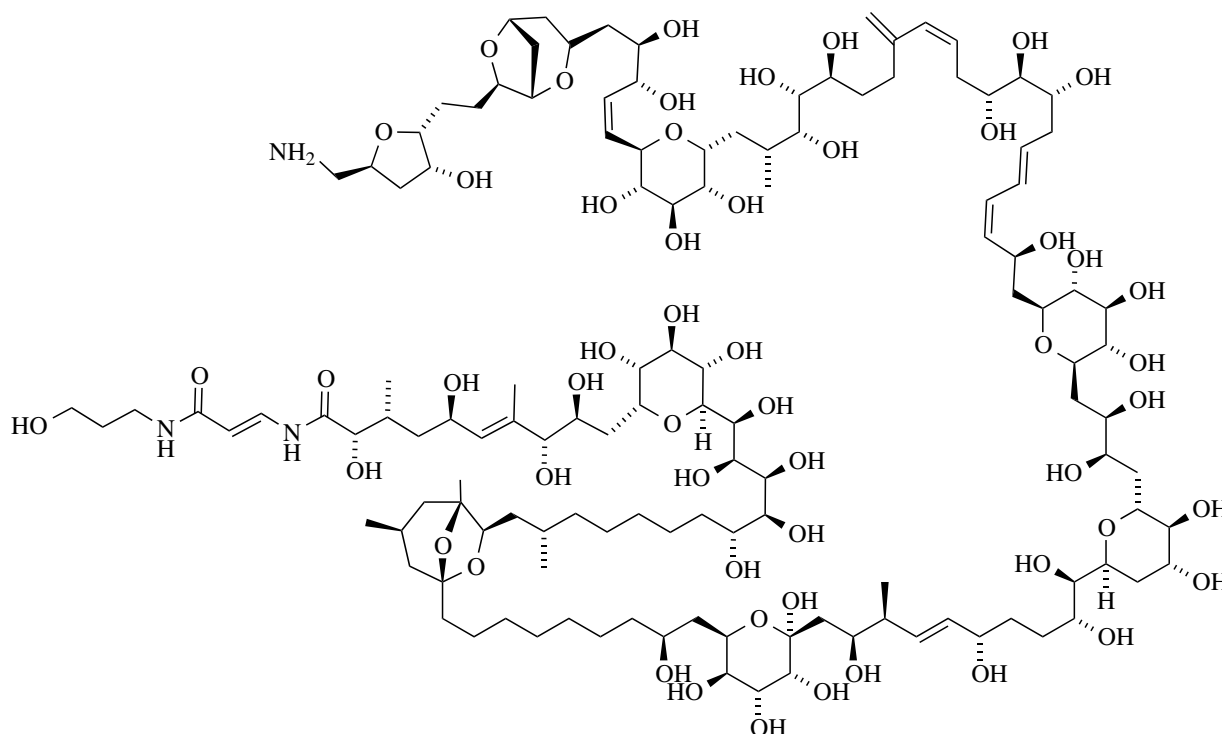


Figure 6: Palytoxin.

A noteworthy and challenging total synthesis employing Suzuki-Miyaura conditions,

was the synthesis of palytoxin (Figure 6), an extremely toxic natural product which is the largest secondary metabolite synthesized up to date, with a molecular weight of 2680.139 Da [69]. During the synthesis of this huge molecule, Kishi *et al* came across many obstacles, especially in a certain step of the synthesis, where the conventional cross coupling conditions were found to be totally inadequate. However, eventually they found ways to overcome the synthetic challenges, improve the reaction rate by employing a thallium base and consequently to refine the Suzuki-Miyaura conditions leading them to the target molecule [37].

Regarding the mechanism of the Suzuki-Miyaura reaction it is following the steps of the general cross-coupling reaction mechanism with the difference that it requires the addition of a base for the activation of the organoboron compound (Figure 7).

Initially the  $R^1X$  halide species is added to the palladium complex  $Pd^0L_2$  via oxidative addition to form a Pd(II)-halide complex I, which upon reaction with a base, e.g. NaOR, results in the exchange of the halide by the base and forms the organopalladium-base complex II. Then transmetallation takes place and the boron species III is activated with the aid of the base NaOR to form IV which can undergo cis-trans isomerization and upon forming V it will go through reductive elimination to afford the desired coupling product  $R^1-R^2$  and regenerate the palladium active species.

However, the palladium catalysts, which are often used for this transformation, have potential toxicity and a substantial cost for larger scale reactions. Nowadays, efforts are undertaken to develop greener cross-coupling reactions and in this regard one of the approaches is to use more active catalysts that are requiring lower catalyst loadings [70–75]. It has to be mentioned that these efforts are widespread, not only in batch but also in flow chemistry [76, 77].

A remarkable contribution in this area was published recently by Noël *et al* [49]. They presented a robust flow protocol for Suzuki-Miyaura reaction between several heteroarylboronic acids and heteroaryl halides which proceed under low loadings (0.05-1.5mol%) of XPhos palladacycle in a packed-bed reactor (Figure 8). Furthermore, a biphasic solvent system was used in order to maintain all the reagents in solution and prevent clogging of the microreactor. It has to be mentioned that the small amount of catalyst provides not

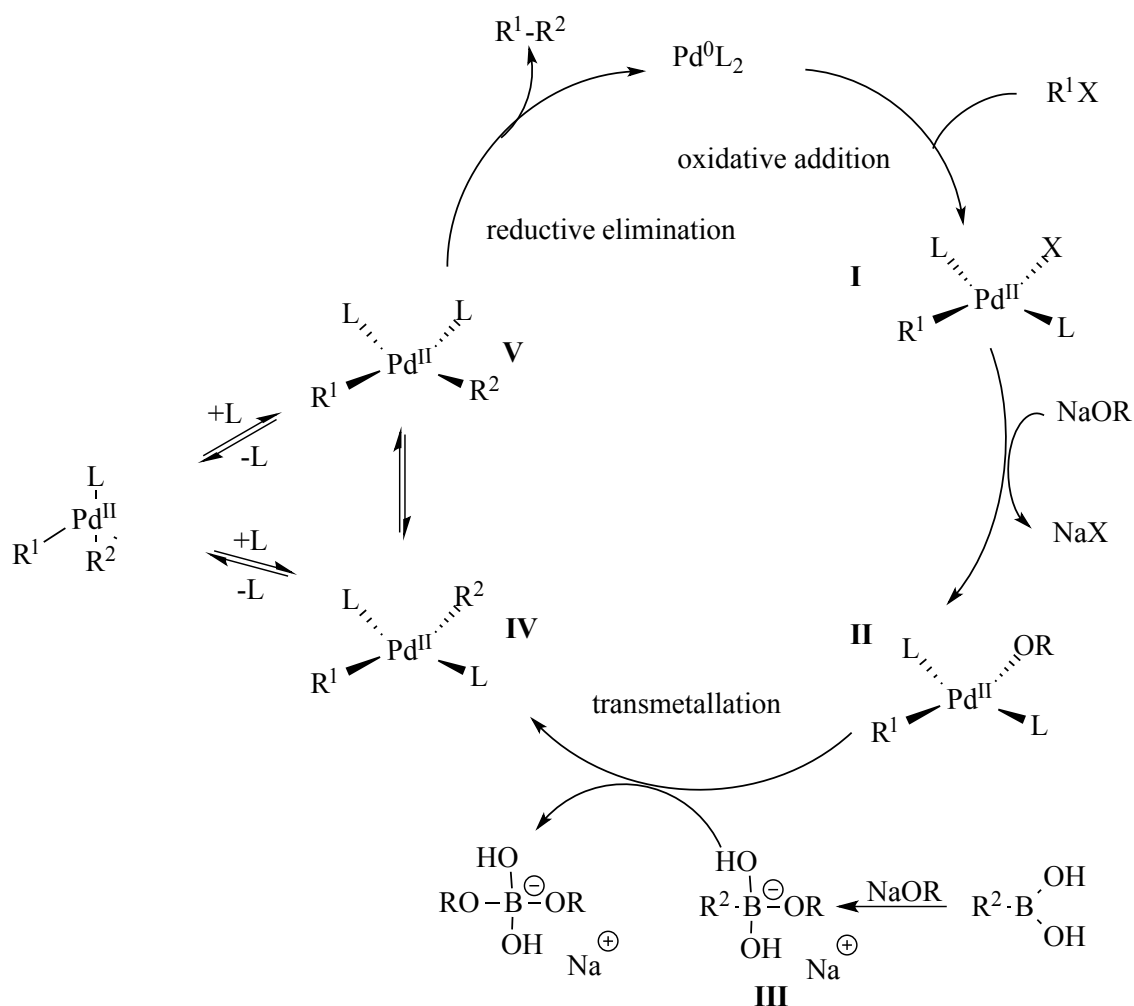


Figure 7: Catalytic cycle of Suzuki-Miyaura cross-coupling reaction.

only a cost effective synthesis but also makes the removal of the palladium residues more facile. The outcome of this synthesis was a series of biaryl compounds obtained in good to excellent yields.

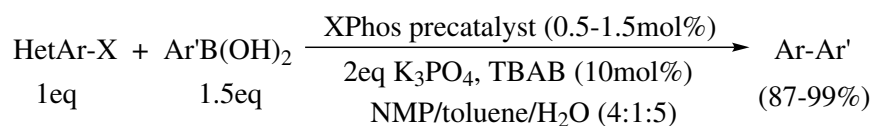


Figure 8: Suzuki-Miyaura reaction in flow.

Another notable contribution in the field of cross coupling chemistry and in particular in heterogeneous catalysis, was made by Ley *et al* in 2005, when they presented a cost effi-

cient continuous flow Suzuki-Miyaura cross-coupling which was catalysed by immobilized  $\text{Pd}(\text{OAc})_2$  under mild conditions (Figure 9). The catalyst was packed in a HPLC column and toluene/methanol was used as solvent. Tetra-*n*-butylammonium salts were used as bases obtaining the best yields (70-85%) with  $\text{Bu}_4\text{NOH}$  and  $\text{Bu}_4\text{NOMe}$  after three passes through the column. Using  $\text{Bu}_4\text{NOMe}$  at  $70^\circ$  they achieved 100% GC yield [78].

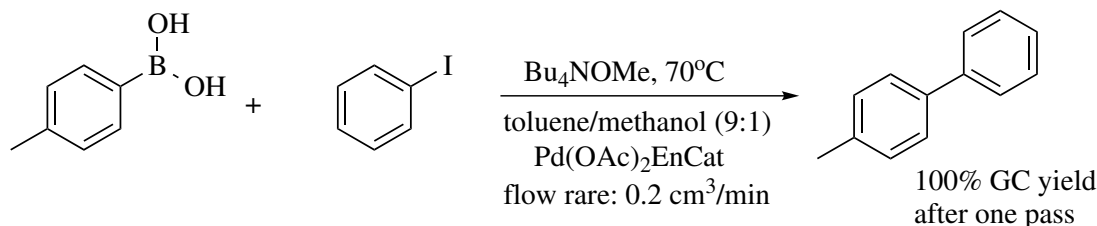


Figure 9: PdEnCat catalysed Suzuki-Miyaura reaction.

Overall, due to the importance of the Suzuki-Miyaura reaction [70, 75] in the pharmaceutical industry as well as in material science, several other contributions have been published up to date, translating this cross coupling reaction in flow [1, 44–50, 79–84].

### 1.2.3 C-H Functionalization

C-H functionalization [77] constitutes an attractive strategy for constructing new carbon-carbon bonds utilizing an otherwise kinetically inert and thermodynamically strong C-H bond [85]. The fact that C-H bonds are so abundant in nature makes this methodology a very useful synthetic tool due to its potential applications as well as its atom efficiency. Utilizing C-H activation, chemists can achieve new disconnections and in a more economic manner since it minimizes reaction steps (e.g protection, de-protection steps) and consequently minimizes the produced waste.

The fore-mentioned transformation takes place via transition metals catalysis [77, 86–88] and it consists of the activation of an  $\text{sp}^3$  or  $\text{sp}^2$  C-H bond which directly interacts with the metal center of the catalyst (it behaves as a functional group) and then upon reaction with the coupling partner, leads to a new C-C bond (Figure 10).



Figure 10: C-C bond formation by C-H activation.

Nowadays the contributions in the field of  $sp^2$  C-H activation [89–92] are manifold but this is not the case for  $sp^3$  C-H activation chemistry [77, 93, 94]. Since these bonds are much more thermodynamically stable, a larger energy barrier has to be overcome in order for the C-H bond to dissociate and of course the ubiquity of such bonds makes it a demanding task to selectively activate one C-H bond over another [85, 92].

To address the arisen selectivity issues, the following methods have been used [85, 92].

First of all, the use of an *N*-heterocycle could be used as a directing group for the metal (e.g. pyridine, pyrimidine rings, pyrroline group) and it could direct it so that the preferred C-H cleavage will take place. In addition, a substrate bearing a functional group could similarly serve the purpose. Furthermore it has been shown that certain catalysts are more effective in C-H functionalization of certain molecules as for example Pd and Rh based catalysts are a good option for the C-H activation of functional arenes and heterocycles [95]. Fagnou *et al* proposed a Pd catalytic cycle shown in Figure 11 to explain the Concerted Metalation-Deprotonation mechanism (CMD) [96]. Initially the ArBr species are added to the Pd(0) via oxidative addition to form complex I, which upon bromine/pivalate ligand exchange forms the complex II. The latter, after reacting with III undergoes a CMD transition-state and leads to complex IV. Then reductive elimination takes place, which leads to V and regenerates the Pd species.

Additionally, C-H activations also undergo one of the four following mechanisms:  $\sigma$ -bond metathesis in early transition metal complexes, oxidative addition in electron-rich late transition metal complexes, electrophilic substitution in electron deficient late transition metal complexes, and 1,2-addition [85, 97, 98].

The  $\sigma$ -bond metathesis mechanism involves, mainly, the early  $d^0$  transition metal complexes of the third and fourth group of the periodic table and consists of concerted



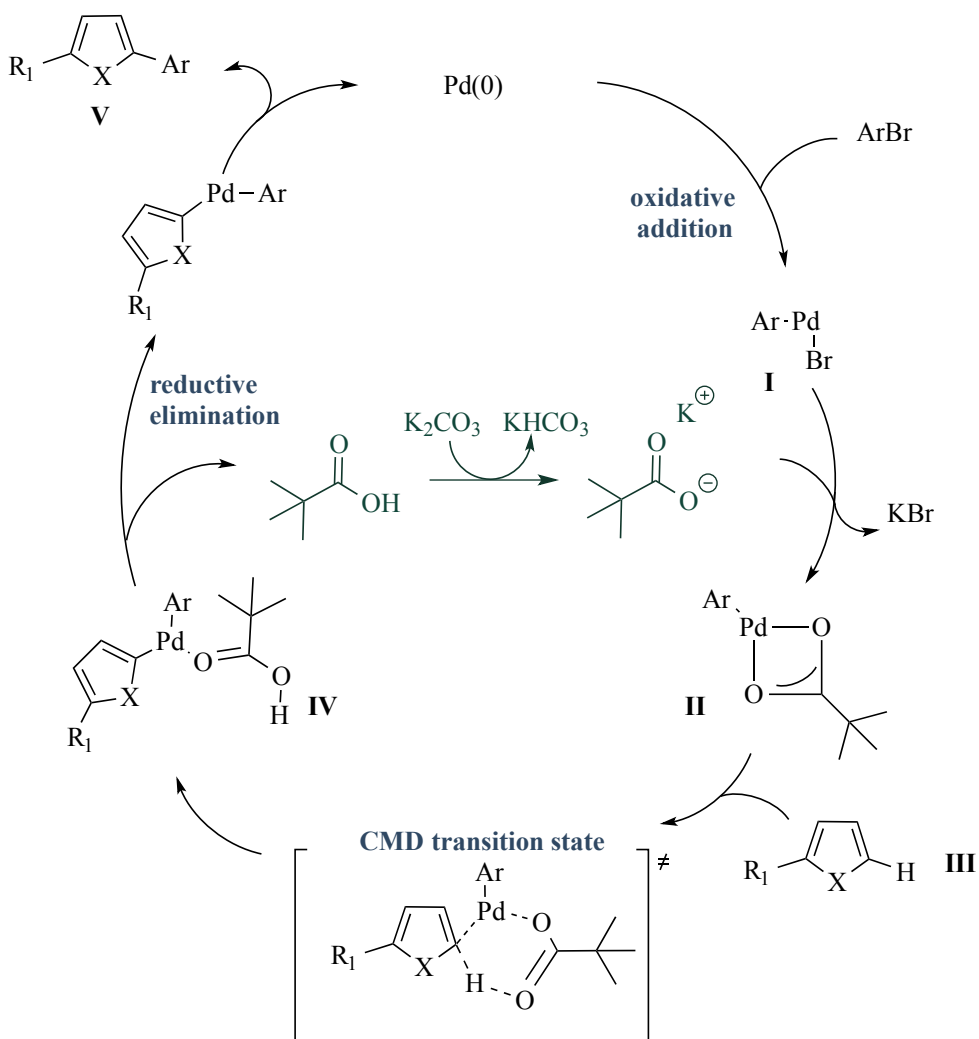


Figure 11: Concerted Metalation-Deprotonation mechanism.

formation and cleavage of bonds at the transition state. During this reaction two bonds are being broken and two new bonds are formed as shown in Figure 12 [85]. In this mechanism, the oxidation state of the metal does not change.

The oxidative addition represents the most common C-H activation mechanism. It proceeds with electron-rich and low valent late transition metal complexes like Ru, Fe, Re, Os, Ir and Pt (Figure 13). At the transition state, the metal is forming a bond with C and H upon reaction with C-H and consequently the geometry of the complex is changing in order to create the space for the two new bonds and the oxidation state notes a rise of two units [85].

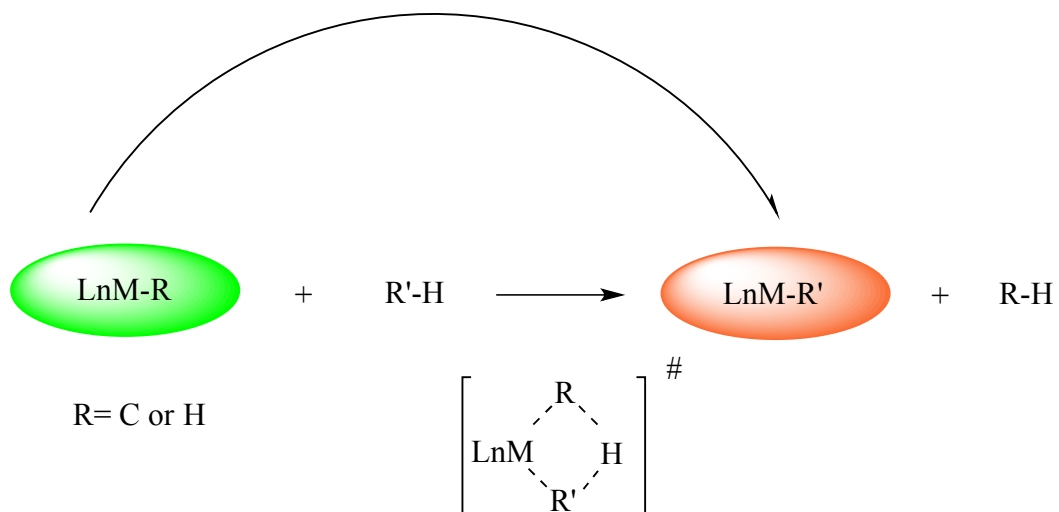
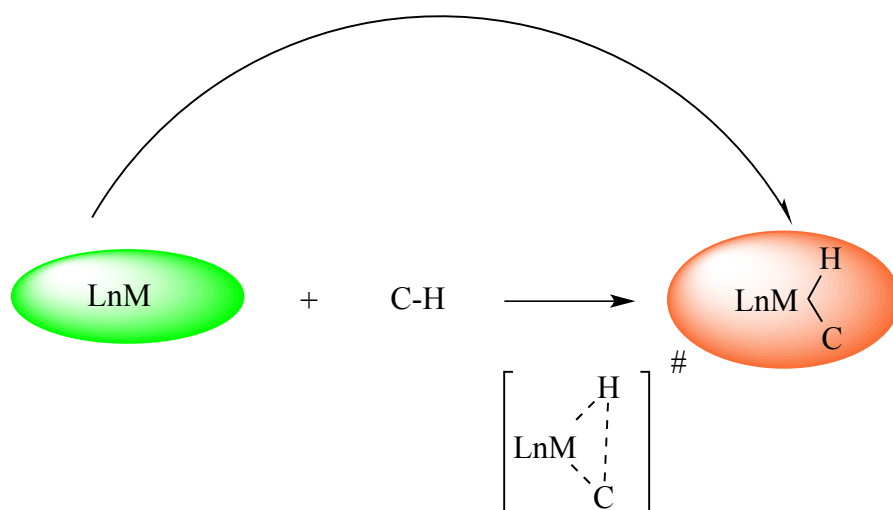
Figure 12:  $\sigma$ -bond metathesis in early transition metal complexes.

Figure 13: Oxidative addition in electron-rich late transition metal complex.

The electrophilic substitution in electron deficient late transition metal complexes involves metals such as  $\text{Pd}^{2+}$ ,  $\text{Pt}^{2+}$  or  $\text{Hg}^{2+}$  (Figure 14) [85].

The 1,2-addition proceeds via addition to a metal-nonmetal double bond and it can involve either early or late transition metals (Figure 15). The ligand in this case has a  $\pi$ -bonding capability and stabilizes the charge in the metal bond upon the addition [85].

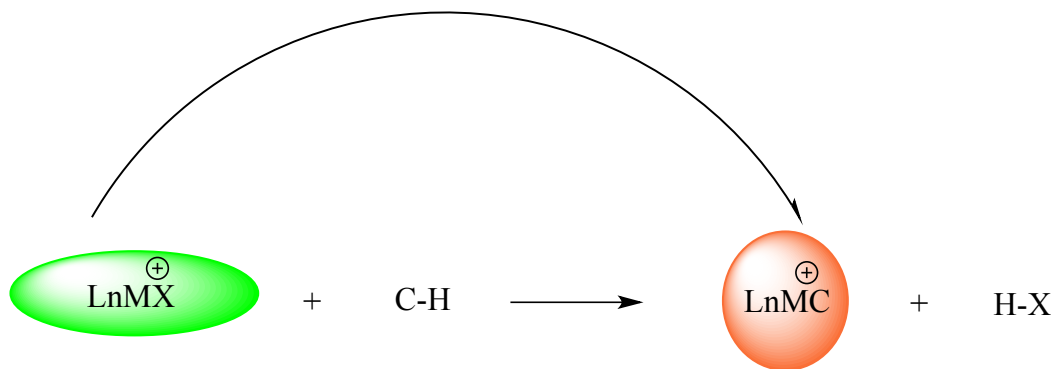


Figure 14: Electrophilic substitution in electron deficient late transition metal complexes.

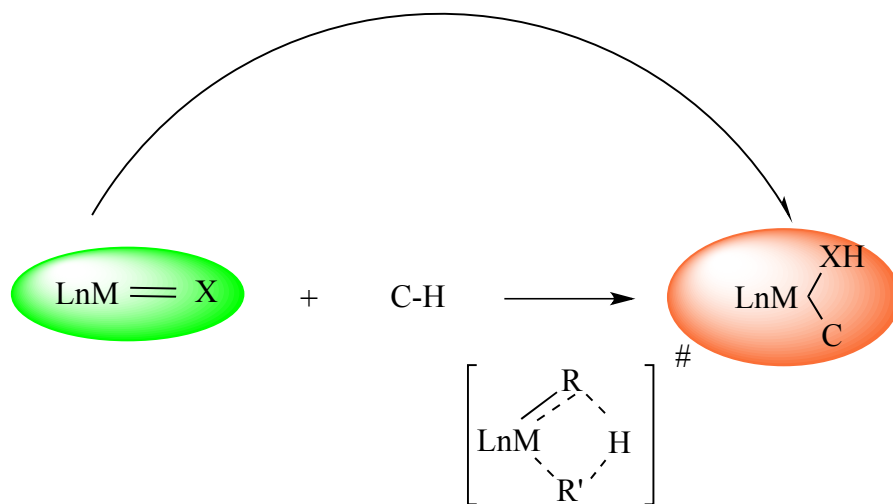


Figure 15: 1,2 addition.

The interest in identifying and developing reactions conditions of this coupling methodology in combination with flow chemistry is continuously increasing and in the future further development is still to follow [1, 99].

## 1.3 Catalysts in organic reactions

The term “catalyst” refers to each substance, which can increase the rate of a chemical reaction without being consumed or changed during the reaction. It participates in the organic reactions, by increasing the stability of the transition state or by increasing the reactivity of an electrophile (making it more prone to nucleophilic attack) or nucleophile. It can also facilitate the dissociation of a leaving group by transforming it to a weaker base [100].

Catalysts can be divided in two major categories: the heterogeneous and the homogeneous ones. They can both serve as catalysts in CF systems and each of them has individual advantages to offer.

### 1.3.1 Heterogeneous catalysts in cross coupling reactions

Nowadays, an increased interest for sustainable green chemistry has arisen. Heterogeneous catalysts provide the researcher with easy handling and are considered to be suitable for continuous flow processes [76] and due to their potential recycling they have favorable properties regarding “greenness” as compared to their homogeneous counterparts. In particular: Pd, Cu, Ru, and Ni can be found immobilized in several different solid supports e.g on silica, monolithic or magnetic nanoparticles or on a polymer complex [79].

Two of the most widely used heterogeneous catalysts are:

- Palladium on charcoal (Pd/C).
- Polyurea-encapsulated palladium(II) acetate.

The main advantages of heterogeneous catalysis can be summarized by the following aspects:

- ability to recover the catalyst (by filtration or centrifugation), recycle it and reuse it is provided and consequently the chemical waste and subsequently the cost of the catalyst loss is minimized [101],

- contamination of the reaction mixture can be avoided and therefore also toxicity issues from the metal to the desired product.

Even though heterogeneous catalysis is a promising field of catalysis there is yet a disadvantage, which should be overcome: the often-occurring catalyst leaching in Pd catalyzed reactions, which subsequently leads to activity loss. This occurs after oxidative addition, when the “Pd” is released to the reaction mixture and after the reductive elimination it re-precipitates, forming the so-called “Pd black”. This phenomenon relies on many different factors as for example the base which is used, the reaction temperature, the type of support and reaction medium [2].

An alternative way for continuous flow systems can be found in homogeneous catalysis.

### 1.3.2 Homogeneous catalysts in cross coupling reactions

Homogeneous catalysts are widely used in cross coupling reactions and the main reason for that is that they are readily available to react immediately after dilution in the reaction mixture. They can be found within single-phase homogeneous systems or in recyclable biphasic systems and they are mainly palladium complexes:  $\text{Pd}(\text{OAc})_2$ ,  $\text{Pd}(\text{PPh}_3)_4$ ,  $\text{Pd}(\text{dppf})\text{Cl}_2$  etc [76].

Palladium complexes are also the first choice of use especially in cross coupling chemistry [42]. They owe their extensive recognition from the synthetic community to their many advantages:

- they are very versatile and require mild conditions to act,
- they are highly selective and contribute to less side product production,
- they can tolerate many functional groups,
- their reactivity is tunable (in the sense that is dependent on the ligands which can be added into the reaction mixture),
- they are resistant to moisture and air.

## 2 Results and Discussion

### 2.1 Towards the synthesis of biologically active Magnolol and Honokiol derivatives in flow

#### 2.1.1 Objective

Within this section, our efforts were focused on the translation of a batch process which was developed in our group and leads to Magnolol and Honokiol bioactive derivatives [102] into a continuous flow process. The compound of interest was 5-allyl-3'-methoxy-[1,1'-biphenyl]-2-ol, which is derivative of Magnolol/Honokiol and was found to enhance  $GABA_A$  induced current ( $I_{GABA}$ ) in a higher intensity than its lead structures [102].  $GABA_A$  ( $\gamma$ -Aminobutyric acid) (Figure 16) is the major receptor for the GABA inhibitory neurotransmitter, which is located in the central nervous system. It consists of five subunits and depending on the structure of the subunit it can show different pharmacological and electrophysiological properties [103, 104]. To reach the target compound, Suzuki-Miyaura coupling reaction was employed via a two step synthesis.

#### 2.1.2 Magnolol and Honokiol properties

Magnolol and Honokiol (Figure 17) are natural compounds, which can be isolated from a tree called *Magnolia officinalis*. They belong to a class of compounds known as neolignans and they are of particular interest due to several therapeutic properties which among others, are the following: antistress [105], anticancer [105], antiangiogenetic [106], antiinflammatory [105], antiepileptic [107], neuroprotective [108, 109], somnogenic (honokiol) [109] etc.

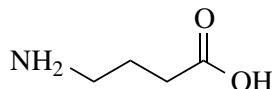


Figure 16:  $\gamma$ -Aminobutyric acid.

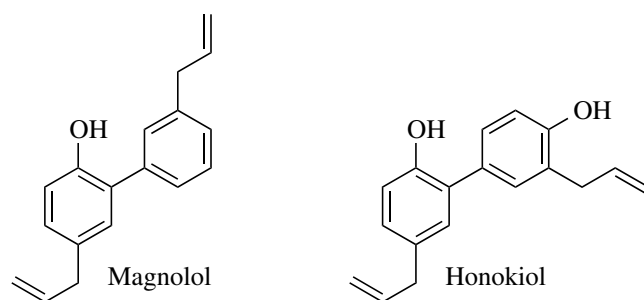
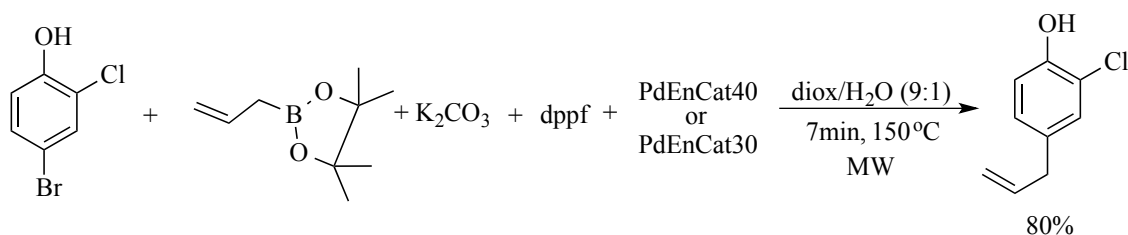


Figure 17: Magnolol, Honokiol.

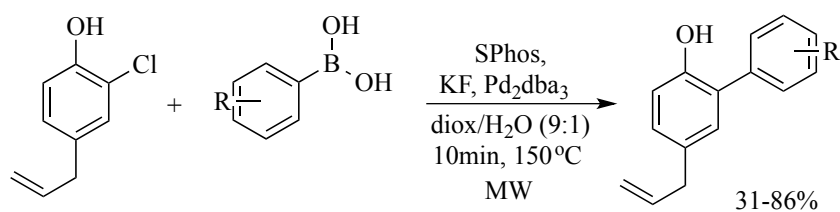
### 2.1.3 Exploration of appropriate conditions to translate the batch process into flow

The batch synthesis consists of two subsequent Suzuki-Miyaura cross coupling reactions (Scheme 4) [102]. In the first step, regioselective allylation at the most reactive bromine position of the 4-bromo-2-chlorophenol takes place and in the second step follows the coupling with the boronic acid of interest in order to access the desired derivative.

Allylation to the bromine position via Suzuki-Miyaura cross coupling



Synthesis of Magnolol/Honokiol derivative  
via Suzuki-Miyaura cross coupling



Scheme 4: Magnolol, Honokiol batch synthesis.

To accomplish the synthesis of our target compound (5-allyl-3'-methoxy-[1,1'-biphenyl]-2-ol) in flow, we started our optimization efforts with the first reaction step, using an in-house developed continuous-flow reactor system.

Since the catalyst, which was used in the batch protocol was immobilized, we used a glass column (60mm Omnifit) to pack the PdEnCat and place it inside a heated reactor from Syrris as it is depicted in Figure 18. The glass column had attached PFA tubing from both ends. In the top, the glass column was connected via the PFA tubing to a syringe pump and in the bottom it leads to a collection flask. The temperature was controlled by a thermometer attached to the reactor. With this flow set-up, the reaction solution could be pumped through the catalyst with the preferred flow rate and the product could be collected after the reaction zone, in the collection flask.

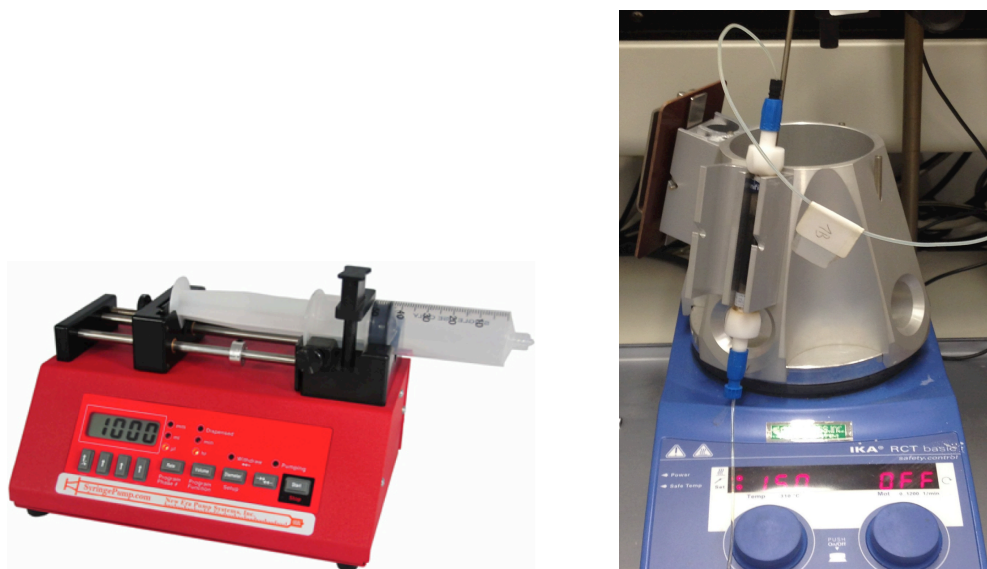


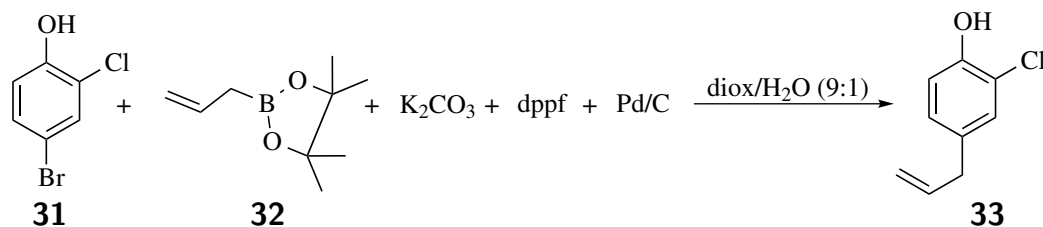
Figure 18: Units of the experimental set-up.

However, this system cannot support external pressurization and consequently the temperature had to be kept at much lower levels than in the batch protocol (150°C), otherwise the solvent system (diox./H<sub>2</sub>O) would boil within the reaction zone. For this reason, we initially conducted a time screening in microwave at 90°C in order to see how the reaction performs using this decreased temperature. Soon it was found that the reaction was not taking place at all at this lower temperature (Table 4, Entries 1-3) and



this was also the case in the flow experiments with our in-house developed continuous-flow reactor system (Table 4, Entries 4-6) (Figure 18).

Table 4: Temperature screening.



Entry <sup>a</sup>	R.T.	T[°C]	Heating mode	Observations	<b>33</b> [%] <sup>d</sup>
1	10	90	MW	-	n.c.
2	20	90	MW	-	n.c.
3	30	90	MW	-	n.c.
4 <sup>b</sup>	30	90	glass column	-	n.c.
5 <sup>b</sup>	60	90	glass column	-	n.c.
6 <sup>b</sup>	120	90	glass column	-	n.c.
7 <sup>c</sup>	5	150	glass column	catalyst leaching	15
8 <sup>c</sup>	10	150	glass column	catalyst leaching	8

*a*: Reaction conditions: 1 eq. of **31**, 2 eq. of **32**, 10 mol% dppf, 2 eq.  $\text{K}_2\text{CO}_3$ , 5 mol% catalyst: Pd/C. *b*: In-house developed continuous-flow reactor system. *c*: AFRICA. *d*: Conversion as determined by GC using dodecane as internal standard.

Therefore we wanted to test next the original batch conditions in flow and for that we had to switch to a more complex continuous flow system, namely AFRICA (see Appendix A), a flow system, which would allow us to use 150°C as reaction temperature,

in combination with the above-mentioned heated reactor, which would allow to proceed with the heterogeneous catalysis. To our disappointment, these trials did not facilitate the process either, resulting in a maximum of 15% conversion (Table 4, Entries 7-8).

Since none of the initial experiments led to a promising result and based on our experience with leaching connected to immobilized catalysts (Chapter 2.3.4) we decided to abandon the “encapsulated type” of catalysts and investigate other catalysts, which could serve the purpose (Table 5). Initially we ran the reaction substituting the immobilized Pd(OAc)<sub>2</sub> with normal Pd(OAc)<sub>2</sub> (Table 5, Entry 1) and then with Pd/C (Table 5, Entries 2-5).

Table 5: Catalyst screening.

<b>Entry<sup>a</sup></b>	<b>Pd source</b>	<b>Heating mode</b>	<b><b>33</b> [%]<sup>d</sup></b>
<b>1</b>	Pd(OAc) <sub>2</sub>	MW	90
<b>2</b>	Pd/C 5% w/w	MW	75
<b>3</b>	Pd/C 10% w/w	MW	90
<b>4<sup>b</sup></b>	Pd/C 10% w/w	MW	n.c.
<b>5<sup>c</sup></b>	Pd/C 10% w/w	glass column	n.c.

*a*: Reaction conditions: 1 eq. of **31**, 2 eq. of **32**, 10 mol% dppf, 2 eq. K<sub>2</sub>CO<sub>3</sub>, 5 mol% of catalyst, R.T.=5min, T=150°C. *b*: In this example no dppf was added. *c*: In AFRICA.

*d*: Conversion as determined by GC using dodecane as internal standard.

From the catalyst’s screening (Table 5) we verified the crucial role of dppf for the reaction performance since in the example where dppf was excluded we had 0% of product (Table 5, Entry 4) in comparison to the same experiment with dppf that led to 90% conversion (Table 5, Entry 3). We also identified Pd/C as well as Pd(OAc)<sub>2</sub> as good

alternatives for PdEnCat30 (Table 5, Entries 1, 3) for translating the protocol in flow. Since Pd(OAc)<sub>2</sub> was not soluble in the reaction mixture and also not supported in a surface that would be prerequisite for packing it in a column; we decided to continue the optimization with Pd/C, which resulted in the same conversion as Pd(OAc)<sub>2</sub> in MW (Table 5, Entries 1, 3) and is one of the widely available catalysts for heterogeneous catalysis. However translating the conditions into flow resulted in 0% conversion (Table 5, Entry 5).

In order to identify the reason behind the 0% conversion and to be able to retain a reproducible flow process for future experiments, we implemented some changes in the experimental set-up, which would allow us to have a better control over the residence time and the dead volume of the system.

First of all, we installed a two ways six port MPLC valve (with an injection and load position) (Figure 19) in between AFRICA and the heated reactor as well as a BPR (250 psi) before the product collection to achieve pressurization of the system allowing for super-heating of the solvents. When the valve was turned to the “Load” position, pure solvent could be pumped from the AFRICA to the reactor. When the valve was turned to the “Inject” position, the reaction mixture could be injected via a syringe to a loop and then transferred to the reactor (Figure 19) in the desired time point, by-passing the dead volume of the AFRICA system.

For determining the dead volume of the reactor we installed a UV detector as shown in Figure 20. We connected a Büchi UV detector directly after the flow reactor and before the product collection flask. Then we fixed the flow rate to a certain value (1mL/min) and recorded the R.T. that was required between the injection of an intensively UV absorbing compound (we used methyl benzoate), till the point that it reached the UV detector (this was noticed due to the significant change of the absorbance value). Knowing the flow rate and the residence time, we could calculate the reactor’s dead volume ( $V_b$ ) as shown in Figure 20. The inner volume of the tubing  $V_a$  and  $V_c$  (Figure 20) was simply calculated by detaching them from the reactor and weighing them empty and then after filling them with water. Using the density of water, and knowing the difference in the weight (between the empty and the filled with water capillary) we could calculate the

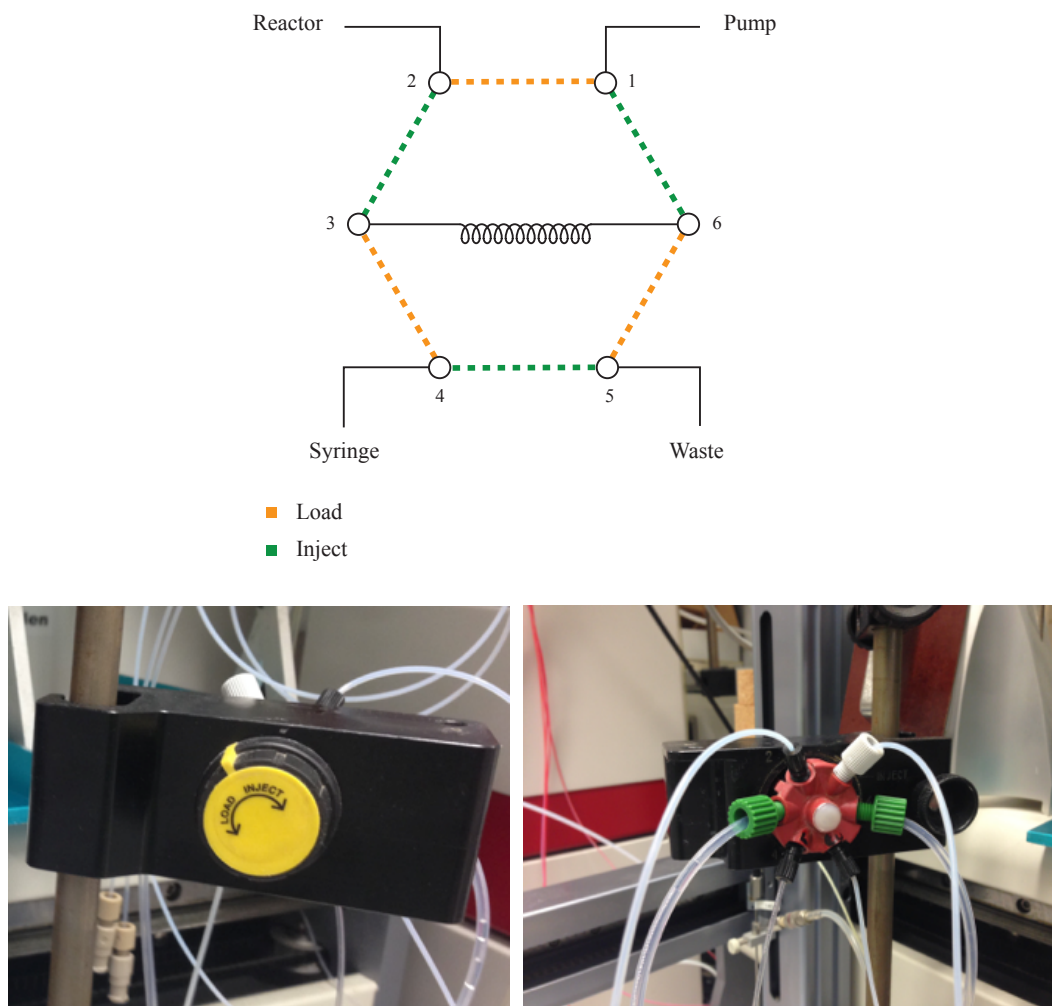


Figure 19: Schematic representation of the MPLC valve in the flow experimental set-up.

inner volume of the tubing. Therefore the overall dead volume was found to be 1.5mL ( $V_a = 0.2218\text{mL}$ ,  $V_b = 0.3445\text{mL}$ ,  $V_c = 0.9337\text{mL} \rightarrow \text{dead volume} = V_a + V_b + V_c = 1.5\text{mL}$ ) (Figure 20).

Since we had the UV detector installed in our flow system we decided to take advantage of a live time analysis during our screenings in order to have an immediate feedback of what is coming out from the reactor at each particular time point. In this way, for example, we would be able to know if we were having ligand leaching or we could immediately have an idea about incomplete conversion to product or the opposite. Therefore, we proceeded to the measurement of the UV absorption of the reaction reagents.

The UV experiment was carried out in two different wavelengths: 254nm and 340nm,

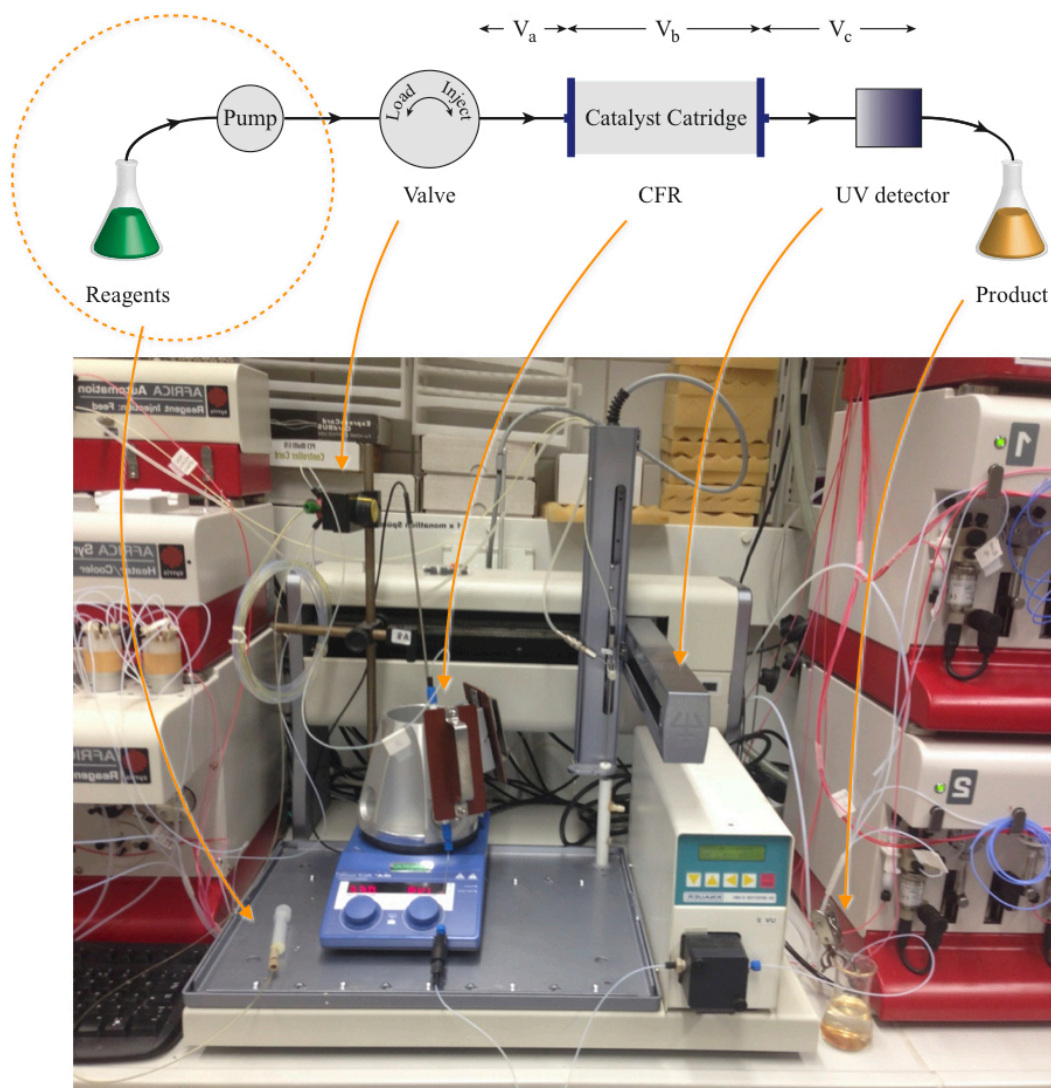


Figure 20: Schematic representation of the flow set-up, used to determine the dead volume of the system.

resulting in the graph in Figure 21. At 340nm, apart from the product's high absorption, the reaction reagents (**31** & **32**) as well as dppf, did not show useful absorptions. At 254nm, dppf absorbed highly, but its value was not far from that of the product. Therefore with the recorded absorptions we could not proceed further to a useful live time analysis.

After the pre-mentioned modifications to maintain sustainable flow conditions and to determine the dead volume of the system we proceeded to a new reaction screening with Pd/C (Table 6), excluding the UV detector from the flow set-up (Figure 22).

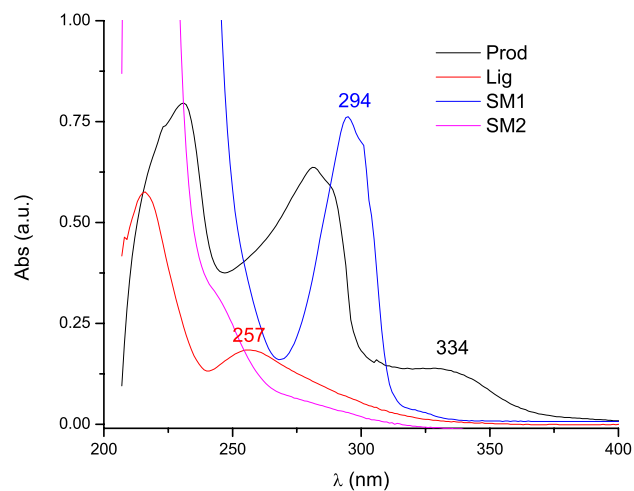


Figure 21: UV experiments in 254nm and 340nm; Prod: **33**, Lig: dppf, SM1: **31**, SM2: **32**.

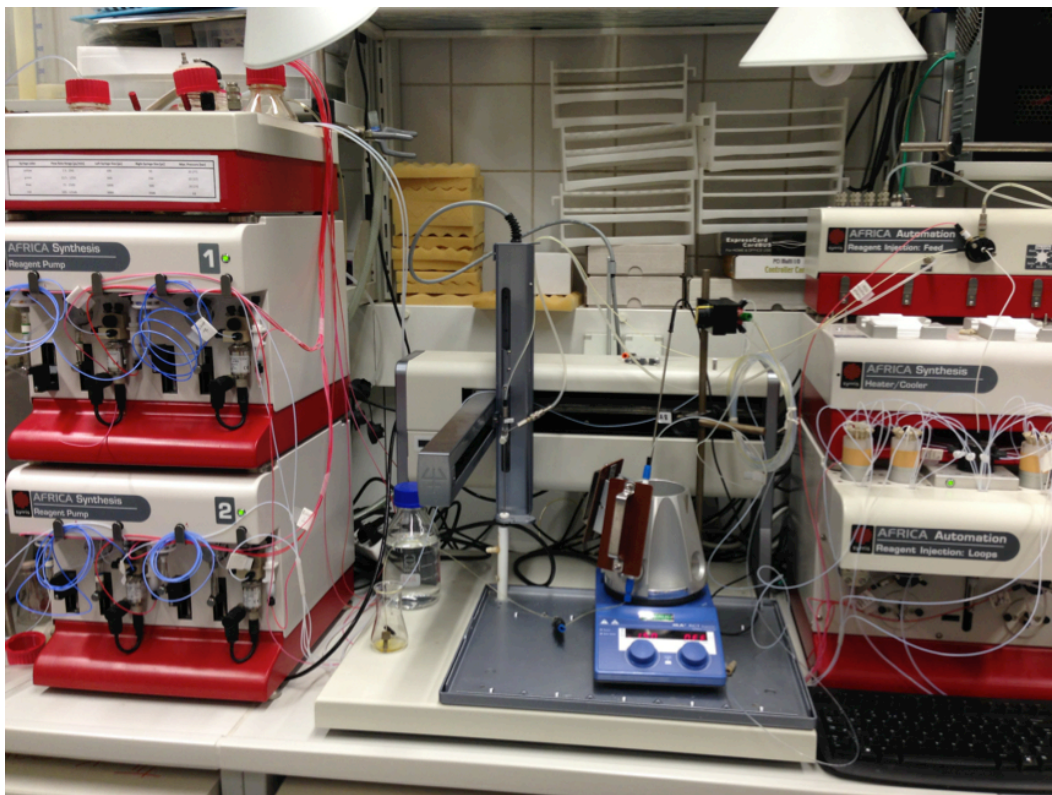
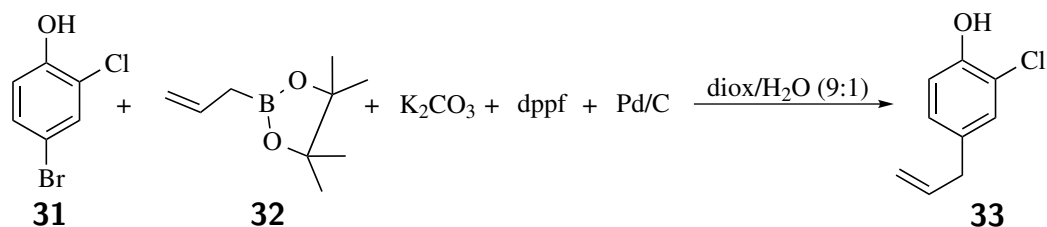


Figure 22: Flow set-up.

Initially, we pre-equilibrated the catalyst with the ligand solution before pumping in

Table 6: Screening in flow.



Entry <sup>a</sup>	Adjustments	<b>33</b> [%] <sup>b</sup>
1	Pre-equilibration of the Pd/C with a solution of dppf, 10min in advance, before the reaction mixture loading	n.c.
2	Pre-equilibration of the Pd/C with a solution of dppf and $K_2CO_3$ , in advance before the reaction mixture loading	n.c.
3	Tenfold amount of Pd/C was added and pre-equilibration of the catalyst with a solution of dppf and $K_2CO_3$ , before the reaction mixture loading took place	n.c.
4	The Pd/C was pre-treated with the dppf before packing it in the glass column and after packing it, was equilibrated with solvent, before the reaction mixture loading	n.c.

*a*: Reaction conditions: 1 eq. of **31**, 2 eq. of **32**, 10 mol% dppf, 2 eq  $K_2CO_3$ , 5 mol% catalyst: 10% w/w of Pd/C, R.T.= 5 min, T=150°C, heating mode: glass column in AFRICA system. *b*: Conversion as determined by GC using dodecane as internal standard.

the reaction mixture solution in order to activate the catalyst species (Table 6, Entry 1). Unfortunately, this resulted in 0% conversion. Then, we repeated the same procedure adding to the dppf solution also the base (Table 6, Entry 2). This did not work either so we increased the catalyst loading in an extreme of ten times more to see if this will make any improvement (Table 6, Entry 3). Unfortunately also this trial did not change

anything. As a last attempt we mixed the catalyst with dppf in the smallest possible amount of DCM (in order to get a solution) and stirred it for 40min. Then the DCM was evaporated and the mixture of the pre-treated catalyst and dppf was packed in the glass column (Table 6, Entry 4). To our disappointment, this attempt was not successful either.

In comparison to the flow experiments, the previously conducted microwave experiment, which had used the same eq. of reagents under the same temperature and time (Table 5, Entry 3) had given a yield of 90%. Our suggestion to explain this difference was that in flow either the dppf does not have the time to form the active species or the Pd leaches completely from the cartridge and results in inactive catalyst leading to 0% conversion. To test our suggestion, we set up a control experiment.

Upon collecting the content of the cartridge (catalyst/ligand mixture) used in Entry 4 (Table 6) and dividing in two equal parts, we subjected them into two microwave reactions, adding all the other required reagents for the reaction to be performed (Reaction conditions: 1 eq. of **31**, 2 eq. of **32**, 2 eq.  $\text{K}_2\text{CO}_3$ ,  $t=5\text{min}$ ,  $T=150^\circ\text{C}$ ). In the one vial we added additionally 10mol% of dppf. Unfortunately, the outcome of the control experiment confirmed our suggestion. In both reaction mixtures (the one which ran with the aid of dppf and catalyst that were recovered from the flow experiment and the other in which additional amount of dppf was added) we observed 0% conversion. That was a strong indication that the catalyst in use was already inactive. Therefore leaching should have taken place during the flow experiment.

Since we were facing difficulties to translate any promising batch conditions in flow and Pd leaching was still a major issue, we decided to use a protocol (Table 20, Entry 6) that is presented in chapter 2.3.4 and which he have developed, optimized and effectively applied for the flow synthesis of 2- and 3-phenylpyridines. In this protocol (Reaction conditions: **31** (1 eq.), **32** (1.2 eq.), 2eq.  $\text{K}_2\text{CO}_3$ , 2.1mol%  $\text{Pd}(\text{PPh}_3)_4$ ,  $90^\circ\text{C}$ , 0.05 M, in flow)  $\text{Pd}(\text{PPh}_3)_4$  was mostly soluble in the solvent mixture and consequently we were targeting for homogenous catalysis also in this particular case. However, we first wanted to test the conditions under MW heating in order to observe if any precipitation occurs during or upon heating, before transferring the reaction in flow. For this reason we



used the temperature (120°C) and time (180sec) from the batch optimization of the same reaction under MW conditions (Table 19, Entry 6). Furthermore, we tried the reaction with two different catalyst loadings: 1mol% and 2.1mol%. Unfortunately also those trials led to 0% conversion.

We also tried the batch conditions for the Magnolol/Honokiol precursor in MW (Reaction conditions: 1 eq. of **31**, 2 eq. of **32**, 2 eq. K<sub>2</sub>CO<sub>3</sub>, R.T.=5min, T=150°C) but using Pd(PPh<sub>3</sub>)<sub>4</sub> instead of PdEnCat30 and adding no ligand, which also resulted in 0% conversion.

Due to the important role of the dppf in the reaction mechanism we again searched for an alternative catalyst, which could ideally be soluble in the reaction mixture. We found Pd(dppf)Cl<sub>2</sub> in which the Pd is in a complex with dppf.

Using the previous reaction conditions now with Pd(dppf)Cl<sub>2</sub> resulted also in heterogeneous solution and 100% conversion to the desired product, under microwave conditions (Table 7, Entry 1). Since in this case dppf was part of the palladium complex, we wanted to check if the added amount of dppf would be still necessary. Therefore we repeated the experiment of Entry 1 (Table 7) but this time without adding dppf and obtained 0% conversion (Table 7, Entry 2) even with higher catalyst loading (Table 7, Entry 3).

Table 7: Pd(dppf)Cl<sub>2</sub> screening in microwave.

Entry <sup>a</sup>	Solubility	Catalyst loading (mol%)	dppf loading (mol%)	<b>33</b> [%] <sup>b</sup>
1	moderate	5	10	100
2	het.	5	-	n.c.
3	het.	10	-	n.c.

*a*: Reaction conditions: 1 eq. of **31**, 2 eq. of **32**, 2 eq. K<sub>2</sub>CO<sub>3</sub>, R.T.= 5 min, T=150°C, heating mode: microwave. *b*: Conversion as determined by GC using dodecane as internal standard.

The solubility at r.t. was moderate only in case of Entry 1 (Table 7) in which dppf

was added. In the other two entries (Table 7, Entries 2-3) we had clearly heterogeneous solutions. In all cases we observed Pd black formation. Transferring the conditions, which in microwave gave 100% conversion (Table 7, Entry 1), in flow, using the Omnifit glass column to pack the catalyst, we got 0% conversion. Since in Entry 1 (Table 7) we had moderate solubility, we wanted to see if it could proceed as a homogeneous solution in flow. Therefore we used a cap disk of 2mL and pumped with AFRICA (see Appendix A) our reaction mixture through. In this case we observed a few percent conversion to product (in GC), but quantification was not possible due to substantial tailing of the peak. Furthermore, to our disappointment, massive precipitation occurred in the reaction zone which led to clogging of the system.

Trying to see if we can improve the solubility of the reaction mixture, we changed the ratio of dioxane/water from 9:1 to 7:3 and 1:1 but these solvent mixtures resulted also in heterogeneous solutions, in microwave reactions.

Due to the previous unsuccessful attempts we decided to investigate other catalysts that could ideally lead to a homogeneous solution. We ran the exact conditions of Entry 1 (Table 7), substituting the Pd(dppf)Cl<sub>2</sub> with Pd<sub>2</sub>dba<sub>3</sub>, which in the batch protocol (Scheme 4) serves as the catalyst of the second Suzuki-Miyaura reaction leading to the desired Magnolol/Honokiol derivative. Adding this catalyst we got a homogeneous solution in r.t. but after a reaction time of 5min (150°C) in the microwave, we observed massive precipitation. Although the conversion was 92% (in GC) we had to abandon also this protocol since it was not suitable for a flow process.

Considering that in microwave screenings we had observed promising conversions but in flow we had almost exclusively 0%, we decided to perform some batch experiments in high pressure resistant glass vial under conventional heating. In this way we wanted to check if the recorded good microwave conversions resulted from a better heating of the catalyst's metal center due to the microwave irradiation, which in turn leads to a better catalyst activity.

For this screening we initially used Pd(dppf)Cl<sub>2</sub> that was the only catalyst with which we got 100% conversion to the desired product (Table 7, Entry 1). We used the exact same conditions as in Entry 1 (Table 7), but we let it react in a high pressure resistant

glass vial (Table 8). We observed massive precipitation together with product formation but the quantification was not possible due to substantial tailing of the product peak and overlapping of this peak and the peak from the substrate. Increasing the time from 5 to 10min and then to 15min and finally 60min, we observed further reaction progressing but unfortunately the quantification of the results was still not possible, due to the mentioned overlapping issue.

Table 8: Screening using conventional heating.

Entry <sup>a</sup>	Ligand & Catalyst	T[°C]	Solubility	Product formation <sup>b</sup>
1	SPhos+Pd <sub>2</sub> dba <sub>3</sub>	75	het.	n.c.
2	dppf+Pd(dppf)Cl <sub>2</sub>	75	moderate till 75min	indication of P( <b>33</b> ) in 90min
3	SPhos+Pd <sub>2</sub> dba <sub>3</sub>	100	het.	indication of two isomers ( <b>33</b> , <b>34</b> ) after 45min
4	dppf+Pd(dppf)Cl <sub>2</sub>	100	moderate till 15min	indication of P( <b>33</b> ) after 15min
5	SPhos+Pd <sub>2</sub> dba <sub>3</sub>	125	het.	indication of two isomers ( <b>33</b> , <b>34</b> ) after 15min
6	dppf+Pd(dppf)Cl <sub>2</sub>	125	moderate till 15min	indication of P( <b>33</b> ) after 15min

*a*: Reaction conditions: 1 eq. of **31**, 2 eq. of **32**, 2 eq. K<sub>2</sub>CO<sub>3</sub>, R.T.= 5 min, catalyst: 5mol% + ligand: 10 mol%, time screening from 15 to 90min in 15min slots. *b*: Product formation was recorded by GCMS analysis.

Trying to control the formation of the precipitant we decided to decrease the temperature and see if this will improve the situation. We also tried Pd<sub>2</sub>dba<sub>3</sub> in combination with SPhos, which are the ligand and catalyst of the second Suzuki-Miyaura coupling reaction (Scheme 4). The reason behind this trial was to see if a one-pot protocol for the synthesis of the desired compounds would be possible.

However, we observed once more massive precipitation occurring during the reaction. Investigating the nature of the precipitant, we found that it was inorganic and corresponded to K<sub>2</sub>CO<sub>3</sub>, which we were using as base.

Although we had product formation, in all the experiments with dppf and Pd(dppf)Cl<sub>2</sub> (Table 8, Entries 2, 4, 6) we could not get quantitative and consequently conclusive results due to the substantial tail of the peak and overlapping of the product to the substrate peak occurred in these cases as well in the GCMS analysis.

In the entries where the ligand/catalyst combination were Pd<sub>2</sub>dba<sub>3</sub> and SPhos (Table 8, Entries 1, 3, 5) we observed formation of two isomers. The desired product **33** along with its isomer **34** (Figure 23).

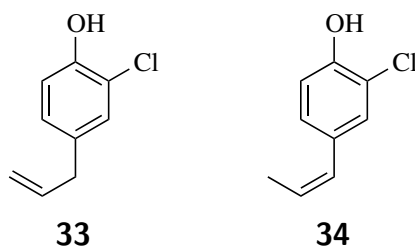


Figure 23: Magnolol/Honokiol intermediate's isomers.

In an attempt to overcome the problem with the precipitation of the base, we ran another experiment in batch, exchanging this time the 2eq. of K<sub>2</sub>CO<sub>3</sub> with 2eq. of NaOH and keeping from Entry 2 (Table 8) the rest of the conditions as they were. In this case, precipitation of the base was observed again after the first 15min of reaction time and it resulted in 0% conversion. Since this attempt was not successful we ran a new experiment, substituting this time the inorganic base with an organic one. We chose DBU and applied the conditions from Entry 6 (Table 8). In this experiment, conversion to product was observed from the first 15min of reaction time and Pd black formation

from 45min onwards. However, the quantification of the peaks was again not possible due to tailing and overlapping of substrate **31** and product **33**.

In order to try this protocol in flow we had to be assured that we could keep Pd in solution and no Pd black formation will take place. PEG 400 is known to be used in flow experiments for this purpose. Therefore, we subjected three reaction mixtures, containing 2eq. DBU instead of  $K_2CO_3$ , in microwave at  $150^\circ C$  for 5min, using in each of them a different percentage (a:5, b:10, c:25% v/v) of PEG 400 as co-solvent. We also prepared a reaction mixture using  $K_2CO_3$  along with 25% of PEG 400 in order to see if the polyethylene glycol could also prevent precipitation of this base. In all cases Pd stayed mostly in solution, but the Pd black formation was not totally prevented. The percentage of PEG 400 did not seem to influence the solubility of the system in a particular manner. Furthermore, in case of the experiment in which  $K_2CO_3$  was used, there was no improvement regarding the precipitation of the base.

However, we wanted to check if these conditions (DBU, PEG 400) could be applicable in flow, so we used the 2 mL cap disk with the AFRICA system (see Appendix A) and taking advantage of the installed MPLC valve (Figure 19), we were manually controlling the loading and injection of the reaction mixture (Figure 24). We ran several experiments varying the residence time from 15 to 45min. Initially we pumped the reaction solution simultaneously through the PFA capillary, but soon blockage was observed due to Pd black formation. In order to solve this problem, we decided to pump the reaction mixture in a “sandwich” fashion. In other words, we were alternating between the same amount of solvent and the same amount of reaction mixture (2 mL of 9:1 dioxane/ $H_2O$  with to 2 mL of reaction mixture solution) in an attempt to wash the precipitating Pd particles in the cap disk, driving them to the outlet of the reactor; preventing it from clogging. Of course, in this way we were increasing the diffusion of the system, but since we were facing Pd black formation we had no other alternatives.

Nevertheless, by applying the “sandwich” fashion, a significant issue arose. We encountered a steep pressure increase whenever we were changing the position of the valve from Load to Inject. The direct effect of this event was that Pd black was not washed out of the system but pushed back to the injection valve (Figure 25). As shown in Figure 24

there is a pressure difference between the loading position and injection position of the valve ( $\Delta P$ ), which was released with the position change, causing the precipitant to return towards the pump. The BPR was insufficient in this case, due to the fact that it was able to regulate the pressure  $P_2$  of the system, but not the overall pressure difference  $\Delta P$ .

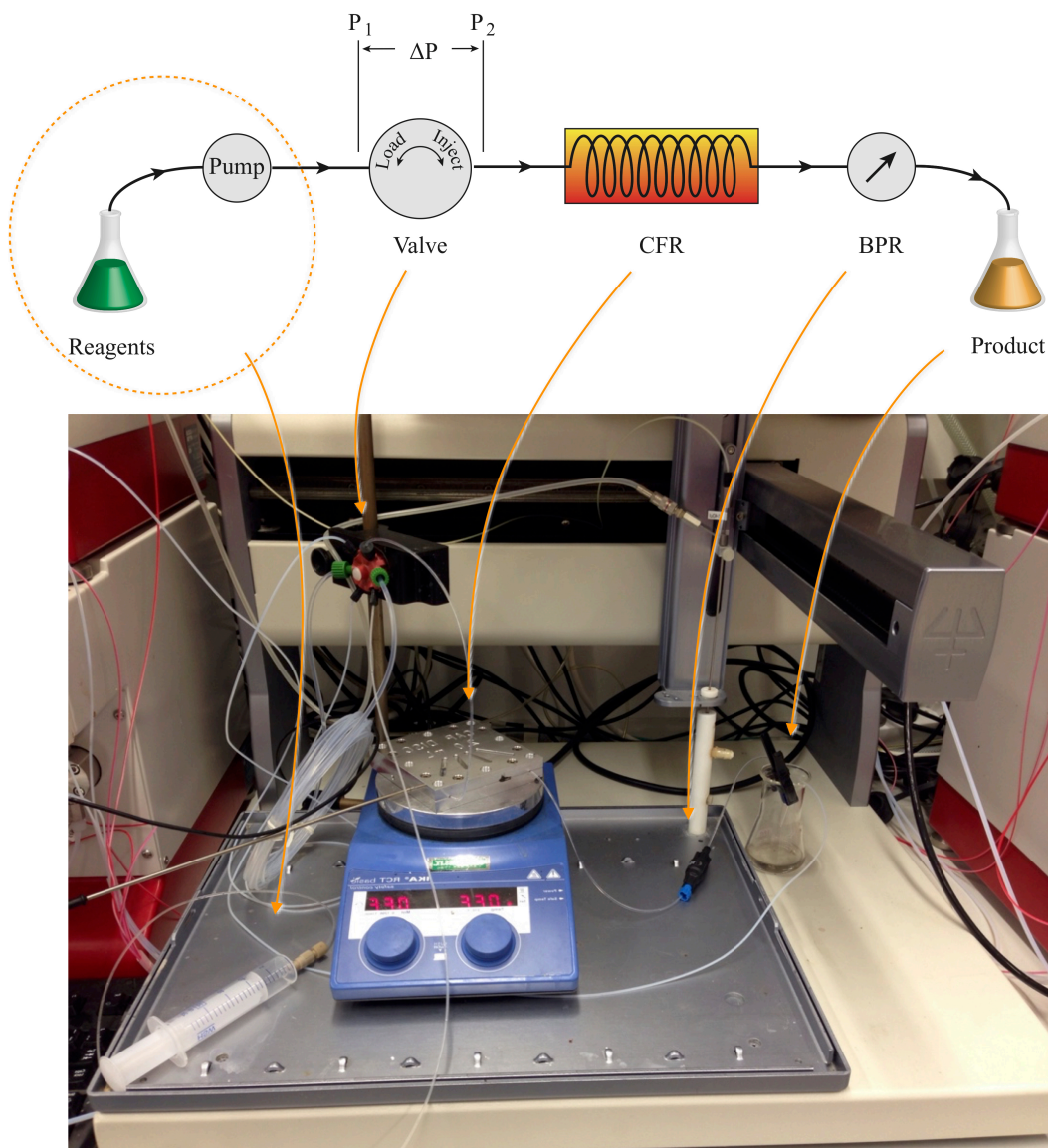


Figure 24: Flow set-up.

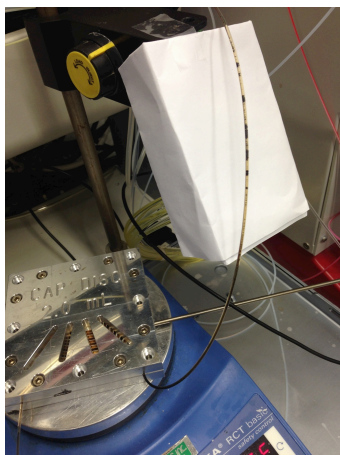
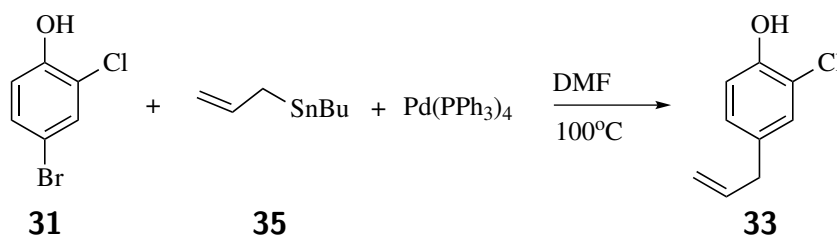


Figure 25: Pd black.

Since we encountered the problem with the pressure release we tried to find other alternatives. We tried to synthesize the desired compound using a Stille protocol [110] (Scheme 5).



*a:* Reaction conditions: 1 eq. of **31**, 1.05 eq. of **35**, 9 mol% Pd(PPh<sub>3</sub>)<sub>4</sub>, R.T.=45min, T=100°C.

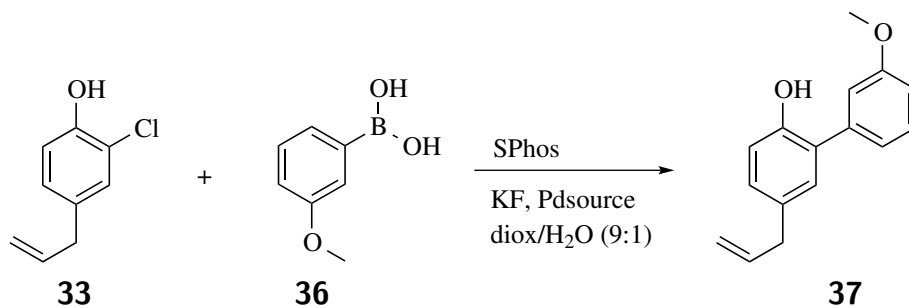
Scheme 5: Stille protocol in flow.

The reaction mixture was homogeneous so we directly tried the protocol in flow. The GCMS analysis showed many peaks of unidentified molecular weight in addition to a small area of product **33** in comparison to the area of the substrate **31**. Since the residence time (45min) was already long for a flow process and the reaction did not show significant progress, we decided to not further investigate this protocol.

In parallel to the translation of the batch process of the first step, in flow, we proceeded to the optimization of the second reaction step (Scheme 4) towards the flow synthesis of 5-allyl-3'-methoxy-[1,1'-biphenyl]-2-ol which was found to modulate recombinantly ex-

pressed  $\alpha 1\beta 2\gamma 2$  GABA<sub>A</sub> receptor from rat (% I<sub>GABA</sub> at 3 $\mu$ M was 136 $\pm$ 32 and it was determined in *Xenopus laevis oocytes*) [102] (Table 9).

Table 9: Screening with (3-methoxyphenyl)boronic acid.



Entry <sup>a</sup>	Pd source	Solubility	<b>37</b> [%] <sup>d</sup>
1 <sup>b</sup>	Pd <sub>2</sub> dba <sub>3</sub>	hom.	93
2 <sup>b</sup>	Pd(dppf)Cl <sub>2</sub>	hom. at r.t. & het. upon heating	76
3 <sup>c</sup>	Pd <sub>2</sub> dba <sub>3</sub>	hom.	n.c.

*a*: Reaction conditions: 1 eq. of **33**, 1.5 eq. of **36**, 2.5 eq. KF, 13.7 mol% SPhos, 6.7 mol% catalyst, T=150°C. *b*: t= 10 min, heating mode: MW. *c*: R.T.= 10 min, heating mode: flow. *d*: Conversion as determined by GCMS using dodecane as internal standard.

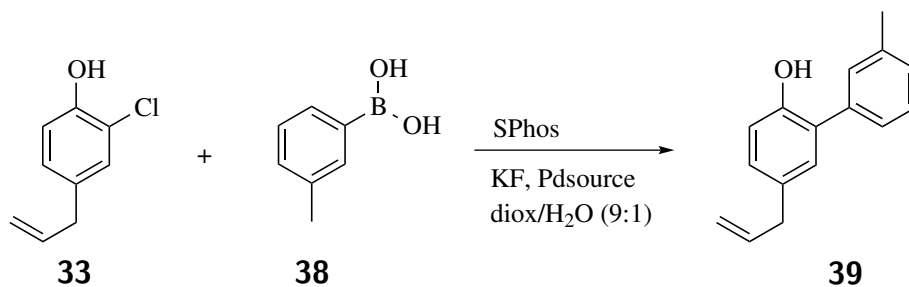
Running the reaction under microwave conditions using Pd<sub>2</sub>dba<sub>3</sub> as our Pd source, we obtained a conversion of 93% (Table 9, Entry 1) whereas when we ran the same reaction substituting the Pd<sub>2</sub>dba<sub>3</sub> to Pd(dppf)Cl<sub>2</sub> we got 76% conversion to the desired product, but precipitation occurred upon heating (Table 9, Entry 2). Since the reaction mixture in Entry 1 (Table 9) was homogeneous during and after the reaction, we decided to run it in flow. For this purpose we used a 500 $\mu$ l cap disk connected to the AFRICA system (Table 9, Entry 3). Unfortunately in the flow experiment we received 0% conversion.

Nevertheless we decided to apply the same conditions in the coupling of **33** with (3-methylphenyl)boronic acid **38** since the latter is also a weakly electron donating boronic acid but sterically less demanding and observe how it will perform.

In all of the entries of Table 10 we observed two products, the desired one **39** and its



Table 10: Screening with (3-methylphenyl)boronic acid in microwave.



Entry <sup>a</sup>	Time (min)	Pd source	Solubility	Product [%] <sup>b</sup>
1	10	5 mol% Pd <sub>2</sub> dba <sub>3</sub>	hom.	53 of two isomers ( <b>39</b> :46% & <b>40</b> :7%)
2	10	5 mol% of Pd/C (10% w/w)	het.	46 of two isomers ( <b>39</b> :45% & <b>40</b> :1%)
3	10	7 mol% of Pd/C (10% w/w)	het.	54 of two isomers ( <b>39</b> :50% & <b>40</b> :4%)
4	10	10 mol% of Pd/C (10% w/w)	het.	54 of two isomers ( <b>39</b> :47% & <b>40</b> :6%)
5	20	5 mol% of Pd/C (10% w/w)	het.	53 of two isomers ( <b>39</b> :46% & <b>40</b> :7%)

*a*: Reaction conditions: 1 eq. of **33**, 1.5 eq. of **38**, 2.5 eq. KF, 13.7 mol% SPhos, 6.7 mol% catalyst, T=150°C. *b*: Conversion as determined by GCMS using dodecane as internal standard.

isomer **40**. All of the reaction mixtures were heterogeneous apart from Entry 1 (Table 10) and in none of them the conversion was satisfactory.

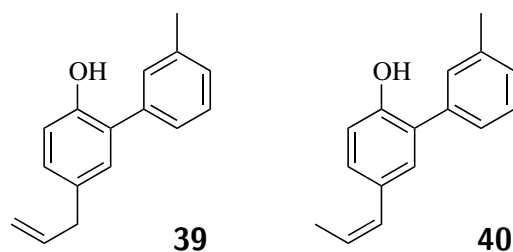


Figure 26: Magnolol/Honokiol isomers.

#### 2.1.4 Summary/Conclusions

As discussed in Chapter 1.3.1, heterogeneous catalysts feature many advantages, but with a common drawback of being susceptible to leaching, which leads to fast loss of catalyst activity. In the case of Magnolol/Honokiol intermediate (Chapter 2.1.3) optimization efforts, we encountered this issue using either PdEnCat30 or Pd/C. Albeit our efforts to circumvent the problem adopting different strategies, we eventually had to switch to a soluble catalyst in order to proceed with the screenings and synthesis. Unfortunately, this adjustment was accompanied also by major obstacles.

Upon a catalyst screening in batch, we identified two catalysts, which could potentially substitute the previously used heterogeneous ones. Pd(dppf)Cl<sub>2</sub> led to a moderately soluble reaction mixture and Pd<sub>2</sub>dba<sub>3</sub> (with SPhos instead of dppf) to a homogeneous solution. However, after heating we observed massive precipitation in both cases and in case of Pd<sub>2</sub>dba<sub>3</sub>, also the formation of the product's isomer. Upon collecting the precipitate we discovered that it was inorganic and corresponded to the base: K<sub>2</sub>CO<sub>3</sub>, which was crashing - precipitating out from the reaction mixture. Of course this protocol would be incompatible with a flow process, because it would immediately clog the system. Substituting K<sub>2</sub>CO<sub>3</sub> with NaOH led to the same result. Using an organic base, DBU resulted in homogeneous solution at r.t., but upon heating we observed substantial Pd black formation. Addition of PEG-400 to the latter solution, in order to prevent Pd black formation, did not improve the situation significantly and running it in flow led to blockage. Trying to access the intermediate compound **33**, we also tried to make the synthesis using a Stille protocol. This gave a homogeneous solution but when transferring

it in flow led to 0% conversion.

Since all previous attempts to synthesize in flow the Magnolol/Honokiol intermediate **33** were unsuccessful, we performed only a few experiments for the second reaction step leading to our target molecule **37** to see if the flow optimization is more promising in this case. Pd(dppf)Cl<sub>2</sub> and Pd<sub>2</sub>dba<sub>3</sub> resulted in homogeneous solutions in r.t. but in the case of Pd<sub>2</sub>dba<sub>3</sub> we observed precipitation upon heating. Therefore, we transferred only the procedure containing Pd(dppf)Cl<sub>2</sub> in flow and this gave 0% conversion.

Overall, the leaching of the heterogeneous catalysts, the precipitation of the base when homogeneous catalysts were used and the Pd black formation when an organic base substituted the inorganic one, constituted inevitable problems in order to translate the batch process into flow and unfortunately did not leave us any further room for improvement. However, regarding the batch process, Pd(OAc)<sub>2</sub>, Pd/C, Pd<sub>2</sub>dba<sub>3</sub> and Pd(dppf)Cl<sub>2</sub> were identified as good alternative catalysts to the initially used PdEnCat30 (Table 5, Entries 1, 3) & (Table 7, Entry 1), resulting to 90%, 90%, 92% and 100% conversion respectively.

## 2.2 Towards streamlining Neurodazine synthesis

### 2.2.1 State of art

Some of the most difficult diseases to treat are the so-called neurodegenerative diseases such as Parkinson's, Alzheimer's and Huntington's disease [111]. They are all occurring by the progressive tissue loss or dysfunction of neuronal cells, which leads gradually to a loss of the quality of life of the patient increasing dependence on other people. Especially nowadays that the life expectancy has increased it is assumed that there will be an increasing of number of individuals suffering from this type of disease and the need to find a curative treatment is more than ever required.

Embryonic stem cells (ECSc) [112] have provided researchers with a potential tool to treat such illnesses but there are ethical and practical issues associated with them making their usage problematic. The main issue, which arises in the first place, is if the quality of a patient's life who suffers, weighs more than the life of an unborn early embryo who will be sacrificed in order to be used as the source of stem cells. Consequently this decision has to be taken before any application of this approach and afterwards practical issues arise, as well. For example, the allogeneic transplants have high probability to be rejected by the receiver's organism so suppression of the patient's immune system has to take place. In addition, the self-renewing ability of the ECSc has to be controlled in order to prevent tumor formation in the recipient.

It becomes clear that the need for alternative strategies is still present and scientists started to focus on alternative routes such as synthetic small molecules (SSMs). SSMs have been found recently to be capable of changing the differentiation of pluripotent cells such as muscle or skin cells into neurons, which are carrying physiological properties. A schematic representation of this transformation is depicted in Figure 27 in which muscles cells from the patient himself are treated with SSMs to generate induced pluripotent stem cells (iPSCs), which in turn will be converted to physiologically functional neurons, and they can be implanted back to the patient. The advantage of this approach is that rejection of the transplanted tissue is avoided since the donor and the host is the same person.

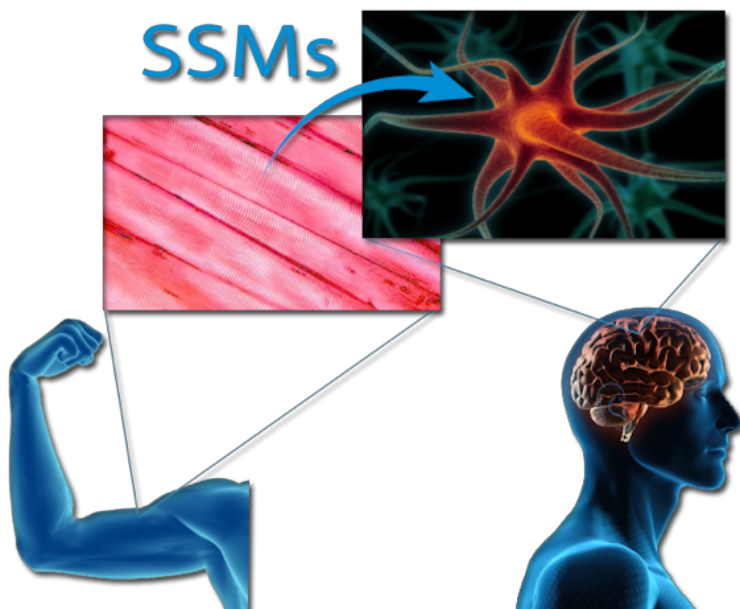
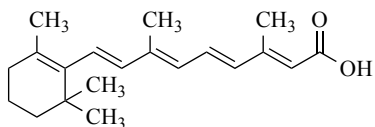


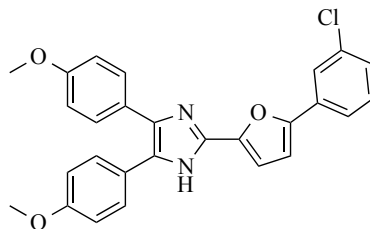
Figure 27: Inducing neuronal differentiation with synthetic small molecules.

A few SSMs that have been identified to show biological ability, up to date, are the following:

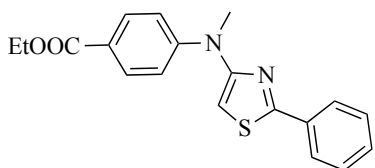
Retinoic acid [113]



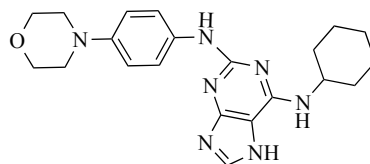
Neurodazine [114]



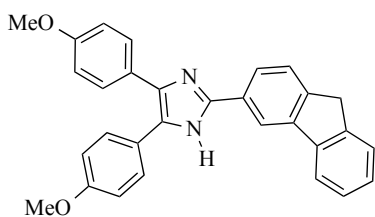
Neuropathiazol [115]



Reversine [116]



Neurodazole [111]



### 2.2.2 Objective

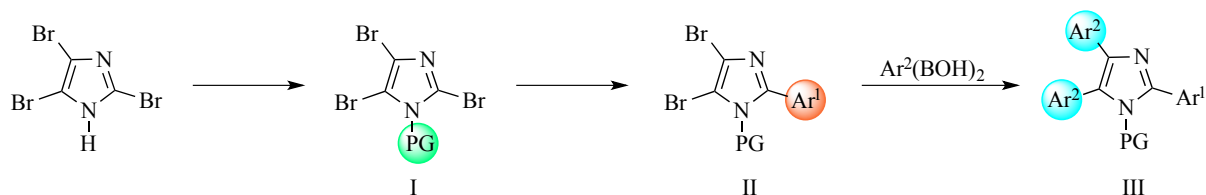
In initial studies, Neurodazine (Nz) has been found to partially convert C2C12 muscle cells derived from mouse [114]. In these studies neuronal marker proteins showed up-regulation but skeletal muscle specific markers were still present showing that the transformation was not complete. In 2014 another group presented Nz to promote P19 embryonic carcinoma cells [111] into functional neurons. They also synthesized Nz derivatives with structural variations and found that the neurogenesis ability of Nz and Neurodazole (Nzl) were in a comparable scale to the one of retinoic acid and they have shown better selectivity regarding their inducing ability than retinoic acid.

Within this section of the Thesis, our efforts were focused on developing an efficient synthetic route towards Neurodazine (Nz), employing C-H methodology and preferably in a continuous flow manner.

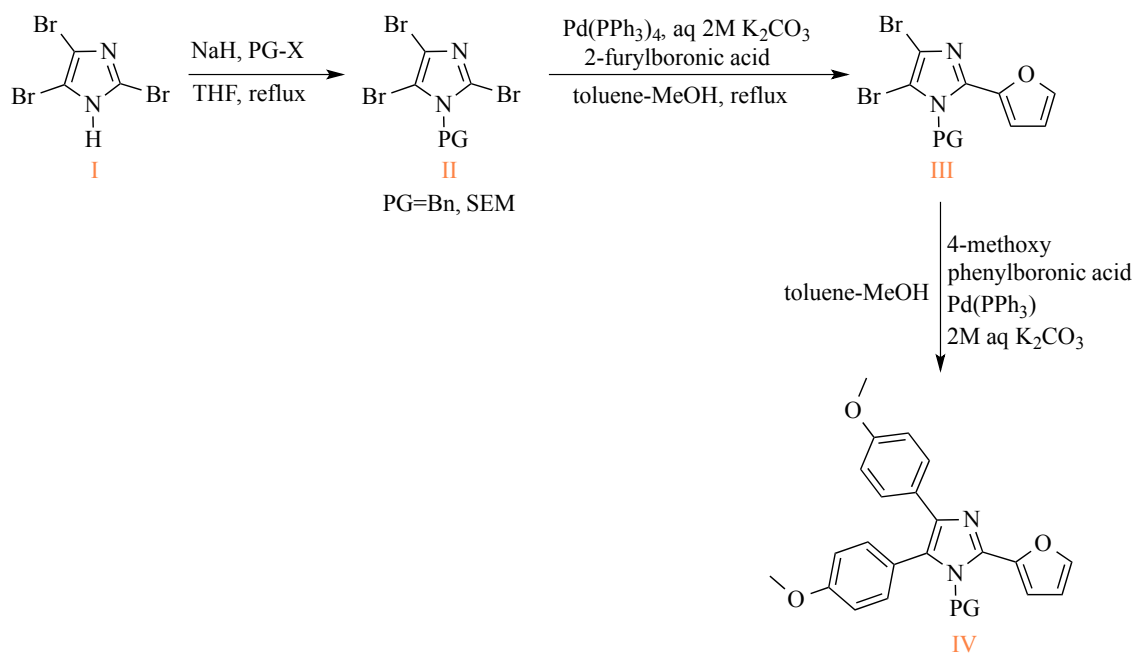
### 2.2.3 Synthetic strategy towards Neurodazine

As discussed thoroughly in the previous chapter, in order for an efficient flow process to take place the crucial reaction parameters have to be identified first in batch reactions and then they have to be transferred to flow conditions.

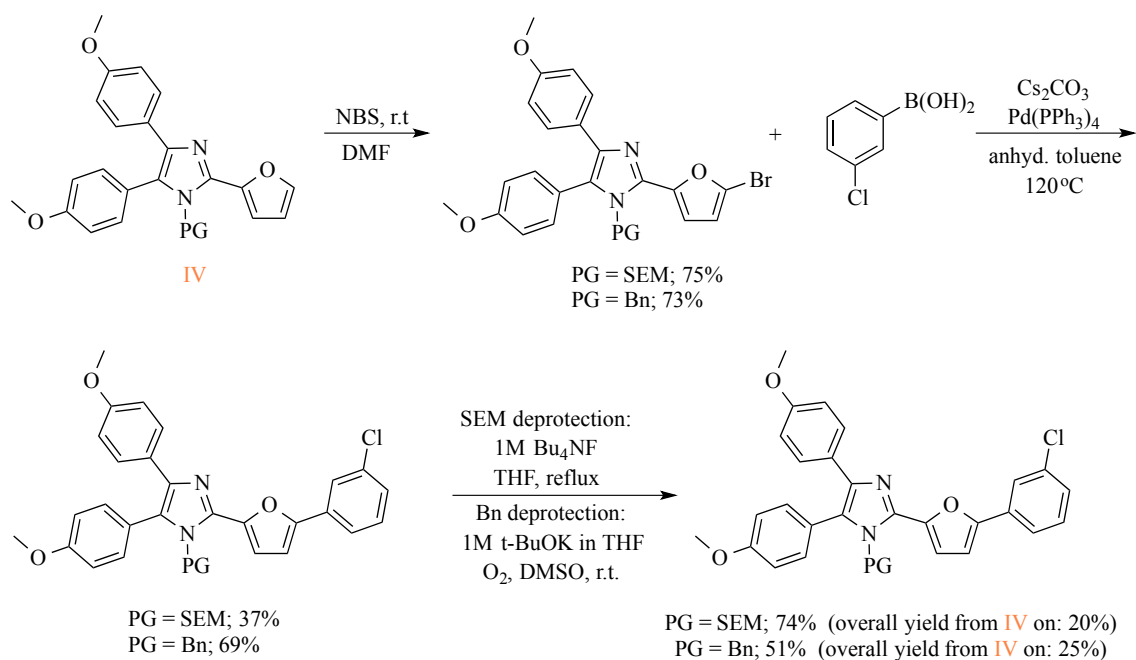
In our group a batch protocol for the synthesis of 2,4,5-triarylated imidazoles was already developed, which in turn was applied for the synthesis of Neurodazine [117]. It was based on sequential Suzuki-Miyaura cross-coupling reaction starting from the commercially available tribromoimidazole, which was protected at the N-position before coupling (Scheme 6). Several protecting groups were screened but finally the Bn and SEM protecting groups were chosen to proceed with, mainly due to their usually facile removal.



Scheme 6: 2,4,5-triarylated imidazole synthesis.



Scheme 7: Synthesis of protected Neurodazine precursor.



Scheme 8: Neurodazine synthesis.

This protocol led to the target compound through six reaction steps. It started with the commercially available tribromoimidazole (I), which after three steps formed the pro-

tected Neurodazine precursor IV (Scheme 7). The actual synthesis of the target compound required additionally three steps and it started from compound IV. Depending upon the protecting group which was in use, it resulted in 20% overall yield starting with the SEM protected precursor and 25% starting with the Bn protected precursor (Scheme 8).

Since this was a multistep synthesis which required stepwise addition of the reagents, control of homogeneity for each individual step, usually long reaction times and resulting in low overall yield, we decided that it was not suitable for a flow process. Our goal was to develop an alternative protocol for the synthesis of Neurodazine, which would ideally have less reaction steps than the previous, it leads to better overall yield and can be done in flow (homogeneity throughout the reaction zone).

The proposed retrosynthetic plan is shown in Figure 28.

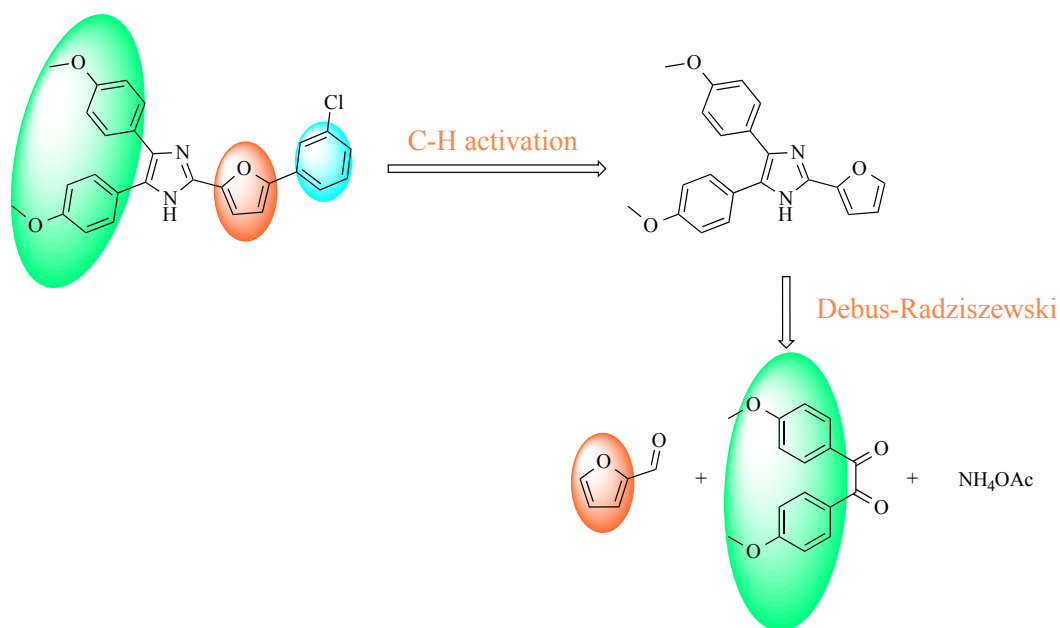
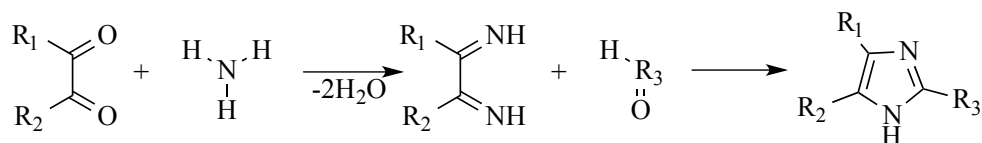


Figure 28: Retrosynthetic analysis.

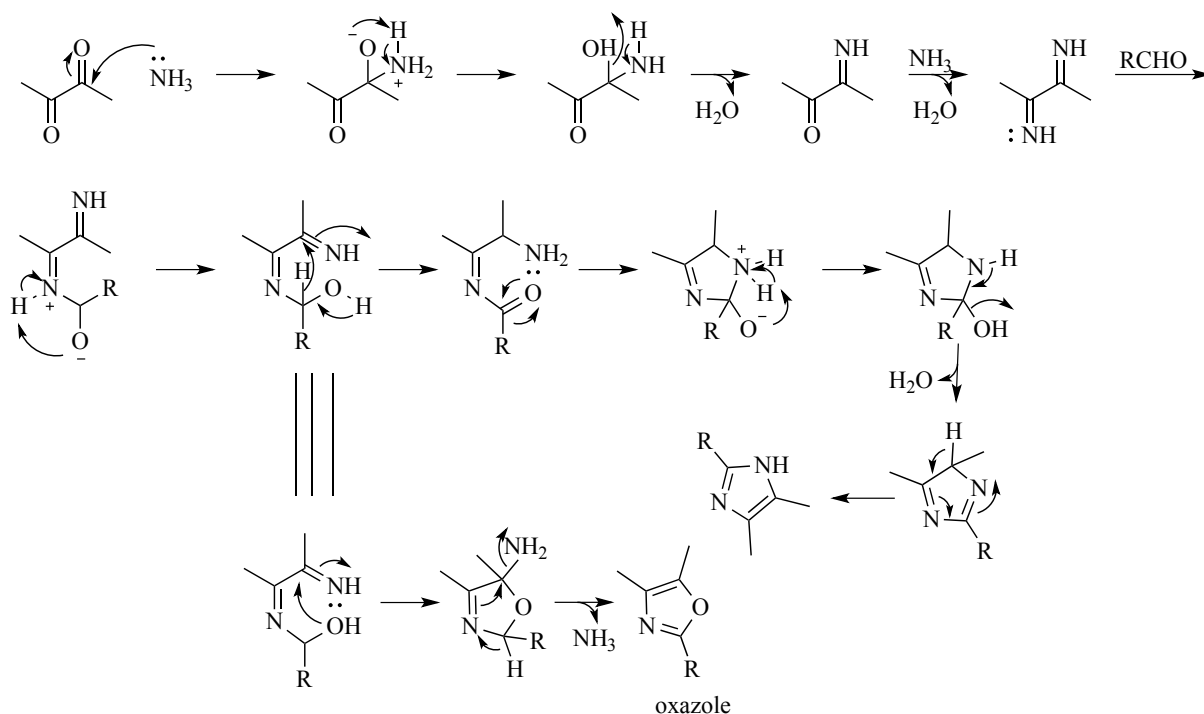
In the first step we envisioned a cyclization protocol taking place, as “Debus-Radziszewski”, used widely in industry for the preparation of imidazole derivatives (Scheme 9). This reaction proceeds through the condensation of a commercially available  $\alpha$ -dicarbonyl compound (e.g. benzil, glyoxal, pyruvaldehyde, porphyrin-2,3-diones) with an aldehyde



and ammonia [118]. A proposed mechanism is depicted in Scheme 10. It initiates with the reaction of ammonia with the  $\alpha$ -dicarbonyl compound to yield an  $\alpha$ -diimine, which upon condensation with the aldehyde leads to the imidazole with a substituent at position 2. As a side-product of this reaction, oxazole formation might occur.



Scheme 9: Debus-Radziszewski reaction.



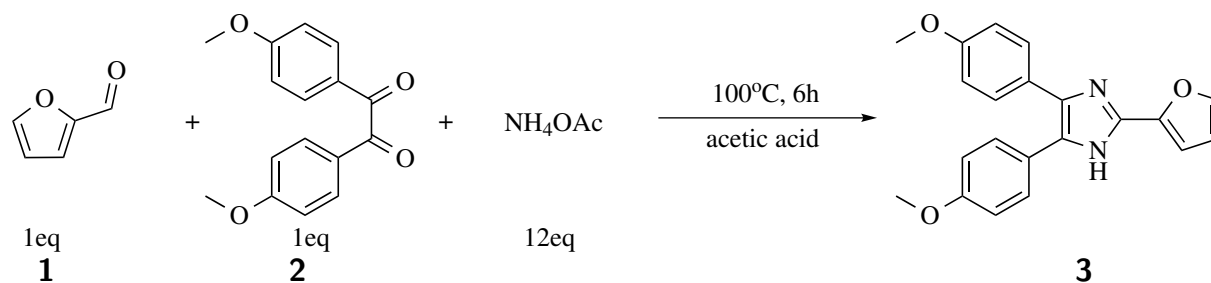
Scheme 10: Debus-Radziszewski mechanism [118].

Varying the aldehyde, diketone or both compounds, we could access different intermediates and hence different final products. Furthermore, in this way, imidazole a common building block for the synthesis of bioactive compounds [119] could be obtained. The final step of the synthesis should be an arylation step via C-H activation strategy, due to its

many advantages, which were discussed thoroughly in Chapter 1.2.3. This methodology would allow us to use many different substituted bromobenzenes (instead of 1-bromo-3-chlorobenzene), which could lead (along with the different structural variations of the first reaction step) to several Neurodazine derivatives bearing different modifications.

#### 2.2.4 Synthesis of Neurodazine / optimization of reaction conditions in batch

We started our optimization with the first step of the synthesis, the cyclization, having as goal to identify suitable conditions for a flow process. The originally published protocol using Debus-Radziszewski reaction to access Neurodazine [114] was under 100°C, using 1eq of furfural **1** (0.096M), 1eq of 1,2-bis(4-methoxyphenyl)ethane-1,2-dione **2**, 12eq of ammonium acetate in acetic acid and in a reaction time of 6h (Scheme 11) (**2**). In the first trial experiment, we found that both diketone and ammonium acetate were not completely soluble in the reaction mixture at room temperature and the reaction time was far too long for a useful flow protocol. We also confirmed the product formation by TLC-MS after 5<sup>1/2</sup>h of reaction time and after work-up and purification we ended up with a yield of 45% (in the literature the obtained yield was not provided).



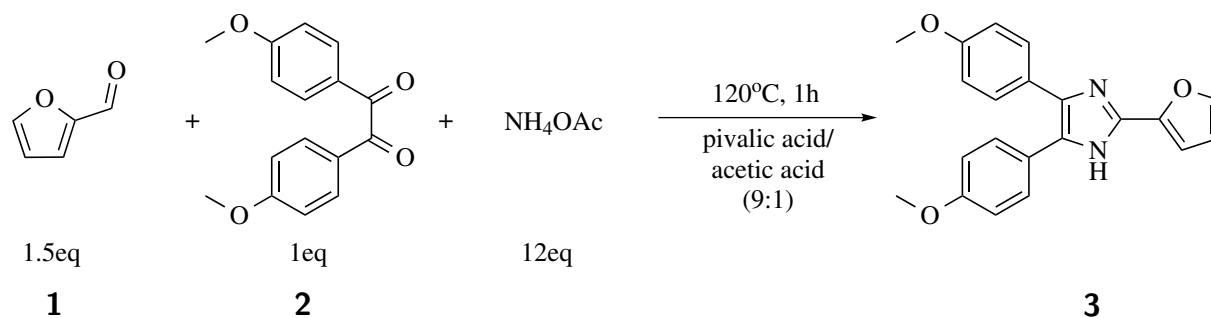
Scheme 11: Debus-Radziszewski.

Since our goal was to translate this process in flow, we initially tried to overcome the solubility issue and then to decrease the reaction time. To work with the first task we conducted some solubility tests at r.t. Adding to the reaction mixture water or methanol, led to emulsion formation and adding propanol or acetonitrile led to a mostly homogeneous solution since **2** was never fully soluble. In order to accelerate the reaction performance and consequently decrease the reaction time we tried two different polar solvents with

higher boiling point than acetic acid and in different amounts: NMP/acetic acid (1:1) and pivalic acid containing 10% acetic acid. Due to the fact that furfural is very volatile and at higher temperature would be more susceptible to evaporation, we increased its equivalents to 1.5eq and we used this amount exclusively in all screening experiments.

Running the reaction mixture in NMP/acetic acid at 120°C and in the literature's concentration of 0.096M, led after 5h to a new spot in TLC, but the NMR spectrum of the crude material did not show the desired product. Changing the solvent system to pivalic acid/acetic acid (9:1), we ran the reaction in the literature's reported concentration of 0.096M and in higher dilution to see if this can improve the dissolution of the reagents. For this reason we also used propanol and acetonitrile in selected experiments. Keeping the temperature at 120°C and reaction time of 1h we received the results presented in Table 11.

Table 11: Batch screening for Debus-Radziszewski.



Entry	C(M)	+ prop. <sup>a</sup>	+ acet. <sup>b</sup>	<b>3</b> [%] <sup>c</sup>
1	0.05	-	-	65
2	0.05	✓	-	42
3	0.05	-	✓	2
4	0.096	✓	-	23
5	0.096	-	-	22

*a*: Propanol. *b*: Acetonitrile. *c*: Relative ratio in HPLC.

The relative ratio in Entry 1 was the best observed in this screening series (Table 11). However, it was decreased when propanol was added (Table 11, Entry 2). In more con-

concentrated reaction mixtures the relative ratio was significantly lower and did not show a difference between the sample containing propanol and the other with no added propanol (Table 11, Entries 4,5). The experiment containing acetonitrile gave the poorest relative ratio among the rest of the experiments (Table 11, Entry 3).

However, we observed that upon stirring there was a good dispersion of the insoluble particles of the diketone and ammonium acetate and for this reason we decided to run in flow Entries 1,2 (Table 11) to observe if the ascertained heterogeneity will be deterrent for the process. We also lowered the concentration at 0.05M in order to facilitate a smoother pumping and it was kept constant for all the experiments of this series. The parameters that initially were of interest were time and temperature, in regards to their influence in the reaction performance.

For conducting the flow experiments, we used a flow system designed in our laboratory consisting of one (or potentially more) syringe pump(s) and an aluminum reactor (for a technical drawing see Appendix A).

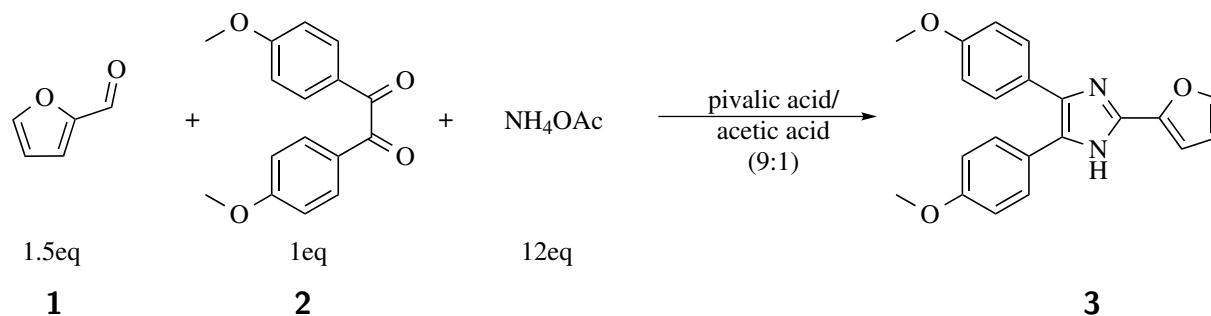


Figure 29: Flow experimental set-up.

The reactor is wrapped around with a coil, which can be of different materials such as steel or perfluoroalkoxy (PFA). In this case, a PFA capillary was used. The reactor is placed on top of a hot plate in order to adjust to the required temperature. The syringe pump is connected with the reactor through the coil as it is shown in the Figure 29.

The results of the flow screening are presented in Table 12.

Table 12: Flow screening for Debus-Radziszewski.



Entry <sup>a</sup>	T[°C]	R.T. (min)	3 [%] <sup>c</sup>
1	120	60	47
2 <sup>b</sup>	120	60	21
3	120	10	27
4	140	10	17
5	130	35	32
6	120	90	18
7	140	90	20
8	130	50	27

*a*: Selection of screening experiments was created by MODDE, C=0.05M. *b*: With added propanol until reaching the best dissolution of reagents. *c*: Relative ratio in HPLC.

Entries 1 and 2 (Table 12) showed much lower relative ratios than the corresponding batch experiments (Table 11, Entries 1, 2). In general all the experiments of this series did not result to satisfying relative ratios and some of them showed inconsistency. For example in Entry 7 after 90min (Table 12) the relative ratio was lower than after 60min and in a lower temperature (Table 12, Entry 1) and in Entry 8 (Table 12) after 50min the relative ratio was lower than at 35 min (Table 12, Entry 5) whereas at 140°C the relative ratio stayed in the same range in both 10 and 90min (Table 12, Entry 4, 7). Furthermore, in all above cases we did not have complete consumption of the substrate, since in a

certain time point the runs had to be interrupted due to massive build-up of undissolved particles in the needle, which led to pulsing of the pump. However, it has to be mentioned, that the reaction solution was homogeneous upon heating, and no blockage occurred in the 1mm PFA capillary. Due to the moderate solubility of the reaction mixtures, which has caused the arisen pre-mentioned issues we could not fully rely on those results.

After these experiments, it became clearer that the homogeneity issue was major and we have not found so far an effective way to overcome it. The solubility of the ammonium acetate was partially improving by the addition of propanol but the one of the diketone was not improving and also in cases that propanol was added in batch, the relative ratio was dropping (Table 12, Entry 2). We could probably replace the source of ammonia in the reaction mixture by replacing the ammonium acetate with gaseous ammonia, which we could bubble through during the reaction, but diketone could not be replaced from another reagent in this synthesis and consequently every flow experiment will fail.

For the pre-mentioned reasons we had to abandon the optimization of the particular reaction in flow and decided to optimize further the batch protocol in terms of time and concentration.

We decided to proceed with 0.075M, which was lower concentration than the literature's published (0.096M) [118] but at 140°C within 60min of reaction time we observed full consumption of the diketone, based on TLC. However in a preparative scale experiment we had great difficulty to work-up the crude mixture. We observed massive emulsion formation during extraction of the crude mixture. In order to neutralize the acid, we have used the extraction strategies, which are presented in the following, but in all cases we could not effectively remove the pivalic acid.

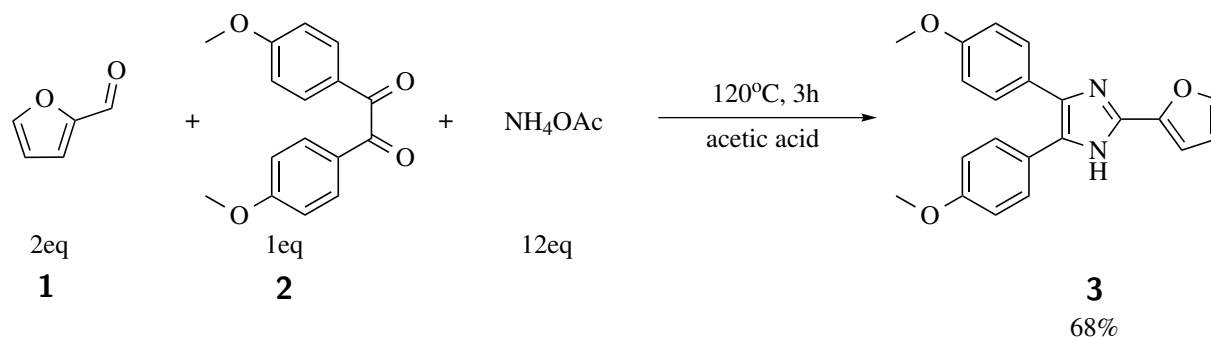
- We have used 2N NaOH with either EtOAc, ether or DCM and we observed massive emulsion which did not break by the addition of EtOH or by swirling with brine. Due to that “phenomenon”, the organic layer was not effectively separated from the aqueous layer and after repeating several times the extraction cycle and filtration through charcoal, substantial loss of material occurred.
- We have also used cold sat. NaHCO<sub>3</sub> with either EtOAc, ether or DCM which led to

slight improvement in terms of how intense was the emulsion appearance, but since this was a weaker base, after work-up we ended up with pivalic acid, which could not be removed fully, even after two times of Kugelrohr distillation. In another run with cold sat.  $\text{NaHCO}_3$  solution we tried to break the emulsion adding Rochelle salt but this did not help either. Likewise, ultrasonic irradiation did not improve the situation.

- Adding to the crude material, solid  $\text{NaHCO}_3$  with a small amount of water until basic and then adding ether and performing the extraction was also resulted in emulsion formation and remaining pivalic acid even upon multiple extraction runs and drying over pulverized  $\text{NaOH}$ .

Overall none of the work-up procedures were sufficient and consequently were resulting in loss of material.

Since for the batch process we were not in the need of a high boiling solvent or for the bulky pivalic acid, which was difficult to remove during the work-up and it was included in the procedure just to accelerate the flow process by enabling us to increase the reaction's temperature, we decided to switch to acetic acid under reflux conditions. Therefore the reaction temperature adjusted accordingly to  $120^\circ\text{C}$  and since furfural is very volatile we increased its equivalents to 2 (Scheme 12) and we performed a preparative scale experiment. The reaction was monitored by TLC and completed after 3h, resulting in 68% isolated yield.

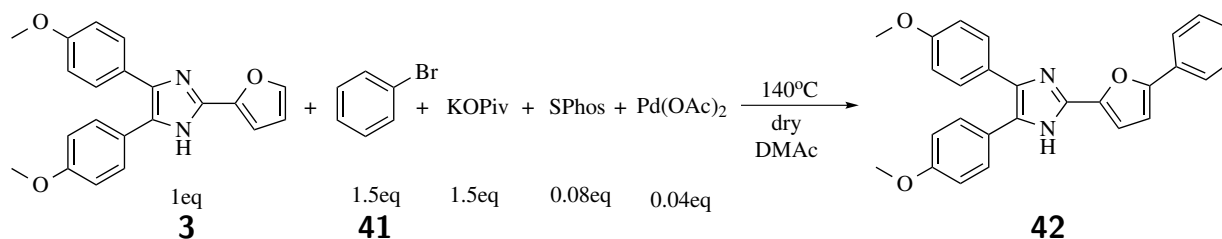


Scheme 12: Synthesis of 2-(furan-2-yl)-4,5-bis(4-methoxyphenyl)-1H-imidazole.

The second step which we wanted to optimize was the C-H activation step, leading to 2-

(5-(3-chlorophenyl)furan-2-yl)-4,5-bis(4-methoxyphenyl)-1*H*-imidazole **8** (Neurodazine).

In preliminary experiments, while we were optimizing the first reaction step, we tried whether a one pot protocol will be feasible in this case. For that, we subjected intermediate compound **3** to direct arylation without a previous work-up, using a protocol developed in our group for C-H activation in benzofuran [120]. This experiment was not at a concentration of 0.075M as it was in the first reaction step instead of the published procedure, which was ran at 0.5M scale. For screening purposes, we used bromobenzene **41** as the arylation partner, instead of 1-bromo-3-chlorobenzene **6**. The added reagents for the second reaction step are presented in Scheme 13.



Scheme 13: C-H activation in compound **3**.

After 24h of reaction time, TLC showed only starting material. Since this reaction was ran under much lower concentration, we wanted to see if this was the reason behind the 0% conversion or due to the one pot experiment, which does not include the intermediate work-up and purification.

Therefore, we repeated the experiment with the isolated compound **3** and using 0.5M concentration. Unfortunately, also this trial resulted in 0% conversion, after running overnight. Furthermore, the reaction solution was not homogeneous in r.t. and this factor would be also problematic for translating this procedure in flow.

In order to proceed with further screening experiments without consuming our actual substrate; we chose a model compound: 2-methylfuran-3-carboxylate **43** and we tried another procedure for C-H activation in furan rings (Table 13) [121]. The reaction mixture was not homogeneous also in this case. We did a temperature screening in microwave for a reaction time of 1h. We evaluated the results by GCMS, comparing the area of substrate, product, side-product in relation to this of dodecane (Table 13). The reaction



worked towards the desired direction with satisfying conversion to product and with minor formation of the transesterification side-product in all cases and with slightly better performance at 120°C.

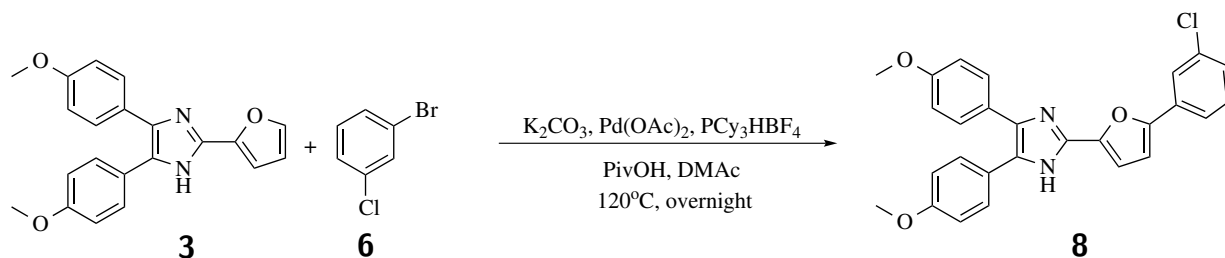
Table 13: Temperature screening.

Entry <sup>a</sup>	T[°C]	43 [%] <sup>b</sup>	Side-Product [%] <sup>b,c</sup>	44 [%] <sup>b</sup>
1	100	21	1	78
2	120	9	7	84
3	140	12	4	82

*a*: Reaction conditions: 1 eq. of **43**, 1 eq. of **41**, 4 mol% PCy<sub>3</sub>HBF<sub>4</sub>, 1.5 eq K<sub>2</sub>CO<sub>3</sub>, 30 mol% PivOH, 2 mol% Pd(OAc)<sub>2</sub>, C=0.3M, heating mode: microwave. *b*: Relative ratios in GCMS using dodecane as internal standard. *c*: Hypothesized structure of side-product based on its molecular weight.

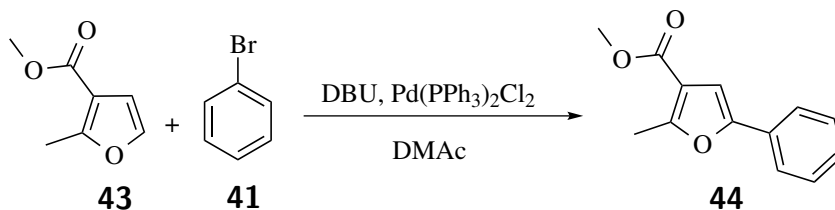
We then transferred these conditions (Table 13, Entry 2) to our actual substrate **3**, but received 0% conversion (Scheme 14) (verified by NMR analysis of the crude product). Repeating the same reaction in the heating block and stirring overnight also gave 0% conversion. Substituting the K<sub>2</sub>CO<sub>3</sub> with KOH, which is a much stronger base; and running the reaction overnight, resulted also in no conversion (verified by crude NMR).

Therefore we abandoned this protocol and after a literature search we tried another published procedure for C-H activation in furan [122]. That procedure used AcONa as base and a “Pd(II)” source as catalyst in DMAc at 150°C for 20h. Since AcONa was not soluble in DMAc, we decided to substitute it with DBU in order to have homoge-

Scheme 14: C-H activation in compound **3**.

neous conditions with the perspective of translating them into a flow system. We ran the reaction under microwave irradiation in 150°C and in 170°C, using our model compound: 2-methylfuran-3-carboxylate **43**. The evaluation of the conversion was done by comparison of the substrate **43**, product **44** and side-product area to dodecane area in GCMS.

Table 14: Temperature screening.



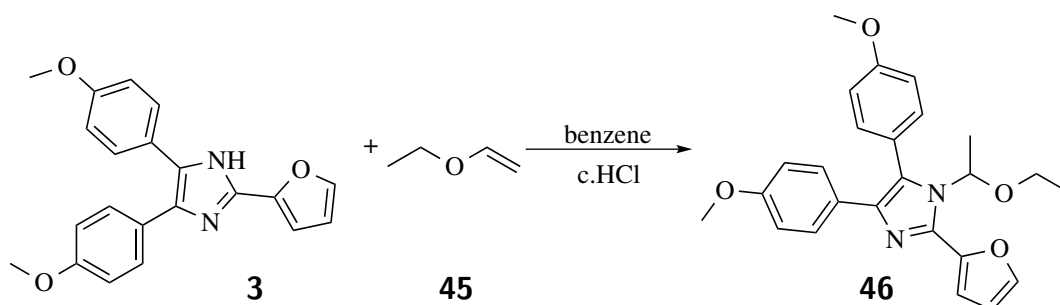
Entry <sup>a</sup>	T[°C]	<b>43</b> [%] <sup>b</sup>	Side-Product [%] <sup>b,c</sup>	<b>44</b> [%] <sup>b</sup>
1	150	93	3	4
2	170	48	7	45
3	190	45	45	10

*a*: Reaction conditions: 1 eq. of **43**, 2 eq. of **41**, 2 eq DBU, 0.01eq Pd(PPh<sub>3</sub>)<sub>2</sub>Cl<sub>2</sub>, C=0.3M, heating mode: microwave. *b*: Relative ratios in GCMS using dodecane as internal standard. *c*: Hypothesized structure of side-product based on its molecular weight.

The reaction mixture was homogeneous but the conversion in this screening (Table 14)

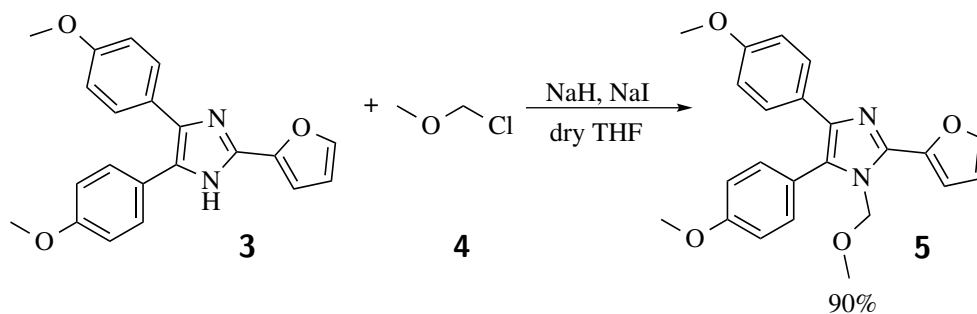
was much lower than in the previous (Table 13). Applying these conditions to our actual substrate **3** resulted to 0% conversion.

Since all previous attempts for C-H activation in our substrate **3** were unsuccessful, we perceived that the protection of the imidazole proton was necessary in order to proceed with the synthesis. After a literature search, we came across with a procedure of protecting azoles using ethyl vinyl ether **45** as the protecting agent [123] and we applied it to our substrate **3** (Scheme 15).



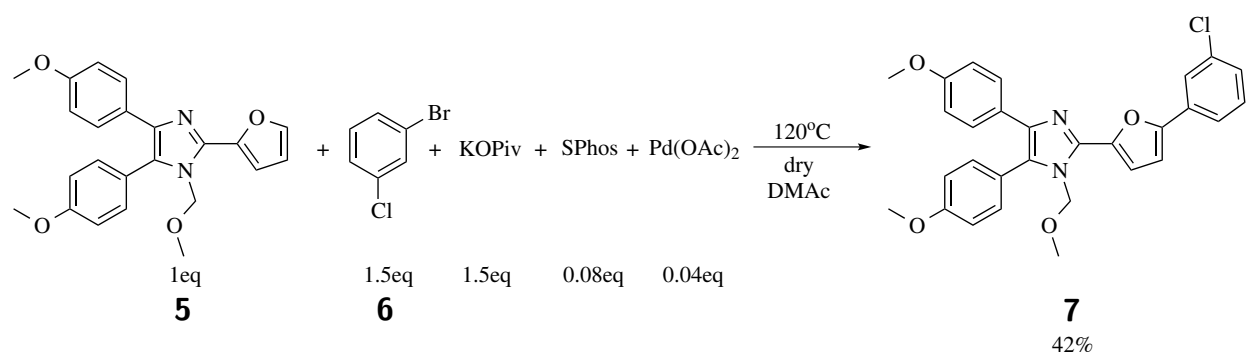
Scheme 15: Attempt to protect compound **3**.

According to NMR analysis of the crude product we had no conversion towards the protected compound **46**. We then turned to another common protecting agent for azoles: chloromethyl methyl ether **4**, abbreviated as MOMCl. We followed a literature published protocol [124] in our substrate (Scheme 16) using MOMCl instead of MOMBr, which resulted to a 59% yield and with the addition of 0.1 eq of NaI we were able to reach 90% yield of isolated product.



Scheme 16: Protection of compound **3**.

Having in hand the protected compound we proceeded again to the C-H activation step. Initially we tried the conditions, which were developed in our group for direct arylation in benzofuran and other benzo-fused heterocycles [120]. In a preparative run, we could obtain 37% isolated yield after running the reaction mixture overnight at 110°C, a slight better isolated yield of 42% after running the reaction mixture overnight at 120°C (Scheme 17) and 28% isolated yield after running the reaction mixture overnight at 140°C. Repeating the reaction which resulted to 42% in shorter reaction time of 6h, we observed no difference in terms of yield.



Scheme 17: C-H activation of compound **5**.

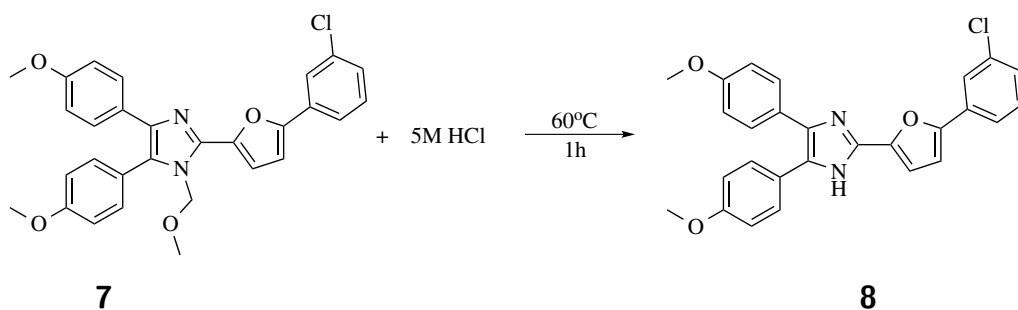
Subsequently, in an attempt to improve the yield we replaced the Pd source with Pd nanoparticles, which they have the advantage of increased surface area and they can potentially increase reaction rate [125]. In particular, we used 0.35% wt. Pd/SiO<sub>2</sub> instead of Pd(OAc)<sub>2</sub> and we repeated the reaction conditions (C=0.5M) showed in Scheme 17, once exactly as they were and once subtracting the SPhos. The reason behind the second experiment was the poor solubility of SPhos in DMAc which in combination with the existing SiO<sub>2</sub> was resulting to an overall bad reaction mixture solubility. Therefore we wanted to see whether SPhos could be omitted. In both cases the isolated yields were discouraging. We obtained 8.7% yield in the example with SPhos and 10.4% in the example without SPhos.

We assumed that activation of the nanoparticles would improve their overall performance and for this reason we tried to pre-activate them using Hydrogen. We repeated the reaction subtracting the SPhos to obtain better solubility. The final reaction con-

centrations in the two follow up experiments were: 0.075M and 0.14M. The activation of the nanoparticles did not facilitate the process either, resulting in 9.3% and 12.7% yield respectively.

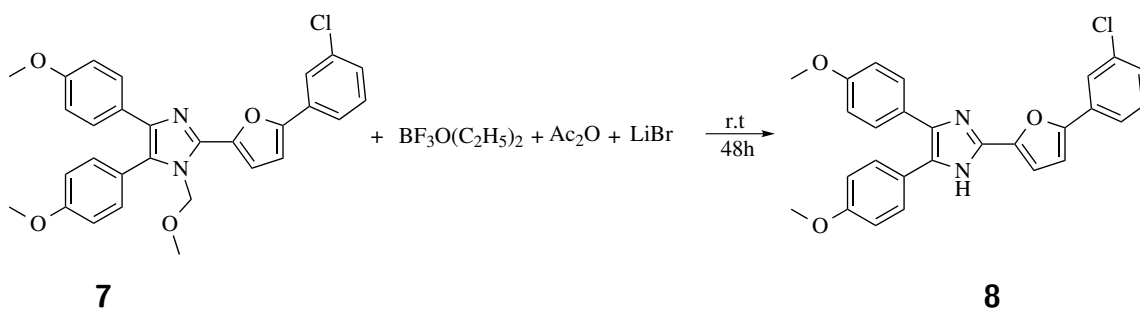
A presumable reason behind the poor yields in all previous cases could be the low amount of Pd in SiO<sub>2</sub> which could probably lead to an improvement if it will be increased. However in this stage we did not investigate this possibility further and we decided to continue with the conditions shown in Scheme 17 and used them for preparative scale experiments hereafter.

Eventually, we proceeded to the deprotection of compound **7**. For this purpose we initially used the conditions presented in the same literature reference where we found the MOM protection protocol [124] (Scheme 18), but we observed no conversion.



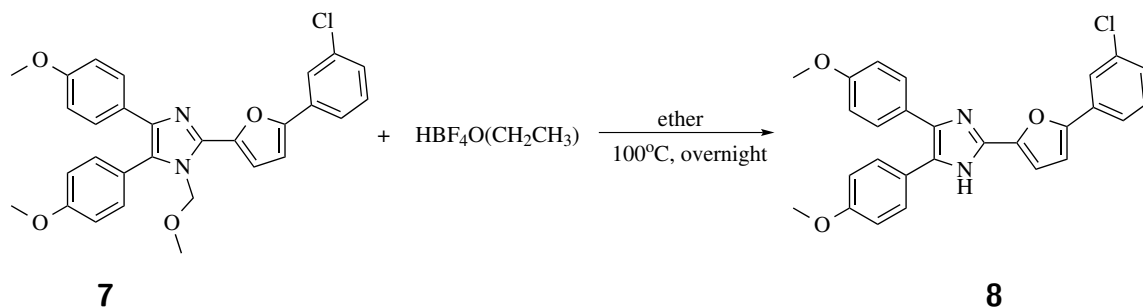
Scheme 18: Attempted deprotection of compound **7**.

Searching the literature for alternative deprotection protocols, we came across with another procedure and we applied it to our substrate [126] (Scheme 19), unfortunately without any change in the conversion.



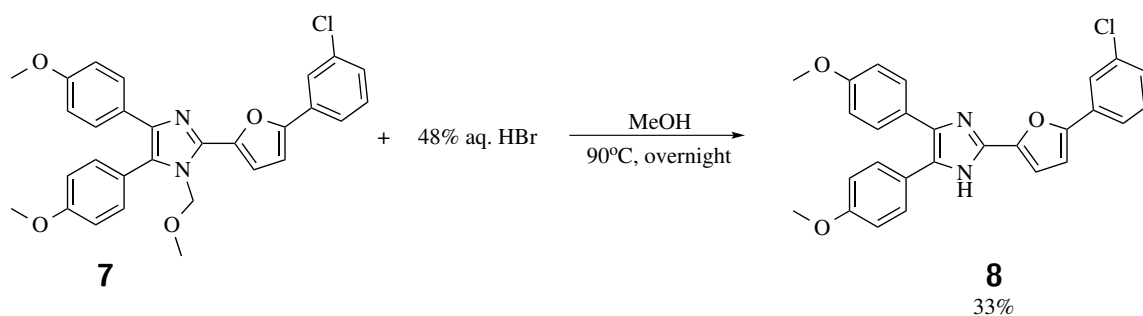
Scheme 19: Attempted deprotection of compound **7**.

We then replaced boron trifluoride diethyl etherate with tetrafluoroboric acid diethyl ether complex and ran the reaction in ether, increasing also the temperature to 100°C (Scheme 20). This attempt gave also 0% conversion.



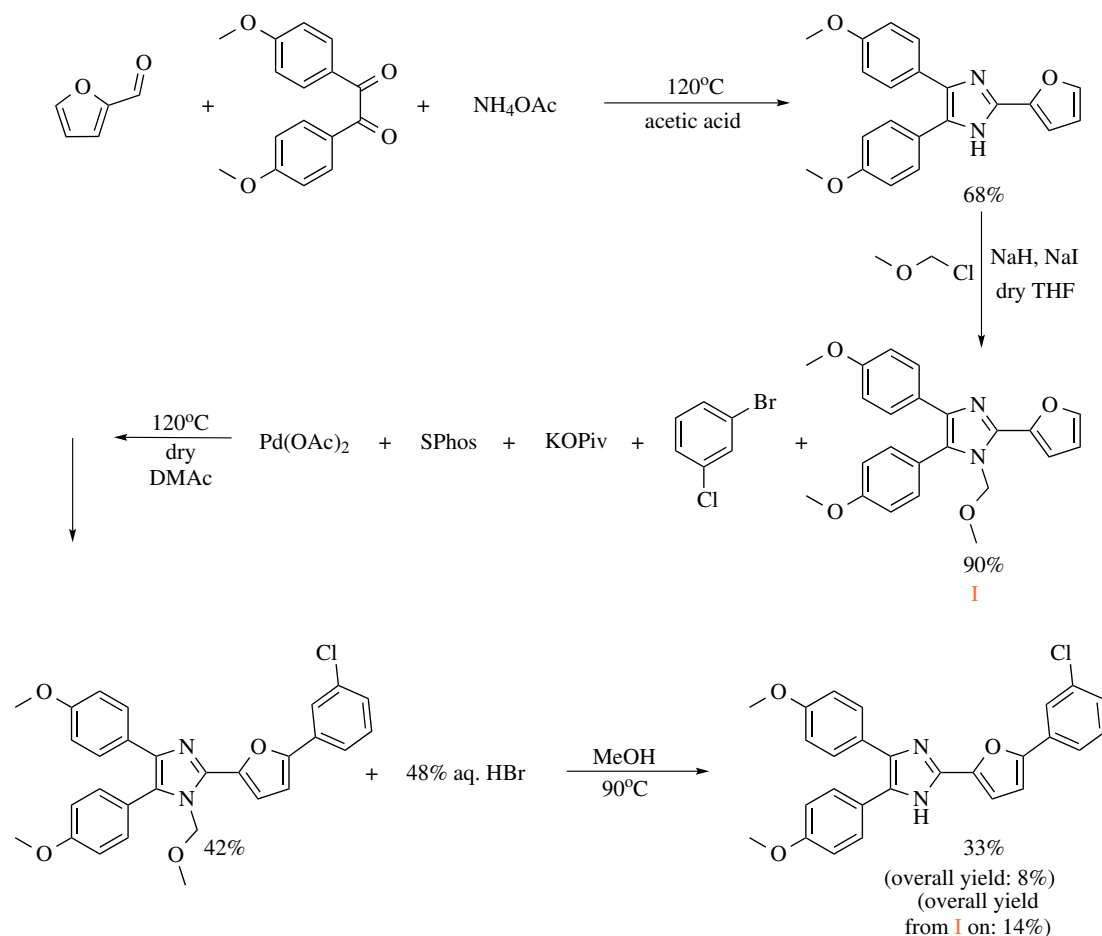
Scheme 20: Attempted deprotection of compound **7**.

We then tried to do the deprotection using HBr in MeOH and we initially ran the reaction overnight in r.t and then in 60°C. Both trials resulted to 0% conversion. However when we increased the temperature to 90°C, we could isolate the deprotected compound **8** in 33% yield.



Scheme 21: Deprotection of compound **7**.

Summarizing, our suggested reaction pathway to achieve our target molecule can be depicted in Scheme 22.



Scheme 22: Neurodazine synthesis.

### 2.2.5 Summary/Conclusions

In the synthesis of Neurodazine we came across homogeneity issues already from the cyclisation step due to the insolubility of the diketone **2** and NH<sub>4</sub>OAc. Furthermore, the batch protocol required ~6h of reaction time, which is far too long for a useful flow process. We tried to deal with these issues adjusting the reaction's concentration, adding a small amount of polar solvents and changing the solvent system and temperature, but unfortunately apart from a slight improvement of NH<sub>4</sub>OAc solubility, by the addition of propanol, the solubility of **2** did not improve. As a consequence, the conducted flow experiments which were done with the aid of a syringe pump, resulted in failure. In all cases we did not have complete consumption of the substrate, since in a certain time point the runs had to be interrupted due to massive built up of undissolved particles

in the syringe and consequently led to pulsing of the pump or complete blockage of the system.

Nevertheless, as a continuation of this project we decided to improve the batch protocol in terms of time and concentration. We identified the best combination using  $C = 0.075\text{M}$  and in reaction time of 3h at  $120^\circ\text{C}$  we obtained an isolated yield of 68% (literature protocol:  $C = 0.096\text{M}$ ,  $100^\circ\text{C}$ , 6h, yield was not provided).

For the C-H activation step of the synthesis, we tried several literature conditions but again we came across with solubility issues (not only due to the catalyst in use, but also due to the base and ligand). Furthermore, all these procedures in batch preliminary experiments resulted to 0% conversion, when were applied to our substrate **3**, and for this reason an optimization to improve the homogeneity of the reaction mixture was pointless. Due to these unsuccessful attempts, we concluded that protection of the free imidazole proton was necessary. Protection using MOMCl led to the protected compound **5** with 90% yield.

We then proceeded with the C-H activation step of the **5** and using a protocol developed in our group, we received in the best case a 42% yield after 6h of reaction time. The deprotection step of the synthesis was the follow up step and in our surprise was one of the more challenging. We tested several different conditions but the MOM group showed great resistance in getting cleaved. Finally the cleavage of the protecting group became possible using HBr in MeOH and stirring overnight at  $90^\circ\text{C}$  we obtained a yield of 33% for the isolated product.

Altogether, the previous existing protocol in our group (Scheme 7, Scheme 8) leading to Neurodazine, required only for the synthesis of the Neurodazine precursor (IV, Scheme 7) three steps and then additionally three steps to complete the synthesis (Scheme 8). In the newly developed protocol (Scheme 22) C-H activation methodology was employed, which gives the advantage of using many different substituted bromobenzenes (instead of 1-bromo-3-chlorobenzene) and could lead in a more facile way (along with the different structural variations which could be applied to the first reaction step) to several Neurodazine derivatives bearing different modifications. Furthermore the reaction pathway in this case is shorter by two reaction steps and it omits the need for bromination in



order for the arylation step to take place, with the overall yield being in the same range (Scheme 22) as was with the previous protocol (Scheme 8).

## 2.3 Arylation of Pyridines via Suzuki-Miyaura Cross-Coupling and Pyridine-Directed C-H Activation Using a Continuous-Flow Approach

### 2.3.1 Objective

Within this section, our efforts were focused on synthesizing several arylated pyridines and further decorating these products via C-H activation chemistry taking advantage of an in-house developed continuous-flow reactor system.

### 2.3.2 Synthesis of 2- and 3-phenylpyridines via Suzuki-Miyaura Cross-Coupling

The objective of this part of the thesis was the synthesis of phenylpyridine derivatives using the Suzuki-Miyaura cross-coupling reaction applying a continuous flow process. As it was discussed in section 1.2.2, Suzuki-Miyaura cross coupling is a process of great significance due to the fact that it provides the researcher with a facile and efficient tool to achieve arylated heterocycles. The latter are considered as a very important class of compounds due to their presence in molecules with interesting biological activities or interesting properties in material science [51–56].

### 2.3.3 Pyridine properties and reactivity

Pyridine is a  $6\pi$ -hetero-aromatic compound, which consists of five C-H bonds and one N atom. Its similar structure with benzene, correlates the two molecules to some extent, especially concerning molecular geometry and spectroscopic properties. The bond angles in pyridine differ slightly to the ones of benzene and also pyridine is a distorted hexagon compared to the benzene [127]. Figure 30 shows a comparison of the bond angles in both molecules.

Furthermore, since nitrogen presents an anisotropic effect, ring positions have different  $\pi$ -electron densities. In the canonical structures of pyridine (Figure 31), it is depicted the electron richer nitrogen in comparison to the 2, 4 and 6 carbon atoms which show less electron density. Due to these electronic properties, pyridine can undergo thermal

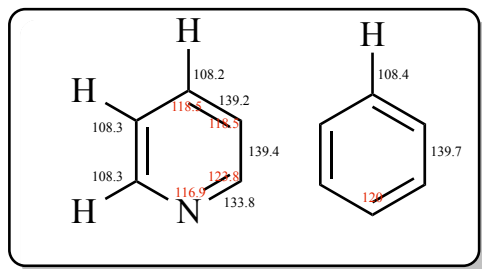


Figure 30: Bond angles in pyridine and benzene (bond angles in degrees).

and photochemical valence isomerization with a similar performance to benzene, nucleophilic substitution (in positions  $\alpha$ -C and  $\gamma$ -C) in an easier “fashion” than benzene and electrophilic substitution (in nitrogen and in  $\beta$ -C) with more difficulty than benzene.

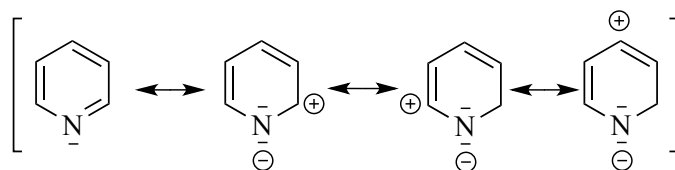


Figure 31: Canonical structures of pyridine.

### 2.3.4 Optimization of reaction conditions

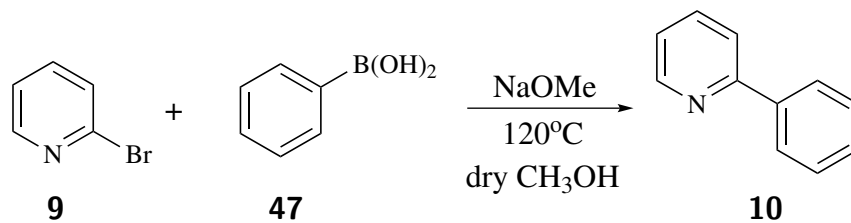
Since pyridine is a common substrate for cross-coupling reactions, we chose 2-bromopyridine **9** for investigating and optimizing the reaction conditions for the Suzuki-Miyaura coupling with phenylboronic acid **47**. After identifying these conditions, we intended to proceed with further Suzuki-Miyaura coupling reactions using other boronic acids and couple them with 2-bromopyridine **9** and 3-bromopyridine **16**. Since the reactions should be carried out in continuous flow ultimately, in this case also had to be assured that the reaction solution is homogeneous at all times at room temperature. The homogeneity factor is crucial because the formation of precipitant during the reaction zone could lead to clogging and it is also important before and after the heated reaction zone where the tubing is at room temperature and can again lead to clogging if the reaction solution is heterogeneous. For this reason, the optimization efforts were directed not only towards

time, yield and atom efficiency but also towards totally soluble reagents in the reaction mixture.

Hence, we conducted several batch experiments, which in majority took place under microwave irradiation, using different catalysts, bases and solvents in order to identify conditions enabling a transfer of the procedure to continuous flow without clogging the system. The results are summarized in the following tables (Table 15, Table 16, Table 17, Table 18, Table 19).

In the initial series of experiments we used encapsulated palladium catalysts exclusively since such heterogeneous catalysts could be packed in a cartridge eventually.

Table 15: Pd(OAc)<sub>2</sub> screening for the Suzuki-Miyaura coupling.



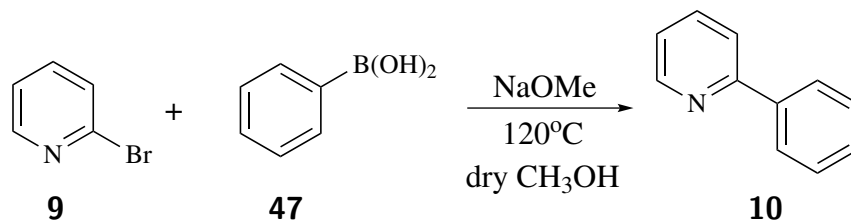
Entry <sup>a</sup>	t	Heating mode	Pd(OAc) <sub>2</sub> EnCat loading (mol%)	Conv. <b>9</b> [%] <sup>b</sup>
1	3h	reflux	1	98
2	24h	reflux	1	98
3	10min	MW	1	34
4	10min	MW	5	33

*a*: 1.2 eq. of **47**. *b*: As determined by GC using dodecane as internal standard.

The combination of NaOMe with Pd(OAc)<sub>2</sub>EnCat gave almost complete conversion under reflux conditions already after 3h of reaction time (Table 15, Entries 1, 2) but in the microwave these conditions did not perform equally well (Table 15, Entry 3), in less time though. Increasing the catalyst loading, had no effect on the conversion (Table 15, Entry 4).

Changing to Pd(PPh<sub>3</sub>)<sub>4</sub>EnCat, under reflux conditions (Table 16, Entry 1), did not lead to comparable good conversion as with the Pd(OAc)<sub>2</sub>EnCat (Table 15, Entries 1, 2) but increasing the equivalents of the base (threefold) lead to twofold increase in the conversion (Table 16, Entry 2). Transferring the latter conditions to microwave we were able to reach almost full conversion (Table 16, Entry 3). Increasing the catalyst loading to fivefold did not cause significant change to the GC conversion (Table 16, Entry 4).

Table 16: Pd(PPh<sub>3</sub>)<sub>4</sub> screening for the Suzuki-Miyaura coupling.



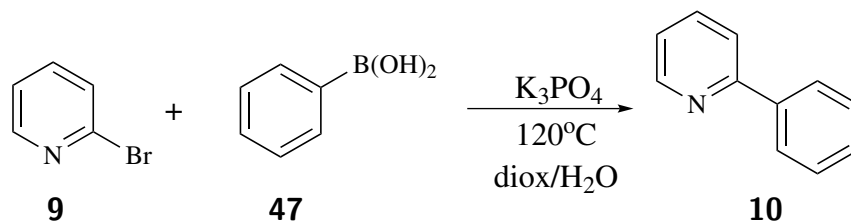
Entry	Eq. of 47	t	Heating mode	Pd(PPh <sub>3</sub> ) <sub>3</sub> EnCat loading (mol%)	Conv. 9 [%] <sup>a</sup>
1	1.2	24h	reflux	1	40
2	4.2	24h	reflux	1	77
3	1.2	10min	MW	1	94
4	1.2	10min	MW	5	98

*a*: As determined by GC using dodecane as internal standard.

Changing the solvent system to dioxane/H<sub>2</sub>O (1:1) and the base to K<sub>3</sub>PO<sub>4</sub>, we observed the best conversion (55%) under MW conditions at 180sec with Pd(OAc)<sub>2</sub>EnCat (Table 17, Entry 3). This was already a noteworthy improvement in comparison to the previous screening using the same catalyst in combination to NaOMe in dry CH<sub>3</sub>OH, since in that case after 10min of reaction time in MW, only 34% conversion was observed (Table 15, Entry 3). Furthermore, using Pd(PPh<sub>3</sub>)<sub>4</sub>EnCat instead of Pd(OAc)<sub>2</sub>EnCat had a significant influence in the reaction performance, since already from 135sec (Table 17, Entry 5) we observed 89% conversion which reached 91% at 270sec (Table 17, Entry 8). Comparing the screening with Pd(PPh<sub>3</sub>)<sub>4</sub>EnCat and K<sub>3</sub>PO<sub>4</sub> in dioxane/H<sub>2</sub>O (1:1)

(Table 17, Entries 5-8) to the screening with NaOMe, Pd(PPh<sub>3</sub>)<sub>4</sub>EnCat in dry CH<sub>3</sub>OH (Table 16, Entry 3), we received similarly good conversions, but in shorter reaction times. After these observations we continued the screenings with different bases exclusively in dioxane/H<sub>2</sub>O (1:1).

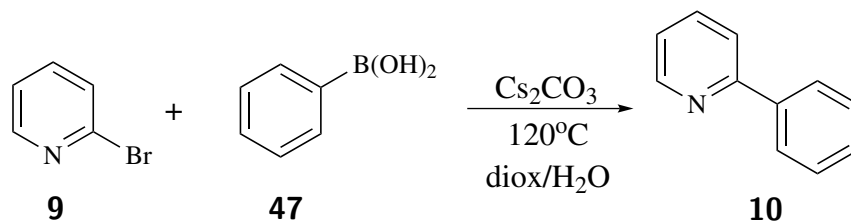
Table 17: K<sub>3</sub>PO<sub>4</sub> screening for the Suzuki-Miyaura coupling, in MW.



Entry <sup>a</sup>	t	EnCat catalyst (1 mol%)	Conv. <b>9</b> [%] <sup>b</sup>
1	90sec	Pd(OAc) <sub>2</sub>	47
2	135sec	Pd(OAc) <sub>2</sub>	48
3	180sec	Pd(OAc) <sub>2</sub>	55
4	90sec	Pd(PPh <sub>3</sub> ) <sub>4</sub>	40
5	135sec	Pd(PPh <sub>3</sub> ) <sub>4</sub>	89
6	180sec	Pd(PPh <sub>3</sub> ) <sub>4</sub>	88
7	225sec	Pd(PPh <sub>3</sub> ) <sub>4</sub>	90
8	270sec	Pd(PPh <sub>3</sub> ) <sub>4</sub>	91

*a*: 1.2 eq. of **47**. *b*: As determined by GC using dodecane as internal standard.

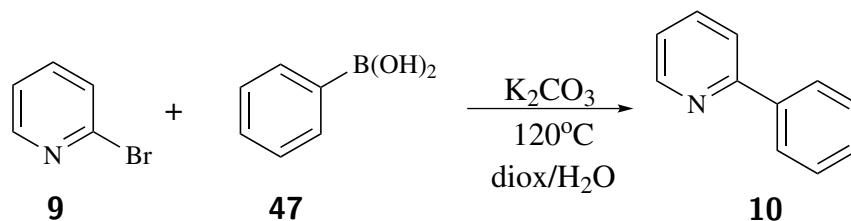
Using Cs<sub>2</sub>CO<sub>3</sub> in combination with Pd(OAc)<sub>2</sub>EnCat resulted in a 60% conversion after 135sec and it stayed constant till 180sec (Table 18, Entries 2,3). Substituting the catalyst with Pd(PPh<sub>3</sub>)<sub>4</sub>EnCat resulted in a 80% conversion already after 90sec (Table 18, Entry 4) and gave the best conversion at (Table 18, Entry 5).

Table 18: Cs<sub>2</sub>CO<sub>3</sub> screening for the Suzuki-Miyaura coupling, in MW.

Entry <sup>a</sup>	t	EnCat catalyst (1 mol%)	Conv. 9 [%] <sup>b</sup>
1	90sec	Pd(OAc) <sub>2</sub>	55
2	135sec	Pd(OAc) <sub>2</sub>	60
3	180sec	Pd(OAc) <sub>2</sub>	60
4	90sec	Pd(PPh <sub>3</sub> ) <sub>4</sub>	80
5	135sec	Pd(PPh <sub>3</sub> ) <sub>4</sub>	95
6	180sec	Pd(PPh <sub>3</sub> ) <sub>4</sub>	92
7	225sec	Pd(PPh <sub>3</sub> ) <sub>4</sub>	92
8	270sec	Pd(PPh <sub>3</sub> ) <sub>4</sub>	92

*a*: 1.2 eq. of **47**. *b*: As determined by GC using dodecane as internal standard.

Using K<sub>2</sub>CO<sub>3</sub> in combination with Pd(OAc)<sub>2</sub>EnCat resulted in a 59% conversion after 135sec (Table 19, Entry 2). Substituting the catalyst with Pd(PPh<sub>3</sub>)<sub>4</sub>EnCat resulted in a 95% conversion already at 180sec (Table 19, Entry 6). A significantly better performance of Pd(PPh<sub>3</sub>)<sub>4</sub>EnCat was observed also in this screening.

Table 19:  $K_2CO_3$  screening for the Suzuki-Miyaura coupling, in MW.

Entry <sup>a</sup>	t	EnCat catalyst (1 mol%)	Conv. 9 [%] <sup>b</sup>
1	90sec	Pd(OAc) <sub>2</sub>	55
2	135sec	Pd(OAc) <sub>2</sub>	59
3	180sec	Pd(OAc) <sub>2</sub>	48
4	90sec	Pd(PPh <sub>3</sub> ) <sub>4</sub>	87
5	135sec	Pd(PPh <sub>3</sub> ) <sub>4</sub>	85
6	180sec	Pd(PPh <sub>3</sub> ) <sub>4</sub>	95
7	225sec	Pd(PPh <sub>3</sub> ) <sub>4</sub>	95
8	270sec	Pd(PPh <sub>3</sub> ) <sub>4</sub>	95

*a*: 1.2 eq. of **47**. *b*: As determined by GC using dodecane as internal standard.

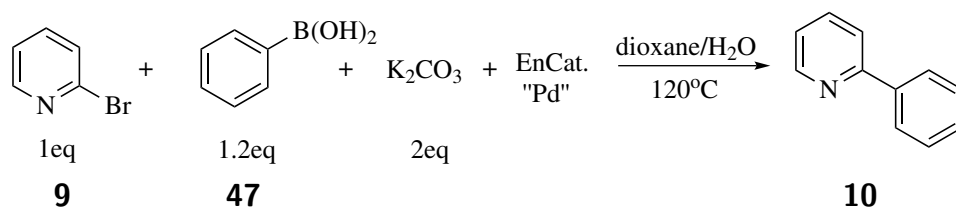
Overall, in the previous screenings with:  $K_3PO_4$ ,  $CS_2CO_3$  and  $K_2CO_3$ , the  $Pd(OAc)_2$  EnCat and  $Pd(PPh_3)_4$ EnCat, using dioxane/water, 1:1 as our solvent system, we observed much better performance with the  $Pd(PPh_3)_4$  (Table 17, Entries 4-6), (Table 18, Entries 4-6), (Table 19, Entries 4-6) in contrast to  $Pd(OAc)_2$ EnCat (Table 17, Entries 1-3), (Table 18, Entries 1-3), (Table 19, Entries 1-3) and almost complete conversion in Entry 5 (Table 18) and Entries 6-8 (Table 19). The different bases showed only negligible differences in conversion. In all cases (with the exception of Entry 4 (Table 16)) bipyridine and biphenyl were observed as side products. We observed the best relation between conversion, homogeneity, and reaction time using the conditions in Entry 6 of Table 19.

Transferring these conditions to a flow process required a second round of optimization in order to adjust the protocol to the respective flow system. Initially, it was tried to use



an immobilized palladium catalyst in a pre-packed cartridge in X-Cube (see Appendix A) repeating the most promising conditions of Entry 6 (Table 19) in flow (1eq of **9**, 1.2eq of **47**, 2eq of  $K_2CO_3$ ,  $C=0.05M$ , flow rate=  $0.5mL/min$ ,  $P=20bars$ ) but we observed substantially lower conversion in comparison to the microwave experiment. All screening experiments for transferring the microwave protocol to the X-Cube were unsuccessful regardless of the catalyst loading (0.35-1mol%) and the applied temperature (90-140°C).

For further investigation of the possible causes for the GC [%] conversion difference between microwave and X-Cube, the stability of the catalyst was investigated and it was found that significant leaching of the catalyst was taking place with concomitant lower conversion over time (Figure 32).



Cat. load.=1mol%,  $C=0.05M$ , f.r.= $0.5mL/min$ ,  $P=20bars$ ,  $T=120^\circ C$ .

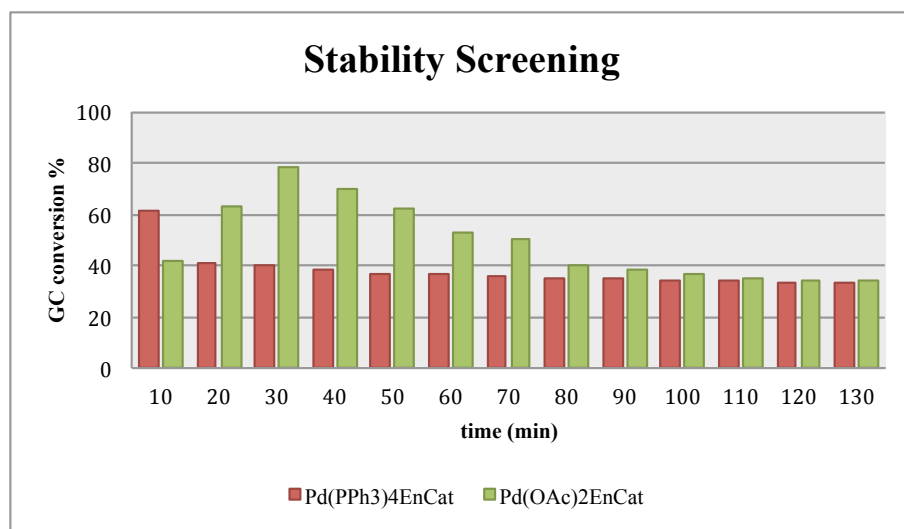


Figure 32: Stability screening for the immobilized catalysts (in X-Cube).

In the case of immobilized  $Pd(OAc)_2$ , an initial increase of the conversion was observed (till 30min, time point) which indicated the formation of more activated Pd species capable

to compensate for the leaching, but increasing time the catalyst amount decreased with an immediate reflection in the observed conversion. In case of  $\text{Pd}(\text{PPh}_3)_4$  the decrease of the conversion took place even faster, from 20min onwards.

Since the stability screening supported our concerns for Pd leaching, this approach was abandoned early on. Alternatively we used a flow system (Figure 33), which was used also for the screening experiments of Debus-Radziszewski reaction and its way of function was presented in chapter 2.2.4 of this Thesis. This system allows performing reactions with ease in flow when it is not required to pressurize a reaction mixture. Therefore the next screenings had to be performed at a lower temperature ( $90^\circ\text{C}$  instead of  $120^\circ\text{C}$  was used), in order to stay below the boiling point of the solvent mixture.



Figure 33: Flow experimental set-up.

Early on,  $\text{Pd}(\text{PPh}_3)_4$  was identified in microwave (Table 19, Entries 4-8) as the best performing catalyst and hence it was chosen for further optimization of the reaction conditions in flow (Table 20) under homogeneous conditions.

Table 20: Optimization in Flow.

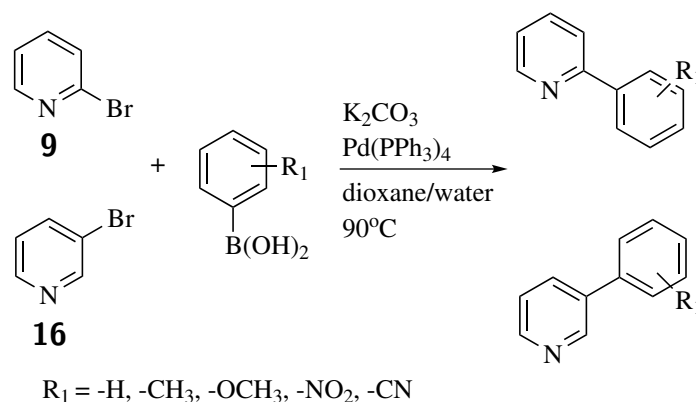
Entry <sup>a</sup>	Cat.load. (mol %)	Flow rate (mL/min)	R.T. (min)	9 [%] <sup>b</sup>
1	0.35	0.5	8	30
2	0.35	0.5	23	40
3	1.05	0.5	23	59
4	1.4	0.5	23	63
5	1.7	0.5	23	80
6	2.1	0.5	23	82

*a*: Reaction conditions: **9** (1 eq.), **47** (1.2 eq.), 2eq. K<sub>2</sub>CO<sub>3</sub>, Pd(PPh<sub>3</sub>)<sub>4</sub>, dioxane-H<sub>2</sub>O (1:1), 90°C, 0.05 M; steel coil. *b*: Conversion as determined by GC using dodecane as internal standard.

Starting with low catalyst loading (0.35 mol%) and a residence time of eight minutes gave only 30% conversion (Table 20, Entry 1). Extending the reaction time to 23 minutes gave only a minor improvement to 40% (Table 20, Entry 2). However, increasing the catalyst loading to an amount of 2.1% ultimately gave a satisfying conversion of 82% (Table 20, Entry 6). These conditions are a good compromise between catalyst loading and flow rate and, hence, subsequent substrate-scope investigations were performed using this protocol. It has to be mentioned that the process in flow takes significantly longer than the batch experiment. This can be attributed to a difference in temperature eventually: temperature measurement in microwave is usually very accurate. In the flow process we measure the temperature of our aluminum block but cannot measure the temperature inside the coil. Hence there could be a significant difference. Additionally, a higher temperature at the metal center in microwave cannot be excluded due to the better microwave absorbing capacity of the metal compared to the solvent.

Since the optimized conditions were identified, the next step was to couple 2-bromopyridine and 3-bromopyridine with various boronic acids bearing electron-donating or electron-withdrawing groups (Scheme 23). We were also interested to investigate if the material

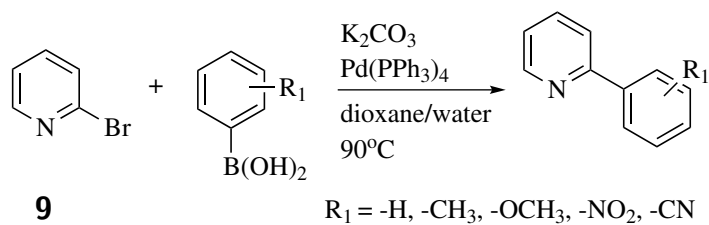
of the coil had any influence on reaction performance. Therefore we conducted experiments either using a steel coil or a PFA coil and in some cases both for comparison. The advantage of the PFA coil is the easier handling and the lower price (approx. 40% less) and easier to wash and unclog when it is necessary.



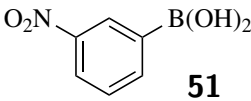
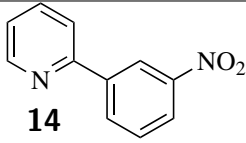
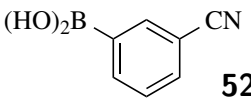
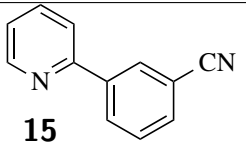
Scheme 23: Suzuki-Miyaura reaction with 2-bromopyridine and 3-bromopyridine with arylboronic acids in dioxane-H<sub>2</sub>O (1:1).

Entries 1-4 (Table 21) show the coupling reaction of **9** with phenylboronic acid (1.2 or 3.0 eq.) in both coil materials. It can be seen that when 1.2 eq. of boronic acid were used the results are comparable for both coil materials (Table 21, Entries 1, 3). However, when 3.0 eq. boronic acid were used the PFA coil performed significantly better (Table 21, Entries 2, 4).

Electron-donating substituents on the boronic acids gave generally better yields. This is also true for sterically hindered *o*-tolylboronic acid (**49**) where 91% yield were obtained in the PFA coil (Table 21, Entry 9). *p*-Methoxyphenylboronic acid (**50**) gave a good yield already in the steel coil (Table 21, Entries 10-11). 3-Nitrophenylboronic acid (**51**) gave a low yield of 12% in the steel coil using 1.2 equivalents of **51** (Table 21, Entry 12). Increasing this to 3.0 equivalents improved the yield to 51% (Table 21, Entry 13). A comparable yield was obtained in the PFA coil with 1.2 equivalents of **51** already (Table 21, Entry 14). 3-Cyanophenylboronic acid (**52**) gave an acceptable yield only in the PFA coil and 3.0 equivalents of **52** (Table 21, Entry 19).

Table 21: Table Suzuki Reaction with 2-Bromopyridine and Arylboronic acids in Dioxane-H<sub>2</sub>O (1:1) and 2.1 mol% Catalyst Loading.

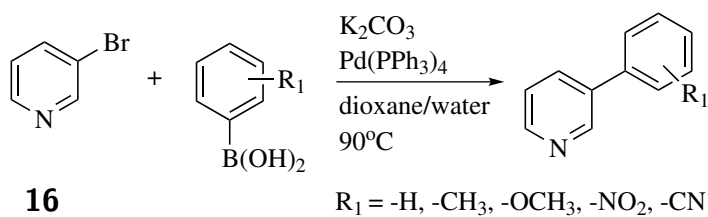
Entry <sup>a</sup>	Boronic acid	Eq. 2	Coil type	Product	Yield. [%] <sup>b</sup>
1	<b>47</b>	1.2	steel	<b>10</b>	64
2	<b>47</b>	3.0	steel	<b>10</b>	76
3	<b>47</b>	1.2	PFA	<b>10</b>	68
4	<b>47</b>	3.0	PFA	<b>10</b>	93
5	<b>48</b>	1.2	steel	<b>11</b>	60
6	<b>48</b>	3.0	steel	<b>11</b>	61
7	<b>49</b>	1.2	steel	<b>12</b>	62
8	<b>49</b>	3.0	steel	<b>12</b>	64
9	<b>49</b>	1.2	PFA	<b>12</b>	91
10	<b>50</b>	1.2	steel	<b>13</b>	85

11	<b>50</b>	3.0	steel	<b>13</b>	89
12	 <b>51</b>	1.2	steel	 <b>14</b>	12
13	<b>51</b>	3.0	steel	<b>14</b>	51
14	<b>51</b>	1.2	PFA	<b>14</b>	44
15	<b>51</b>	3.0	PFA	<b>14</b>	45
16	 <b>52</b>	1.2	steel	 <b>15</b>	4
17	<b>52</b>	3.0	steel	<b>15</b>	6
18	<b>52</b>	1.2	PFA	<b>15</b>	24
19	<b>52</b>	3.0	PFA	<b>15</b>	45

*a*: Reaction conditions: 1eq. of **9**, 1.2 or 3 eq. of aryl boronic acid, 2 eq.  $K_2CO_3$ , 2.1 mol%  $Pd(PPh_3)_4$ , dioxane- $H_2O$  (1:1),  $90^\circ C$ , 0.05 M. *b*: As determined by GC using dodecane as internal standard.

Using **16** as substrate in combination with **47** gave the best result (80% yield) using 3.0 equivalents of **47** and the PFA coil (Table 22, Entry 4). Hence, all subsequent coupling reactions on **16** were carried out under these conditions. Methyl substituents were best tolerated no matter whether in 2- or 4-position of the boronic acid (Table 22, Entries 5-6). 4-Methoxy-, 3-nitro-, and 3-cyanophenylboronic acids gave similar yields just below 60% (Table 22, Entries 7-9). Furthermore in all of the cases, which we have synthesized used 1.2 equivalents of the aryl source when we increased to 3 eq. a better yield of **17**, **18**, **19**, **20**, **21**, **22** was obtained.

Table 22: Suzuki Reaction with 3-Bromopyridine and Arylboronic acids in Dioxane-H<sub>2</sub>O (1:1) and 2.1 mol% Catalyst Loading.



Entry <sup>a</sup>	Boronic acid	Eq. 2	Coil type	Product	Yield. [%] <sup>b</sup>
1	<b>47</b>	1.2	steel	<b>17</b>	18
2	<b>47</b>	3.0	steel	<b>17</b>	53
3	<b>47</b>	1.2	PFA	<b>17</b>	64
4	<b>47</b>	3.0	PFA	<b>17</b>	80
5	<b>48</b>	3.0	PFA	<b>18</b>	87
6	<b>49</b>	3.0	PFA	<b>19</b>	75
7	<b>50</b>	3.0	PFA	<b>20</b>	58
8	<b>51</b>	3.0	PFA	<b>21</b>	58

9		<b>52</b>	3.0	PFA		<b>22</b>	56
---	---	-----------	-----	-----	--	-----------	----

*a*: Reaction conditions: 1eq. of **16**, 1.2 or 3 eq. of aryl boronic acid, 2 eq.  $K_2CO_3$ , 2.1 mol%  $Pd(PPh_3)_4$ , dioxane- $H_2O$  (1:1),  $90^\circ C$ , 0.05 M. *b*: As determined by GC using dodecane as internal standard.

The synthesis of 3-phenyl pyridines (Table 22, Entries 5, 6, 8, 9) led in general, to better yields in comparison to the 2-phenyl pyridines (Table 21, Entries 6, 8, 15, 19), which were synthesized using the same boronic acids, with the exception of (Table 21, Entries 4, 11 (2-phenylpyridine **10**) & (2-(4-methoxyphenyl)pyridine **13**), that had a better yield under similar conditions. However, it has to be mentioned that in case of Entries 5 & 6 (Table 22), the experiments took place in the PFA coil instead of steel coil which was used in case of Entries 6 & 8 (Table 21).

Comparing results using the steel and the PFA coil material it was found that PFA performed significantly better. The overall better performance of the PFA coil could be due to the fact that the metal coil might undergo metal-metal interactions with the metal center of our palladium catalyst resulting in decreased catalyst activity. However, for a detailed explanation more experiments would be necessary (e.g. analyzing the inner surface of the steel coil) which was beyond the scope of this work.

### 2.3.5 Arylation of 2-phenylpyridine via C-H activation in flow

Besides Suzuki-Miyaura coupling, we were also interested in direct arylation reactions under continuous flow. 2-Phenylpyridine **10** constitutes a common substrate for direct functionalization reactions where the pyridine nitrogen directs the catalyst in ortho-position of the adjacent phenyl ring [95,128–133]. Since we could efficiently synthesize this compound with our flow process, we decided to investigate its further application in C-H activation chemistry, also via a continuous-flow approach.



### 2.3.6 Optimization of reaction conditions

Prerequisites for direct arylation in flow are of course the same as for cross-coupling, most importantly homogeneity of the reaction solution at all times. Initially we wanted to use a Pd catalyst as well since then it would be possible to combine both reaction steps in a single operation eventually.

In our group, we have developed a protocol for direct arylation of *N*-(2-pyridyl) substituted anilines and decided to start our screenings using these conditions (3eq of arylboronic acid, 10mol% Pd(OAc)<sub>2</sub>, 1eq of Ag<sub>2</sub>O, 0.5eq of BQ in dry THF) to study if they can efficiently be applied in the direct arylation of 2-phenylpyridine [134].

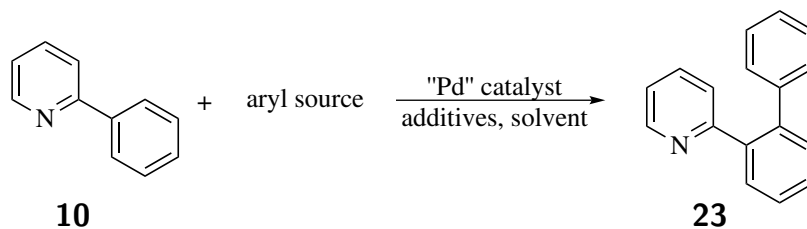
We started our optimization using phenyl boronic acid as aryl source **47** and we checked initially if the reaction mixtures are homogeneous and if they result in good GC yields. We ran two experiments increasing the BQ from 0.5 to 1eq (Table 23, Entries 1-2), which resulted to an increase of the yield up to 57%. However Ag<sub>2</sub>O was not soluble in dry THF.

After a literature search we found that 1,4-dioxane is a common solvent in use on such transformations in combination with BQ, AgF and aryltrimethoxysilane as aryl source [135]. Initially we substituted the dry THF with a mixture of dioxane/H<sub>2</sub>O (1:1) or plain 1,4-dioxane (Table 23, Entries 3-5) and then used the aryltrimethoxysilane with AgF instead of phenyl boronic acid **47** and Ag<sub>2</sub>O (Table 23, Entry 6), but those experiments resulted also in heterogeneous solutions and hence we did not proceed to GC analysis.

In search for another C-H activation protocol, we found a procedure to ortho arylate 2-phenylpyridines with aryltrifluoroborates by Wu *et al* [136], which we used as starting point for our next screening experiments. In this protocol Cu(OAc)<sub>2</sub> was used in place of Ag<sub>2</sub>O in combination with BQ in dioxane. Using phenyl potassium trifluoroborate, we received in the first two experiments moderately homogeneous reaction mixtures and the best GC yield was at range of 36% after increasing the temperature from 90°C to 120°C (Table 23, Entries 7-8). Furthermore, phenyl potassium trifluoroborate showed slightly better solubility in comparison to phenyl boronic acid **47** so we decided to continue the screenings with it.

Trying to identify a solvent which could dissolve our reagents in a satisfying manner, we tried another aprotic but polar solvent: DMSO. The latter has a much higher boiling point (189°C) in comparison to dioxane (101°C); and it could serve as a more versatile choice of a polar aprotic solvent in case that it would be necessary to increase the reaction temperature e.g for accelerating the reaction rate. Entry 9 (Table 23) was the most promising in the DMSO series (Table 23, Entries 9-20) but unfortunately it was not possible to improve the GC yield neither with the portion-wise addition of the aryl source (Table 23, Entry 15) nor with extra addition of aryl source after 3h (Table 23, Entry 16) or extra addition of catalyst (Table 23, Entry 17). Addition of both catalyst and aryl source after 3h (Table 23, Entry 18) or addition of Cs<sub>2</sub>CO<sub>3</sub> (Table 23, Entries 19-20) did not facilitate the process either.

Table 23: Batch screening of Pd(OAc)<sub>2</sub> catalyzed C-H activation protocols.

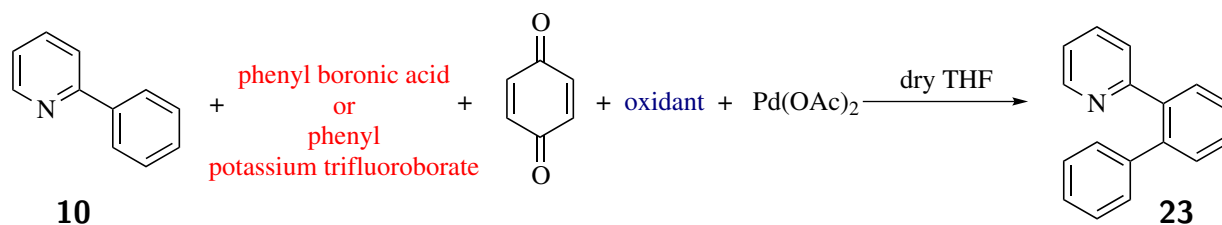


Entry	Aryl Source	Oxidant	Solvent	T[°C]	GC yield [%] <sup>k</sup>
1 <sup>a</sup>	<b>47</b>	Ag <sub>2</sub> O	dry THF	80	18
2 <sup>b</sup>	<b>47</b>	Ag <sub>2</sub> O	dry THF	80	57
3 <sup>b</sup>	<b>47</b>	Ag <sub>2</sub> O	dioxane/H <sub>2</sub> O (1:1)	90	-
4 <sup>b</sup>	<b>47</b>	Ag <sub>2</sub> O	dioxane	90	-
5 <sup>c</sup>	<b>47</b>	-	dioxane/H <sub>2</sub> O (1:1)	90	-
6 <sup>b</sup>	Ar-Si(OMe) <sub>3</sub>	AgF	dioxane	90	-
7 <sup>b</sup>	C <sub>6</sub> H <sub>5</sub> BF <sub>3</sub> K	Cu(OAc) <sub>2</sub>	dioxane	90	12

8 <sup>b</sup>	C <sub>6</sub> H <sub>5</sub> BF <sub>3</sub> K	Cu(OAc) <sub>2</sub>	dioxane	120	36
9 <sup>b</sup>	C <sub>6</sub> H <sub>5</sub> BF <sub>3</sub> K	Cu(OAc) <sub>2</sub>	DMSO	120	50
10 <sup>b</sup>	C <sub>6</sub> H <sub>5</sub> BF <sub>3</sub> K	Cu(OAc) <sub>2</sub>	DMSO	140	46
11 <sup>b</sup>	C <sub>6</sub> H <sub>5</sub> BF <sub>3</sub> K	Cu(OAc) <sub>2</sub>	DMSO	160	42
12 <sup>c</sup>	C <sub>6</sub> H <sub>5</sub> BF <sub>3</sub> K	Cu(OAc) <sub>2</sub>	DMSO	120	33
13 <sup>c</sup>	C <sub>6</sub> H <sub>5</sub> BF <sub>3</sub> K	Cu(OAc) <sub>2</sub>	DMSO	160	42
14 <sup>b,d</sup>	C <sub>6</sub> H <sub>5</sub> BF <sub>3</sub> K	Cu(OAc) <sub>2</sub>	DMSO	120	45
15 <sup>b,e</sup>	C <sub>6</sub> H <sub>5</sub> BF <sub>3</sub> K	Cu(OAc) <sub>2</sub>	DMSO	120	29
16 <sup>b,f</sup>	C <sub>6</sub> H <sub>5</sub> BF <sub>3</sub> K	Cu(OAc) <sub>2</sub>	DMSO	120	42
17 <sup>b,g</sup>	C <sub>6</sub> H <sub>5</sub> BF <sub>3</sub> K	Cu(OAc) <sub>2</sub>	DMSO	120	28
18 <sup>b,h</sup>	C <sub>6</sub> H <sub>5</sub> BF <sub>3</sub> K	Cu(OAc) <sub>2</sub>	DMSO/H <sub>2</sub> O (3:1)	120	26
19 <sup>b,i</sup>	C <sub>6</sub> H <sub>5</sub> BF <sub>3</sub> K	Cu(OAc) <sub>2</sub>	DMSO/H <sub>2</sub> O (3:1)	120	5
20 <sup>b,j</sup>	C <sub>6</sub> H <sub>5</sub> BF <sub>3</sub> K	Cu(OAc) <sub>2</sub>	DMSO/H <sub>2</sub> O (3:1)	120	7

*a*: Reaction conditions: 1 eq. of **10**, 3 eq. of aryl source, 0.5 eq. of BQ, 1 eq. of oxidant, 10 mol% Pd(OAc)<sub>2</sub>. *b*: 1 eq. of **10**, 3 eq. of aryl source, 1 eq. of BQ, 2 eq. of oxidant, 10 mol% Pd(OAc)<sub>2</sub>. *c*: 1 eq. of **10**, 3 eq. of aryl source, 2 eq. of BQ, 3 eq. of oxidant, 10 mol% Pd(OAc)<sub>2</sub>. *d*: As (c) but with 5 mol% of Pd(OAc)<sub>2</sub>. *e*: Portionwise addition of the aryl source. *f*: Addition of 2.5 eq. of the aryl source after 3h. *g*: Addition of 10 mol% catalyst after 3h. *h*: Addition of 2.5 eq. of the aryl source +10 mol% catalyst after 3h. *i*: Addition of 1 eq. of Cs<sub>2</sub>CO<sub>3</sub> after 3h. *j*: Addition of 2 eq. of Cs<sub>2</sub>CO<sub>3</sub> after 3h. *k*: As determined by GC using dodecane as internal standard.

Since the experiment with the best GC yield at that point was the one in Entry 2 (Table 23) although it was not homogeneous, we decided to optimize further this protocol for transferring the process to flow.



Scheme 24: Batch screening of Pd(OAc)<sub>2</sub> catalyzed C-H activation protocol.

The screening of the reaction shown in Scheme 24 was oriented towards temperature (between 60°C and 80°C), aryl source (between **47** and C<sub>6</sub>H<sub>5</sub>BF<sub>3</sub>K), and oxidant (between silver oxide and copper acetate). Furthermore the addition of the aryl source was done portion-wise. The reaction mixture at time t = 0h contained 1 eq. of phenyl boronic acid or C<sub>6</sub>H<sub>5</sub>BF<sub>3</sub>K. At t = 3h a sample was taken for GC analysis and directly after that 1 more eq. of the aryl source was added. The same procedure was repeated at 6h and for the mixtures, which showed promising GC yield (Table 24, Entry 6) (Table 25, Entry 5) a final sample was taken after 24h reaction time (Table 24, Entry 7) (Table 25, Entry 6). In an initial attempt to increase the yield, we left **47** at 80°C to react for 24h (Table 25, Entry 1), in comparison to the same experiment which at 60°C was left for 3h or 6h (Table 24, Entries 1, 2), because in these cases the GC yield stayed constant at the range of 20%. An increase of 30% was noticed after that change (57% GC yield, Table 25, Entry 1). In all cases dry THF was used and biphenyl formation was observed (Table 24, Table 25).

Table 24: Batch screening of Pd(OAc)<sub>2</sub> catalyzed C-H activation protocol at 60°C.

Entry <sup>a</sup>	Oxidant	Aryl Source	t	GC Yield [%] <sup>b</sup>
1	Ag <sub>2</sub> O	<b>47</b>	3h	20
2	Ag <sub>2</sub> O	<b>47</b>	6h	20
3	Cu(OAc) <sub>2</sub>	<b>47</b>	3h	12
4	Cu(OAc) <sub>2</sub>	<b>47</b>	6h	10

5	Ag <sub>2</sub> O	C <sub>6</sub> H <sub>5</sub> BF <sub>3</sub> K	3h	46
6	Ag <sub>2</sub> O	C <sub>6</sub> H <sub>5</sub> BF <sub>3</sub> K	6h	52
7	Ag <sub>2</sub> O	C <sub>6</sub> H <sub>5</sub> BF <sub>3</sub> K	24h	68
8	Cu(OAc) <sub>2</sub>	C <sub>6</sub> H <sub>5</sub> BF <sub>3</sub> K	3h	17
9	Cu(OAc) <sub>2</sub>	C <sub>6</sub> H <sub>5</sub> BF <sub>3</sub> K	6h	19

*a*: Reaction conditions: 1 eq. of **10**, 3 eq. aryl source added portionwise, 0.5 eq. BQ, 1 eq. of oxidant, 10 mol% Pd(OAc)<sub>2</sub>. *b*: As determined by GC using dodecane as internal standard.

Table 25: Batch screening of Pd(OAc)<sub>2</sub> catalyzed C-H activation protocol at 80°C.

Entry <sup><i>a</i></sup>	Oxidant	Aryl Source	t	GC Yield [%] <sup><i>b</i></sup>
1	Ag <sub>2</sub> O	<b>47</b>	24h	57
2	Cu(OAc) <sub>2</sub>	<b>47</b>	3h	2
3	Cu(OAc) <sub>2</sub>	<b>47</b>	6h	11
4	Ag <sub>2</sub> O	C <sub>6</sub> H <sub>5</sub> BF <sub>3</sub> K	3h	54
5	Ag <sub>2</sub> O	C <sub>6</sub> H <sub>5</sub> BF <sub>3</sub> K	6h	58
6	Ag <sub>2</sub> O	C <sub>6</sub> H <sub>5</sub> BF <sub>3</sub> K	24h	63
7	Cu(OAc) <sub>2</sub>	C <sub>6</sub> H <sub>5</sub> BF <sub>3</sub> K	3h	20
8	Cu(OAc) <sub>2</sub>	C <sub>6</sub> H <sub>5</sub> BF <sub>3</sub> K	6h	19
9 <sup><i>b</i></sup>	-	C <sub>6</sub> H <sub>5</sub> BF <sub>3</sub> K	24h	60

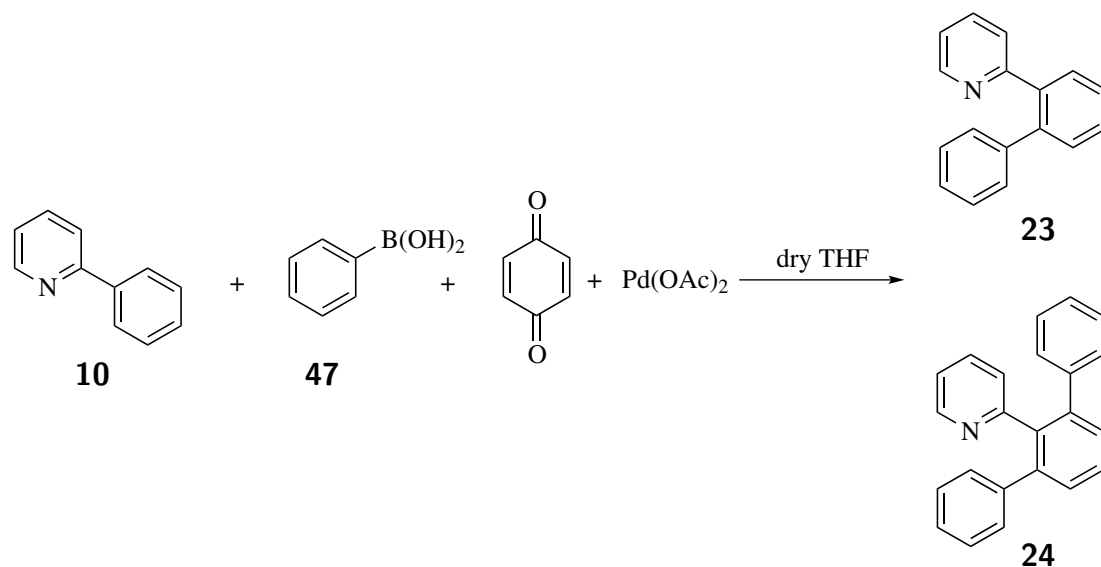
*a*: Reaction conditions: 1 eq. of **10**, 3 eq. of aryl source added portionwise, 0.5 eq. BQ, 1 eq. of oxidant, 10 mol% Pd(OAc)<sub>2</sub>. *b*: With 4 eq. of BQ *c*: As determined by GC using dodecane as internal standard.

Substituting dry THF with “normal” THF led to a significant drop in GC yield. This was a strong indication that water free conditions were important for the reaction performance. The best GC yield that we could obtain using dry THF was at the range of 68% at 60°C (Table 24, Entry 7) and at 63% at 80°C (Table 25, Entry 6) and still the

protocol was not ideal since the silver oxide was not completely soluble in the reaction mixture. Using 4eq of benzoquinone instead of 0.5eq and excluding the silver oxide (Table 25, Entry 9) we could obtain moderate solubility and a GC yield of 60% comparable to the one in Entry 6 (Table 25).

Since these last conditions still required a long reaction time (24h) it was doubtful whether this could be transferred to a useful flow process since there, residence times > 1h are already difficult to handle and take away the advantages of a flow process. Nevertheless, we ran the reaction in the flow system we had previously used in the Suzuki-Miyaura coupling reaction, with a maximum residence time of 90 minutes. The optimized batch conditions (Table 24, Entry 7) did not result in a GC yield of more than 10%. Tuning of the individual parameters e.g doubling the equivalents of benzoquinone, increasing the equivalents of the aryl source (even eleven-fold times more), increasing the solution's concentration (till three-fold times more), did not facilitate the process either. Always the GC yield was below 10%. The same was also the case when instead of 2-phenyl pyridine, 2-(o-tolyl) pyridine or 2-(m-tolyl) pyridine was used, because the electronic properties of the methyl substituent in pyridine did not influence the coupling either.

A last attempt to increase the reaction rate, reducing the reaction time and ideally increasing the yield was to run the reaction in microwave conditions but at a significantly higher temperature of 220°C and 18 bars (maximum temperature and pressure which we could run a THF solution in our microwave system). The purpose of this experiment was to see if we could obtain a good yield in a reasonable time and then translate the protocol using a flow system, which can withstand pressurized conditions (AFRICA or X-Cube, see Appendix A). We proceeded to the reaction and we screened the GC yield varying the equivalents of BQ from 1-4 (Table 26).

Table 26: Microwave screening of Pd(OAc)<sub>2</sub> catalyzed C-H activation protocol.

Entry <sup>a</sup>	Eq. of BQ	GC yield <b>23</b> [%] <sup>b</sup>	GC yield <b>24</b> [%] <sup>b</sup>	GC yield <b>10</b> [%] <sup>b</sup>
1	1	29	7	64
2	2	20	4	76
3	4	9	3	88

*a*: Reaction conditions: 1eq. of **10**, 3 eq. of **47**, 1-4eq. BQ, Pd(OAc)<sub>2</sub> (10 mol%), 30min, 220°C. *b*: As determined by GC using dodecane as internal standard.

Since the latter microwave screening (Table 26) did not result in a significant improvement either, we decided to abandon Pd catalyzed methods and switch to ruthenium catalysts, which have been used in many C-H activation protocols up to date efficiently [97, 137].

Again we started screening for homogeneous reaction conditions. Oi *et al* reported a promising method in which NMP was used as solvent, benzeneruthenium(II)chloride dimer as catalyst and K<sub>2</sub>CO<sub>3</sub> as the base at 120°C for 20h [138, 139]. Even though the base was insoluble in this case, NMP allowed increasing the reaction temperature and shortening the reaction time below 1h simultaneously. The initial screening was conducted with **10** as substrate, bromobenzene **41** as aryl source, and different Ru(II) cat-

alysts: benzeneruthenium(II)chloride dimer and dichloro(p-cymene)ruthenium(II)dimer (shown from left to right in Figure 34) and the GC yield (overall: mono-arylated+bis-arylated product) was recorded after performing the reactions in different temperatures under air and inert conditions with microwave irradiation (Table 27). It was soon found that both catalysts investigated gave almost identical results in terms of conversion. Since dichloro(p-cymene)ruthenium(II)dimer was significantly cheaper we continued further optimization using this catalyst.

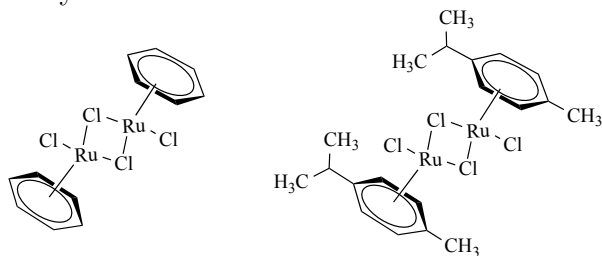
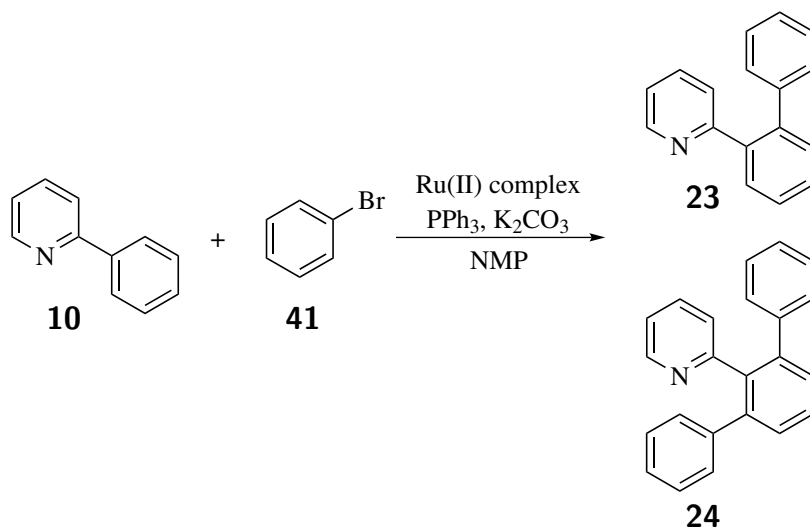


Figure 34: Ru(II) catalysts, used for the screening.

Table 27: Screening conditions for Ru(II) catalyzed C-H activation protocol.



Entry <sup>a</sup>	Time [min]	T[°C]	GC yield	
			23 [%] <sup>i</sup>	24 [%] <sup>i</sup>
1 <sup>b,d,g</sup>	30	120	44	24
2 <sup>b,e,g</sup>	30	120	54	17



3 <sup>c,e,g</sup>	30	120	55	25
4 <sup>c,e,f,g</sup>	30	120	59	15
5 <sup>b,e,g</sup>	30	160	58	28
6 <sup>c,e,g</sup>	30	160	50	34
7 <sup>b,d,g</sup>	30	160	58	17
8 <sup>b,e,g</sup>	15	160	37	9
9 <sup>b,e,h</sup>	30	160	29	60
10 <sup>b,e,h</sup>	30	160	57	15

*a*: Reaction conditions: 2eq. of base, 10mol% PPh<sub>3</sub>, in MW. *b*: 1 eq. of **41**, concentration 0.5M. *c*: 1.5 eq. of **41**, concentration 0.5M. *d*: Under inert conditions. *e*: Under air. *f*: Concentration 0.25M. *g*: Dry K<sub>2</sub>CO<sub>3</sub>, dry NMP. *h*: Bench quality K<sub>2</sub>CO<sub>3</sub>, bench quality NMP *i*: As determined by GC using dodecane as internal standard.

Although some initial conclusions could be drawn from this screening, the biggest issue to deal with was the bad solubility of the base. We observed slightly better yields at 160°C (Table 27, Entries 5, 6, 9) so we continued the screening at this temperature. We also noticed a slight improvement in the overall yield when we increased the equivalents of the aryl source to 1.5eq. (Table 27, Entries 3-6). By decreasing the concentration (Table 27, Entry 4) in an attempt to increase the solubility of the base the GC yield was undermined even though 1.5eq. of aryl source was also used in this case. Furthermore we observed no difference under inert conditions as used by Oi *et al.* or under air (Table 27, Entries 1, 2, 5, 7). A finding that comes in accordance with the general trend of Ru(II) complexes, which are stable in air and water [140]. Therefore all screening reactions as well as compound syntheses have been carried out under air.

Since, the solution of reagents had to be homogeneous at r.t. as well after the reaction zone and because K<sub>2</sub>CO<sub>3</sub> was not soluble in NMP, we conducted an extensive base screening in several solvents in order to identify a soluble base (Table 28).

Table 28: Base screening of Ru(II) catalyzed C-H activation protocol.

Entry <sup>a</sup>	Base	Solvent	Solubility	GC overall yield [%] <sup>e</sup>
1 <sup>d</sup>	dry K <sub>2</sub> CO <sub>3</sub>	dry NMP	n.h	80
2 <sup>d</sup>	Cs <sub>2</sub> CO <sub>3</sub>	bench quality NMP	n.h	74
3 <sup>b</sup>	Cs <sub>2</sub> CO <sub>3</sub>	bench quality NMP	n.h	-
4 <sup>c</sup>	Cs <sub>2</sub> CO <sub>3</sub>	bench quality NMP	n.h	-
5	Cs <sub>2</sub> CO <sub>3</sub>	Acetylacetone	n.h	-
6	Cs <sub>2</sub> CO <sub>3</sub>	ethyl glycol diethyl ether	n.h	-
7	Cs <sub>2</sub> CO <sub>3</sub>	NMP/H <sub>2</sub> O	n.h	17
8	K <sub>3</sub> PO <sub>4</sub>	bench quality NMP	n.h	
9	KOtBu	bench quality NMP	moderate	2
10	NaOtBu	bench quality NMP	moderate	3
11	DABCO	bench quality NMP	moderate	1
12	<i>N,N</i> -diisopropylethylamine	bench quality NMP	moderate	3
13	Stoichiometric amount of DABCO & sub-stoichiometric amount of Cs <sub>2</sub> CO <sub>3</sub>	bench quality NMP	moderate	1
14	NaOH	bench quality NMP	n.h	-
15	KPV	bench quality NMP	n.h	-
16	KOAc	bench quality NMP	n.h	-

*a*: Reaction conditions: 1.5 eq. of **41**, catalyst: dichloro(*p*-cymene)ruthenium(II)chloride dimer, 2 eq. of base, 10mol% PPh<sub>3</sub>, concentration 0.25M, 30min reaction time, microwave, 160°C. *b*: Ultrasonic irradiation. *c*: Addition 10% and 20% of dicyclohexano-18-crown-6. *d*: Was tested also in NMP/H<sub>2</sub>O, DMF, anisole. *e*: As determined by GC using dodecane as internal standard.

We tested several bases. With  $\text{Cs}_2\text{CO}_3$  we observed a promising GC yield (Table 28, Entry 2) but the reaction mixture was not homogeneous and when adding various amounts of water to dissolve the base, a significant drop of the GC yield was observed. In other solvents such as DMF, anisole, or mixtures of NMP-EtOAc, the base was not soluble at all.

When KOtBu and NaOtBu were used (Table 28, Entries 9-10), we observed better solubility but again a significant drop of the GC yield to only 2-3%. Using NaOH or KOAc (Table 28, Entries 14 & 16) gave inhomogeneous solutions as well.

Changing to an organic base such as DABCO or Hunig's base (Table 28, Entries 11-12) solved the solubility issue but led again to a significant drop in yield (1-3% GC yield). Attempts to improve solubility by changing the concentration did not help either.

For this reason we decided to continue our screenings and finally the breakthrough came by switching to DBU where we obtained a homogeneous solution, which we used for further optimization in flow. We performed several screenings regarding equivalents of bromobenzene, DBU, catalyst loading (with both benzeneruthenium(II)chloride dimer and dichloro(p-cymene)ruthenium(II)) and a comprehensive table of the most important results is provided in Table 29. In all cases we found that mixtures of **23** and **24** were formed. However, for the optimization we looked at overall conversion and yield.

Table 29: Screening conditions for Ru(II) catalyzed C-H activation protocol.

Entry <sup>a</sup>	Eq. 41	Eq. DBU	Time (min)	T[°C]	GC yield <b>23</b> [%] <sup>d</sup>	GC yield <b>24</b> [%] <sup>d</sup>
1 <sup>b</sup>	1.5	1	30	160	9	20
2 <sup>b</sup>	1.5	2	30	160	13	22
3 <sup>b</sup>	1.5	4	30	160	20	35
4 <sup>b</sup>	1.5	6	30	160	18	20
5 <sup>b</sup>	1.5	4	10	160	13	10
6 <sup>b</sup>	1.5	4	20	160	23	17
7 <sup>b</sup>	2	4	30	160	13	25
8 <sup>b</sup>	3	4	30	160	20	22

9 <sup>b</sup>	4	4	30	160	21	30
10 <sup>b</sup>	6	4	30	160	23	39
11 <sup>c</sup>	3	4	30	140	27	41
12 <sup>c</sup>	3	4	30	160	26	69
13 <sup>c</sup>	3	4	30	180	14	73

*a*: Both dichloro(p-cymene)ruthenium(II)chloride dimer and benzeneruthenium (II) chloride dimer were tested resulting in similar results, heating mode: microwave. *b*: 2.5 mol% catalyst loading. *c*: 5 mol% catalyst loading. *d*: As determined by GC using dodecane as internal standard.

One equivalent of DBU gave 29% GC yield of **23** and **24** (Table 29, Entry 1). Increasing the amount up to 4 equivalents and retaining the time at 30 min gave an improvement to 55% (Table 29, Entry 3). With the same amount of DBU at a shorter time of 10min, decrease of the yield to 23% was noticed (Table 29, Entry 5), but at 20min since the reaction was still progressing there was an increase of the yield to 40% (Table 29, Entry 6). Keeping constant the equivalents of DBU and increasing the equivalents of **41** lead to a maximum yield of 62% (Table 29, Entry 10). Increasing the catalyst loading to 5% and the equivalents of bromobenzene to 3 finally gave a good overall GC yield of 95% of **23** and **24** (Table 29, Entry 12). Next we tried to transfer these conditions to a continuous flow process.

Applying the optimized conditions in flow (Table 29, Entry 12) to a preparative scale experiment, we were able to isolate **23** in 26% and **24** in 69% yield respectively (ratio 1:2.65) (Table 30). This result differs from Oi's findings where a total yield of 82% of the same two products was obtained but in favor of the mono-arylated one (6.7:1). However, in his case only 1 eq. of bromobenzene was used. Using 2.2 or 3.0 equivalents, **24** was formed exclusively. Of course a different base was applied which can be responsible for the observed differences [138, 139].

The electronic nature of the halide (Figure 35) had a significant influence on the product distribution.

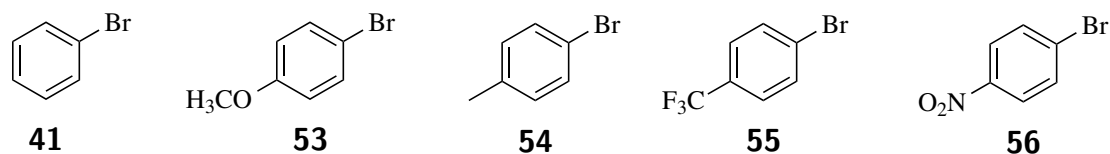
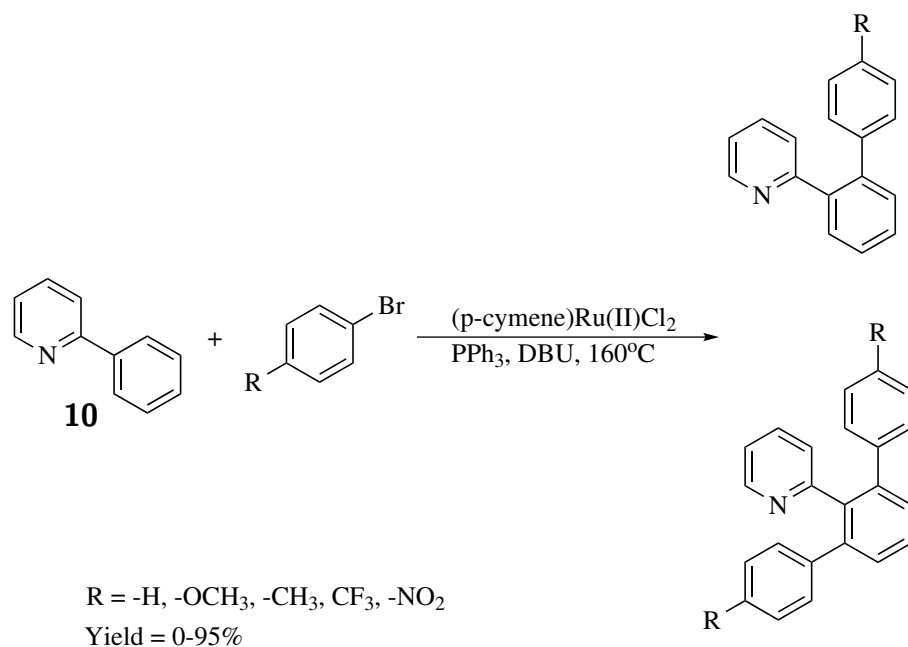


Figure 35: Substitute bromobenzenes.

Table 30: Isolated yields.

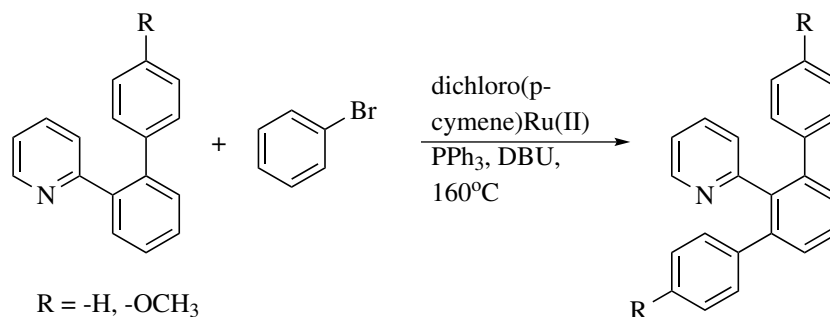


Entry <sup>a</sup>	R	mono-arylated product [%]	bis-arylated product [%]	Combined Yield [%]
1	-H ( <b>41</b> )	26 ( <b>23</b> )	69 ( <b>24</b> )	95
2	-OCH <sub>3</sub> ( <b>53</b> )	59 ( <b>25</b> )	0 ( <b>30</b> )	59
3	-CH <sub>3</sub> ( <b>54</b> )	17 ( <b>26</b> )	34 ( <b>27</b> )	51*
4	-CF <sub>3</sub> ( <b>55</b> )	3 ( <b>28</b> )	71 ( <b>29</b> )	74
5	-NO <sub>2</sub> ( <b>56</b> )	0	0	0

<sup>a</sup>: Reaction conditions: 3 eq. of **10**, 4 eq. DBU, 5 mol% catalyst, 10mol% PPh<sub>3</sub>, solvent: NMP, concentration 0.25M, 30 min residence time, 160°C. \*For this example we isolated an inseparable mixture of the mono- and bis-arylated product and their ratio was determined by NMR to 1:2, mono- to bis-arylated product.

Electron rich 4-bromoanisole **53** gave exclusively the mono-arylated product **25** (Table 30, Entry 2). 4-Bromotoluene **54** favored the formation of bis-arylated **27** over mono-arylated **26** ((1:2), Table 30, Entry 3). When an electron withdrawing substituent was present as in 4-bromo-trifluoromethylbenzene **55**, the bis-arylated product **29** was overwhelmingly favored (1:23.7) with good overall yield (Table 30, Entry 4). A nitro group **56** was not tolerated (Table 30, Entry 5), however this we have observed in Ru catalyzed arylations previously and can be attributed to the ability of the nitro group to coordinate to ruthenium leading to catalyst inactivation [137]. Overall these results show that an increase in electron density favors mono-arylation and vice versa.

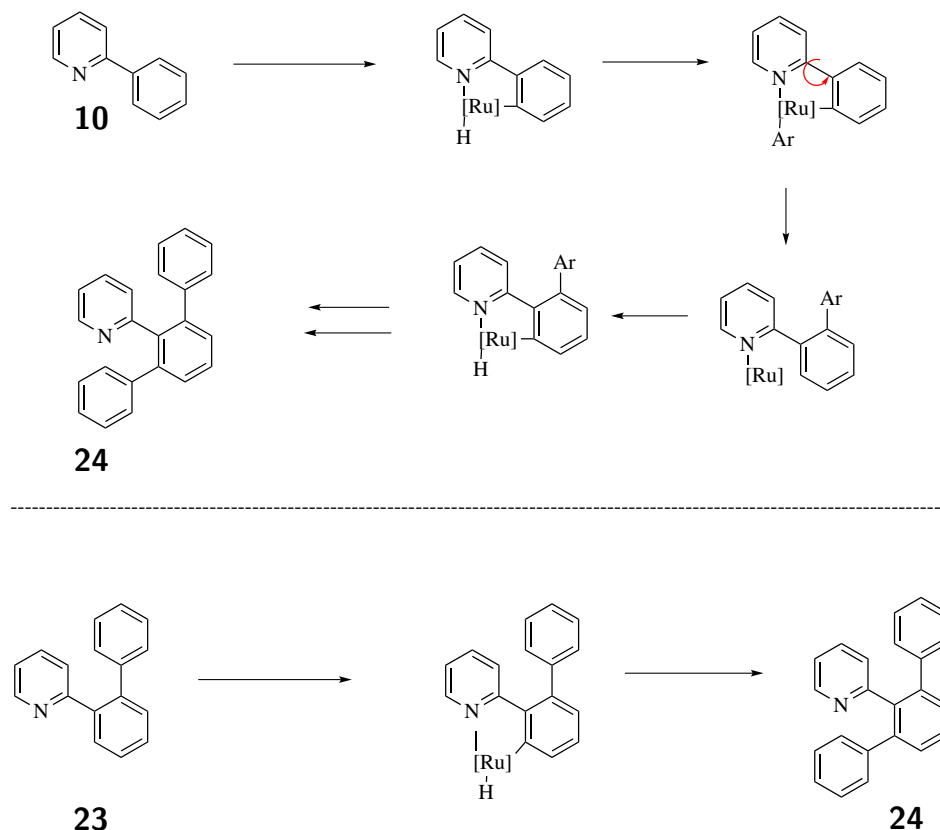
Next, we aimed at the synthesis of bis-arylated compounds. Mono-arylated products **23** and **25** were used as starting materials for a second arylation step with bromobenzene (Scheme 25).



Scheme 25: Arylation of the mono-arylated substrates with bromobenzene.

To our surprise the yield of **24** was significantly lower starting from **23** (44%) compared to the reaction starting from 2-phenylpyridine **10** (69%). The reason for this observation is not clear. A possible explanation is that after the insertion of the Ru(II) into the C-H bond and the first arylation, ruthenium stays coordinated to the pyridine nitrogen (to some extent) leading to rapid second arylation. However when the substrate is the already mono-substituted compound **23** the phenyl group exhibits steric hindrance and pre-coordination of ruthenium to the pyridine nitrogen might be more difficult and hence the reaction might be slower overall (Scheme 26).

By increasing the catalyst loading to 7.5 mol% we received 59% yield, which is in agree-



Scheme 26: Proposed mechanism.

ment with our explanation. In order to support our hypothesis further, we performed a time course for the arylation of **10** with bromobenzene **41** (Figure 36). If the catalyst dissociates from pyridine completely after the first arylation step, we should see accumulation of **23** at the beginning and only small amounts of **24**. When the concentration of **23** increases and simultaneously that of **10** decreases, **23** becomes the preferred substrate and the amount of **24** will increase. However, if our hypothesis is true, we should see formation of **24** to a similar extent compared to **23** already from the beginning and no accumulation of **23**. Indeed, **24** is the major product from the very beginning (Figure 36) which supports our line of argument.

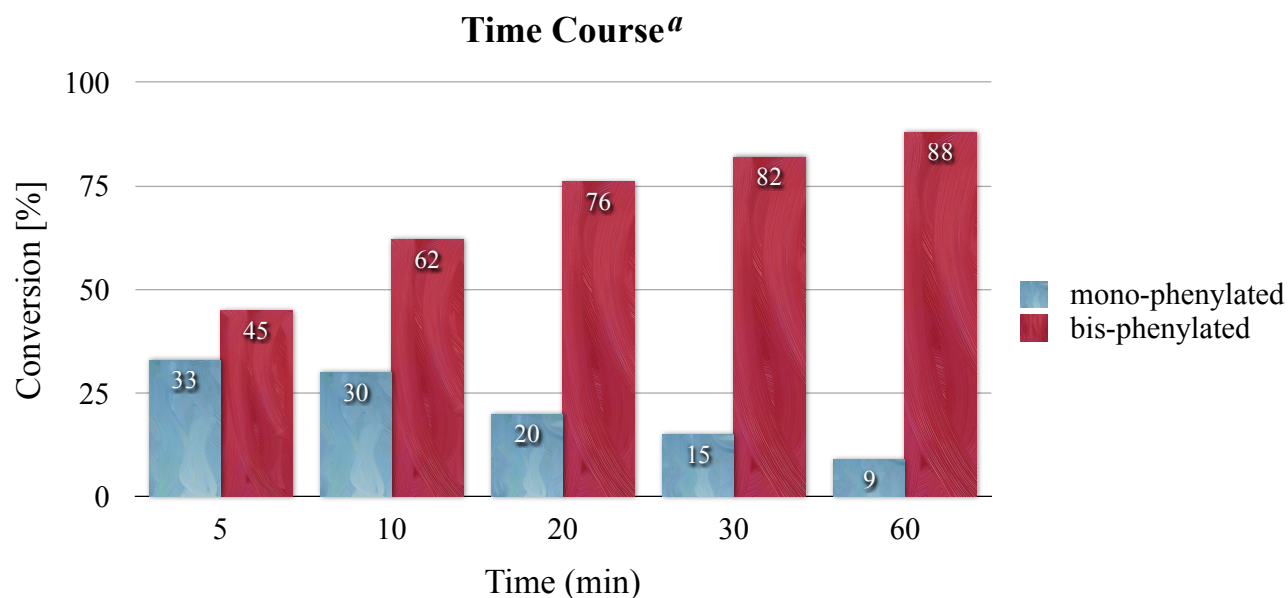


Figure 36: Time course using bromobenzene as coupling partner.

*a*: Conversion as determined by GC using dodecane as internal standard, mono-phenylated: **23**, bis-phenylated: **24**.

We also subjected **25** to a second arylation step. From the previous result (Table 30, Entry 2), it can be expected that arylation of **25** might be difficult and slow. Indeed, a yield of only 24% was obtained (with 7.5mol% catalyst) which underlines the importance of electronic effects on the aryl substituents.

### 2.3.7 Summary/Conclusions

The task on this part of the Thesis was to identify suitable reaction conditions for the synthesis of 2-phenyl pyridine (**10**) via Suzuki-Miyaura cross coupling in flow and its subsequent direct arylation. The main prerequisite in this case was again to achieve homogeneity of the reaction solution at all times, which would enable a transfer of the procedure in flow without clogging. Apart from homogeneous catalysts, heterogeneous catalysts can also serve this purpose. Since they could be packed in cartridges, a homogeneous reaction solution can go through the cartridge, react with the aid of the catalyst and form the final product. The crucial prerequisite that has to be ensured is that no precipitation will occur at all times during the reaction zone, because this could lead to



clogging and consequently to reaction termination.

The batch optimization of the reaction conditions for the synthesis of the target molecule (**10**) in this section of the Thesis, directed towards time, yield, atom efficiency and soluble reagents in the reaction mixture.  $\text{K}_2\text{CO}_3$  was soon identified as the best performing base in combination with dioxane/ $\text{H}_2\text{O}$  (1:1) as solvent and immobilised  $\text{Pd}(\text{PPh}_3)_4$  as catalyst. After 3min of reaction time under microwave irradiation in  $120^\circ\text{C}$ , 95% of GC conversion was observed. However, efforts to transfer these conditions in a continuous flow system such as X-Cube (see Appendix A) were unsuccessful regardless of the catalyst loading and the applied temperature. Suspecting leaching of the catalyst, we conducted a stability screening which confirmed our concerns for Pd leaching.

Substituting the immobilised  $\text{Pd}(\text{PPh}_3)_4$  with “normal”  $\text{Pd}(\text{PPh}_3)_4$ , we received a homogeneous solution, which we were able to directly run in flow for an optimization screening. We used our in-house developed flow reactor, a simpler to operate flow system (see Appendix A), since X-Cube which we have previously used for the heterogeneous catalysed protocol was not longer necessary. Due to the fact that this system does not support pressurization, we had to decrease the reaction temperature in order to stay below  $90^\circ\text{C}$  so that we will not exceed the boiling point of the solvent.

We identified the optimized reaction conditions in using 1.2eq of phenyl boronic acid **47**, 2eq of  $\text{K}_2\text{CO}_3$  and 2.1mol% of  $\text{Pd}(\text{PPh}_3)_4$ , reaching a GC conversion of 82% after 23min of residence time. We then applied these conditions in coupling of 2-bromopyridine **9** with several arylboronic acids containing both electron withdrawing and donating groups and we isolated the corresponding 2-phenyl pyridines in generally good yields. Since we were interested to investigate if the material of the coil had any influence on the reaction performance, we conducted experiments either using a steel coil or a PFA coil and in some cases both for comparison.

Furthermore, it has to be mentioned that we also investigated the influence of the equivalents of the aryl source to the yield. We discovered that when 1.2eq of boronic acid was used, the results were comparable for both coils. However, when 3eq of boronic acid was used, the PFA coil performed significantly better. Electron donating substituents on the boronic acids gave generally better yield. Even with the sterically hindered o-

tolylboronic acid **49** a 91% yield was obtained using the PFA coil. For electron withdrawing substituents on the boronic acid, improvement of the yield was noticed when instead of 1.2eq we used 3eq of boronic acid.

Then we transferred the same conditions to the couplings of 3-bromopyridine **16** with arylboronic acids but using almost exclusively the PFA coil and 3eq of the aryl source and we obtained in general better yields in the corresponding 3-phenyl pyridines in comparison to the 2-phenyl pyridines.

Overall, we synthesized a series of Suzuki-Miyaura coupling products employing the efficient and robust technology of a continuous flow system, using a reactor designed in-house (see Appendix A) and Pd(PPh<sub>3</sub>)<sub>4</sub> as cheap catalyst.

Besides Suzuki-Miyaura coupling, we were also interested in direct arylation reactions under continuous flow. 2-Phenylpyridine (**10**) constitutes a common substrate for direct functionalization reactions and since we could efficiently synthesize this compound with our flow process, we decided to investigate its further application in C-H activation chemistry, also via a continuous-flow approach.

Initially we wanted to use a Pd catalyst since then it would be possible to combine both reaction steps in a single operation eventually. When testing literature known Pd catalyzed protocols it turned out that none of the reaction mixtures were absolutely homogeneous, due to insolubility of the oxidants in use or of the aryl source and the catalyst in the reaction solution. However, we conducted several screenings in batch trying to optimize the yield and at the same time to improve the solubility of the reaction mixture. Unfortunately, the best GC yields that we were able to obtain were in the range of 60% and most importantly we could not improve significantly the solubility of the reagents in the reaction mixture. Therefore, we decided to abandon Pd catalyzed methods and switch to ruthenium catalysts, which are often used in C-H activation protocols.

We identified a protocol from Oi *et al* in which NMP was used as solvent, benzeruthenium(II)chloride dimer as catalyst and K<sub>2</sub>CO<sub>3</sub> as the base at 120°C for 20h [138, 139]. The initial screening was conducted with **10** as substrate, bromobenzene **41** as aryl source, and different Ru(II) catalysts: benzeruthenium(II)chloride dimer and dichloro(p-cymene)ruthenium(II)dimer with microwave irradiation. It was soon found

that both catalysts investigated, gave almost identical results in terms of conversion. Since dichloro(p-cymene)ruthenium(II)dimer was significantly cheaper we continued further optimization using this catalyst. Furthermore we observed no difference under inert conditions as used by Oi *et al* or under air. A finding that comes in accordance with the general trend of Ru(II) complexes, which are stable in air and water [140]. Therefore all screening reactions as well as compound syntheses have been carried out under air.

The major problem that we came across during this optimization was the solubility of the base. We tested several inorganic and organic bases in combination with different solvents and additives, in order to substitute the insoluble  $K_2CO_3$  in the reaction mixture, but none of them resulted to a clearly homogeneous solution. In the best cases we received moderately homogeneous reaction mixtures but those resulted in very poor GC yields. Attempts to improve solubility by changing the concentration did not help either. Finally the breakthrough came by switching to DBU where we obtained a homogeneous solution, which we used for further optimization in flow. In all cases we found that mixtures of **23** and **24** were formed.

When we identified the best compromise between equivalents of bromobenzene **41**, DBU and catalyst loading, we applied the optimized conditions in flow using several substituted bromobenzenes. The electronic nature of the halide had a significant influence on the product distribution. Electron rich 4-bromoanisole **53** gave exclusively the mono-arylated product **25**. 4-Bromotoluene **54** favored the formation of bis-arylated **27** over mono-arylated **26**. When an electron withdrawing substituent was present as in 4-bromo-trifluoromethylbenzene **55**, the bis-arylated product **29** was overwhelmingly favored (1:23.7) with good overall yield and a nitro group **56** was not tolerated. Overall these results show that an increase in electron density favors mono-arylation and vice versa.

Next, we aimed at the synthesis of bis-arylated compounds and we have made an interesting observation. The yield of **24** was significantly lower starting from **23** (44%) compared to the reaction starting from 2-phenylpyridine **10** (69%). The reason for this observation was initially not clear but after conducting a time course for both reactions we concluded to the following explanation. After the insertion of the Ru(II) into the C-H

bond and the first arylation, ruthenium stays coordinated to the pyridine nitrogen (to some extent) leading to a second arylation rapidly. However when the substrate is the already mono-substituted compound **23** the phenyl group exhibits steric hindrance and pre-coordination of ruthenium to the pyridine nitrogen might be more difficult and hence the reaction might be slower (Scheme 26).

Overall, to the best of our knowledge, in this work we presented for the first time the possibility of performing metal catalyzed C-H activation, using a continuous flow process in an intermolecular fashion, since only one intramolecular example was disclosed, so far [99]. Furthermore the transformation is operationally simple since it does not require inert techniques making it user-friendly and effective at the same time.

## 3 Experimental Section

### 3.1 General notes

Unless otherwise noted, chemicals were purchased from commercial suppliers and used without further purification.

Microwave reactions were performed on a Biotage Initiator Sixty microwave unit.

Continuous flow reactions as far as concerned the synthesis of the phenylpyridine derivatives, were performed using a syringe pump (model NE: 1000) from New Era Pump Systems connected to an aluminum reactor designed in our group. A technical drawing is provided in Figure 37. For optimization purposes the X-Cube (Figure 38) from ThalesNano was also used. Regarding the optimization towards the flow synthesis of the magnolol/honokiol precursors, flow reactions were performed mainly using the AFRICA system from Syrris (Figure 39) with a cap disk (Figure 40) which was designed in our group or a reactor from Syrris, which allows the use of a glass column for encapsulation of heterogeneous additives (base/catalyst) (Figure 41) as well as a syringe pump (model NE: 1000). Flash column chromatography was performed by using a Büchi Sepacore™ MPLC system.

Kugelrohr distillation was carried out using a Büchi GKR-51 apparatus.

Preparative HPLC runs were performed on a Shimadzu LC-8A device with an SIL-10AP autosampler, SPD-20A detector and FRC-10A fraction collector. For separation a Phenomenex Luna RP18, 10  $\mu$ m, 100A, 250 x 21.20 mm. The injection volume was 2-4  $\mu$ L and the column flow 20 mL/min. The detection wavelength was 254 nm.

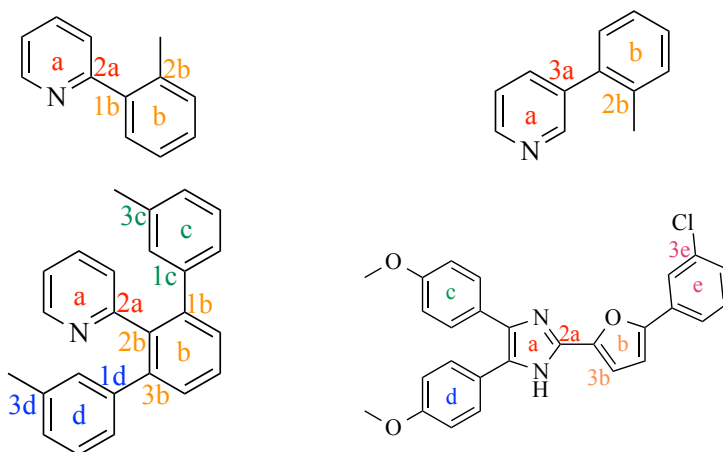
For TLC analysis aluminum-backed silica gel from Merck was used.

NMR-spectra were recorded either in CDCl<sub>3</sub> or DMSO-d<sub>6</sub> on a Bruker AC 200 (200 MHz) or a Bruker Avance Ultrashield (400 MHz) spectrometer and chemical shifts are reported in ppm relative to the nominal residual solvent signals: CDCl<sub>3</sub>:  $\delta$  = 7.26 ppm (<sup>1</sup>H),  $\delta$  = 77.16 ppm (<sup>13</sup>C); DMSO-d<sub>6</sub>:  $\delta$  = 2.50 (<sup>1</sup>H),  $\delta$  = 39.52 (<sup>13</sup>C). For assignment of <sup>13</sup>C multiplicities standard <sup>13</sup>C spectra were recorded. The assignments were presented when they could be unequivocally assigned to a certain carbon. The chemical shifts are

reported in parts per million (ppm).

The abbreviations used are as follows: s, singlet; d, doublet; dd, doublet of doublets; t, triplet; m, multiplet; td, triplet of doublets; ddd, doublet of doublet of doublet.

In order to assign the chemical shifts of each carbon and proton in a consistent way, each of the different ring systems is marked with a, b, c, d as shown in the following example.

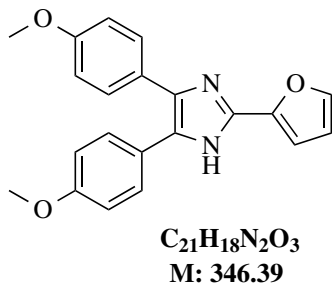


Melting points were determined using a Kofler-type Leica Galen III micro hot stage microscope and are uncorrected.

GC-MS runs were performed on a Thermo Finnigan Focus GC/DSQ II with a standard capillary column BGB 5 (ID=30m×0.32mm).

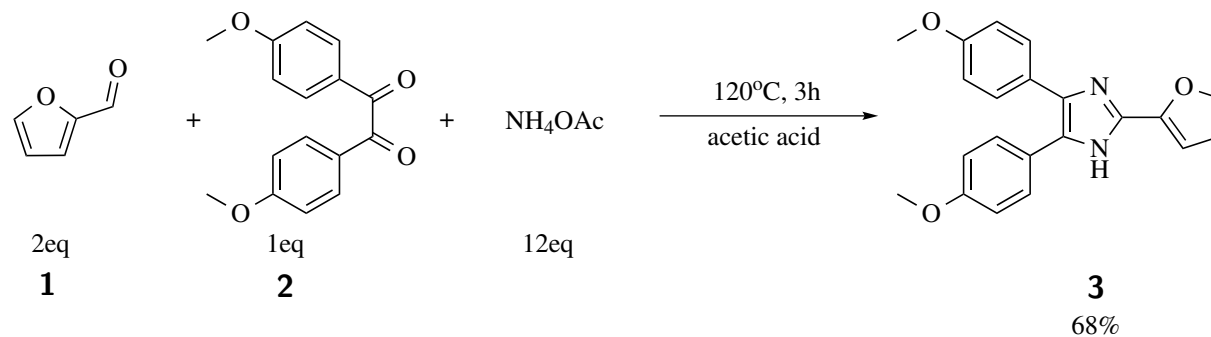
## 3.2 Towards streamlining Neurodazine synthesis

### 3.2.1 Synthesis of 2-(furan-2-yl)-4,5-bis(4-methoxyphenyl)-1*H*-imidazole (**3**)



This compound [141] was synthesised according to the following procedure.

1,2-Bis(4-methoxyphenyl)ethane-1,2-dione (1 eq, 1.56 g, 5.7 mmol) **2**, furfural (2 eq, 0.95 mL, 11.56 mmol) **1**, NH<sub>4</sub>OAc (12 eq, 5.27 g, 68.4 mmol) and 60 mL acetic acid were placed in a dry three-necked flask which was equipped with a thermometer, a reflux condenser, a magnetic stir bar and a septum. The mixture was heated at 120°C for 3h.



Subsequently, the reaction mixture was poured into an ice cooled NaHCO<sub>3</sub> solution and the aqueous phase was extracted three times with diethylether. The organic layer was washed with brine, dried over sodium sulfate, filtered and evaporated under vacuum. The crude product was purified via MPLC on silica gel (P.E: EtOAc= 2:1).

- Yield: 68% (1.348 g, 3.89 mmol)
- Appearance: brown powder
- M.p: 169-172°C

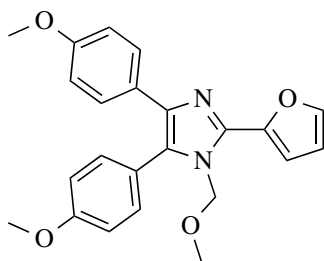
- TLC:  $R_f = 0.5$  (P.E: EtOAc= 1:1)

**$^1\text{H}$  NMR (200 MHz,  $\text{CDCl}_3$ ):**  $\delta$  3.81 (s, 6H,  $\text{OCH}_3$ ), 6.50 (dd, 1H,  $J = 3.4, 1.8$  Hz, H4b), 6.77 - 6.96 (m, 5H, H3c/5c/3d/5d/H3b), 7.34 - 7.50 (m, 5H, H5b/2c/6c/2d/6d).

**$^{13}\text{C}$  NMR (50 MHz,  $\text{CDCl}_3$ ):**  $\delta$  55.3 (s,  $\text{CH}_3$ ), 60.4 (s), 107.5 (s, C3b), 112 (s, C2b), 114 (s), 125.2 (s, C2a/5a), 129.2 (s, C5b), 138.5 (s, C4b), 142.3 (s, C4c), 145.6 (s, C4d), 158.9 (s, C3c), 168.0 (s), 171.0 (s).



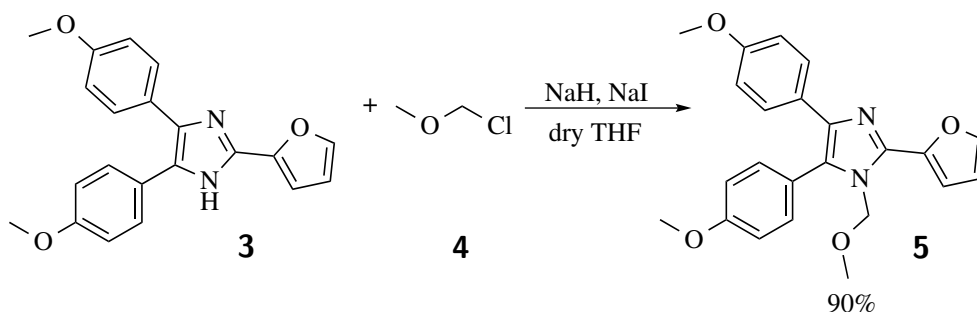
### 3.2.2 Synthesis of 2-(furan-2-yl)-1-(methoxymethyl)-4,5-bis(4-methoxyphenyl)-1*H*-imidazole (**5**)



**C<sub>23</sub>H<sub>22</sub>N<sub>2</sub>O<sub>4</sub>**  
**M: 390.44**

This compound was synthesised according to the following procedure.

2-(Furan-2-yl)-4,5-bis(4-methoxyphenyl)-1*H*-imidazole **3** (1 eq, 534 mg, 1.54 mmol) was placed in an oven dried vial with 1.5 mL of freshly distilled THF. In another oven dried vial, NaH (1.2 eq, 77 mg, 1.85 mmol) was weighed and then cooled in an ice bath. Afterwards, 1.7 mL of freshly distilled THF was added under an Ar atmosphere and the solution was stirred for a few minutes until complete dissolution of the NaH. Then the 2-(furan-2-yl)-4,5-bis(4-methoxyphenyl)-1*H*-imidazole solution was added to the NaH solution via syringe. It was let to stir for 10min in 0°C and then MOMCl was added dropwise **4** (1.2 eq, 0.140 mL, 1.85 mmol). At last, NaI was added to the reaction mixture (0.1 eq, 22.5 mg, 0.15 mmol) and it was stirred for 2h until the substrate **3** was fully converted to the protected compound **5** (evaluation by TLC).



Subsequently, the reaction mixture was poured in an ice cooled NaHCO<sub>3</sub> solution and the aqueous phase extracted with diethylether for three times. The organic layer was

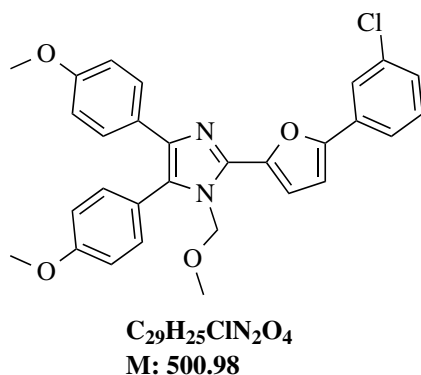
washed with brine, dried over magnesium sulfate and evaporated under vacuum. Further purification was not required.

- Yield: 90% (539 mg, 1.38 mmol)
- Appearance: light brown oil
- TLC: Rf = 0.62 (P.E: EtOAc= 1:1)

**<sup>1</sup>H NMR (200 MHz, CDCl<sub>3</sub>):** δ 3.21 (s, 3H, NCH<sub>2</sub>OCH<sub>3</sub>), 3.76 (s, 3H, OCH<sub>3</sub>), 3.87 (s, 3H, OCH<sub>3</sub>), 5.23 (s, 2H, NCH<sub>2</sub>), 6.54 (dd, 1H, J = 3.4, 1.8 Hz, H4b), 6.72 - 6.81 (m, 2H, H3c/5c), 6.94 - 7.03 (m, 3H, H3b/3d/5d), 7.30 - 7.38 (m, 2H, H2c/6c), 7.43 - 7.52 (m, 2H, H2d/6d), 7.57 (dd, J = 1.7, 0.6 Hz, 1H).

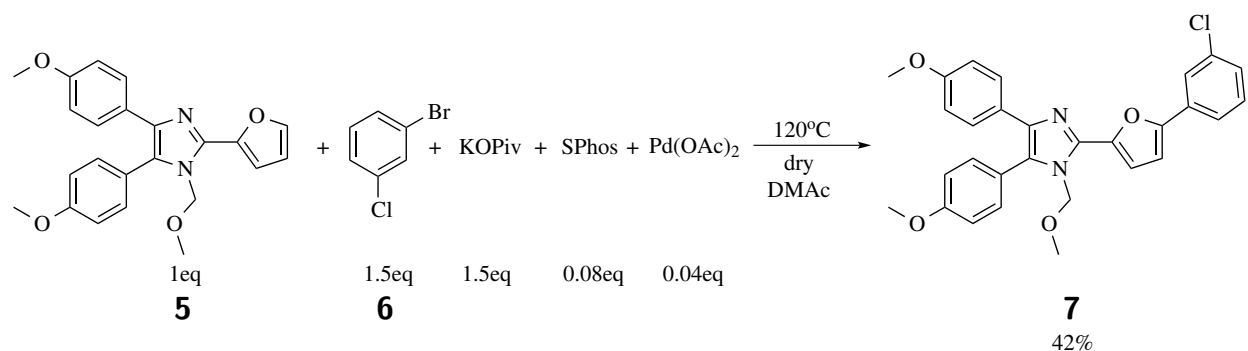
**<sup>13</sup>C NMR (101 MHz, CDCl<sub>3</sub>):** δ 55.0 (s, OCH<sub>3</sub>), 55.2 (s, OCH<sub>3</sub>), 55.6 (s, NCH<sub>2</sub>OCH<sub>3</sub>), 74.4 (s, NCH<sub>2</sub>), 110.3 (s, C4b), 111.4 (s, C3b), 113.4 (s, C3c/5c), 114.3 (s, C3d/5d), 122.1 (s, C1d), 126.8 (s, C1c), 128.2 (s, C2c/6c), 128.8 (s, C5a), 132.5 (s, C2d/6d), 138.0 (s, C4a), 139.2 (s, C5b), 142.9 (s, C2a), 145.1 (s, C2b), 158.3 (s, C4c), 159.8 (s, C4d).

### 3.2.3 Synthesis of 2-(5-(3-chlorophenyl)furan-2-yl)-1-(methoxymethyl)-4,5-bis(4-methoxyphenyl)-1H-imidazole (7)



This compound was synthesised according to the following procedure.

2-(Furan-2-yl)-1-(methoxymethyl)-4,5-bis(4-methoxyphenyl)-1*H*-imidazole **5** (1 eq, 175 mg, 0.45 mmol) with 1-bromo-3-chlorobenzene **6** (1.5 eq, 129 mg, 79  $\mu$ l, 0.675 mmol), potassium pivalate (1.5 eq, 157 mg, 0.675 mmol), Sphos (8 mol%, 0.014 mg, 0.036 mmol) and Pd(OAc)<sub>2</sub> (4 mol%, 0.004 mg, 0.018 mmol) were placed in an oven dried vial. The vial was evacuated and flushed with argon 3 times. Then 0.9 mL of degassed DMAc were added via syringe. The mixture was heated to 120°C for 6 h.



Subsequently, the organic phase was washed with saturated ammonium chloride solution for three times. Then was washed with brine, dried over sodium sulfate and evaporated under vacuum. The crude product was purified via MPLC on silica gel (P.E: Ether= 3:1).

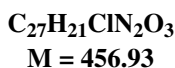
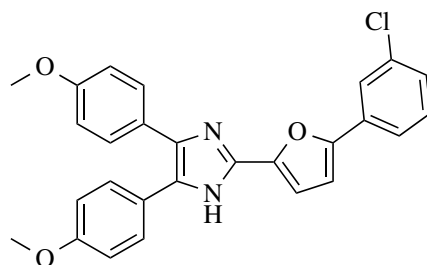
- Yield: 42% (9.2 mg, 0.19 mmoles)

- Appearance: yellow oil
- TLC: Rf = 0.73 (P.E: Ether= 1:1)

**<sup>1</sup>H NMR (400 MHz, CDCl<sub>3</sub>):**  $\delta$  3.28 (s, 3H, NCH<sub>2</sub>OCH<sub>3</sub>), 3.80 (s, 3H, OCH<sub>3</sub>), 3.90 (s, 3H, OCH<sub>3</sub>), 5.33 (s, 2H, NCH<sub>2</sub>), 6.77 - 7.13 (m, 6H, H3c/5c/3d/5d/3b/4b), 7.23 - 7.45 (m, 4H, H2c/6c/4e/5e), 7.45 - 7.55 (m, 2H, H2d/6d), 7.60 - 7.68 (m, 1H, H6e), 7.77 (t, J = 1.8 Hz, 1H, H2e).

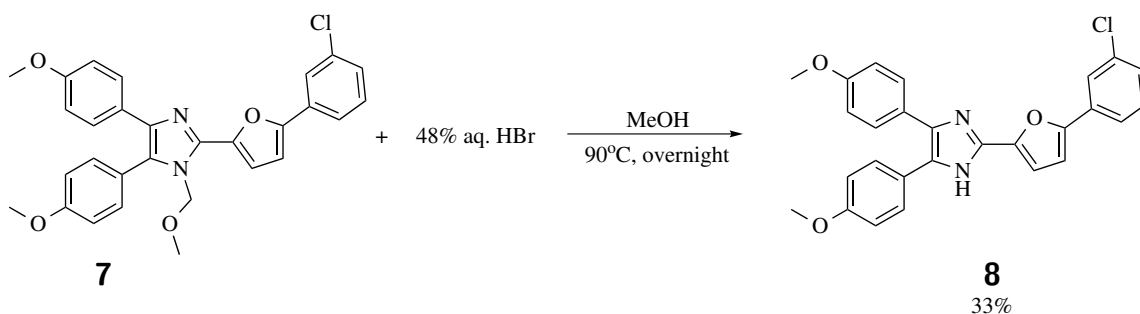
**<sup>13</sup>C NMR (101 MHz, CDCl<sub>3</sub>):**  $\delta$  55.2 (s, OCH<sub>3</sub>), 55.3 (s, OCH<sub>3</sub>), 55.8 (s, NCH<sub>2</sub>OCH<sub>3</sub>), 74.8 (s, NCH<sub>2</sub>), 108.1 (s, C4b), 112.6 (s, C3b), 113.6 (s, C3c/5c), 114.4 (s, C3d/5d), 122.0 (s, C6e), 122.1 (s, C2e), 124.0 (s, C1d), 126.9 (s, C4e), 127.6 (s, C5e), 128.3 (s, C2c/6c), 129.3 (s, C1c), 130.1 (s, C5a), 132.0 (s, C1e), 132.6 (s, C2d/6d), 134.8 (s, C3e), 138.5 (s, C4a), 138.9 (s, C2b), 145.4 (s, C2a), 152.8 (s, C5b), 158.5 (s, C4c), 160.0 (s, C4d).

### 3.2.4 Synthesis of 2-(5-(3-chlorophenyl)furan-2-yl)-4,5-bis(4-methoxyphenyl)-1H-imidazole (8)



This compound [117] was synthesised according to the following procedure.

2-(5-(3-Chlorophenyl)furan-2-yl)-1-(methoxymethyl)-4,5-bis(4-methoxyphenyl)-1H-imidazole **7** (1 eq, 30 mg, 0.06 mmol) with 48% aq. HBr (0.2 ml) and 0.6 mL of MeOH were placed in an oven dried vial. The mixture was heated to 90°C and let it stirred overnight.



Subsequently, the reaction mixture was poured in an ice cooled NaHCO<sub>3</sub> solution and the aqueous phase extracted with diethylether for three times. The organic layer was washed with brine, dried over sodium sulfate and evaporated under vacuum. The crude product was purified via prep. TLC (P.E: EtOAc= 2:1).

- Yield: 33% (9 mg, 0.02 mmoles)
- Appearance: yellow oil

- TLC: Rf = 0.38 (P.E: EtOAc= 2:1)

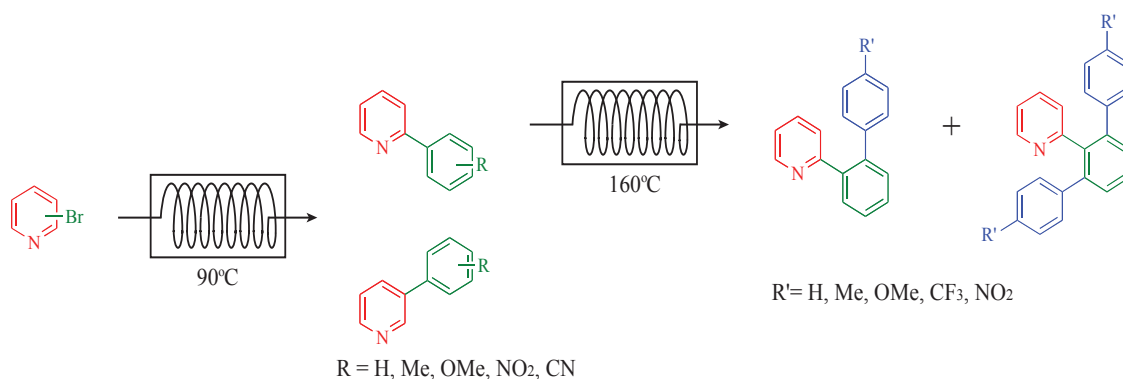
**<sup>1</sup>H NMR (400 MHz, CDCl<sub>3</sub>):**  $\delta$  3.73 (s, 6H, OCH<sub>3</sub>), 6.66 (d, J = 3.6 Hz, 1H, H3b), 6.68 - 6.81 (m, 4H, H3c/5c/3d/5d), 6.98 (d, J = 3.6 Hz, 1H, H4b), 7.14 (dt, J = 8.4, 1.4 Hz, 1H, H4e), 7.19 (m, 1H, H5e), 7.31 - 7.39 (m, 4H, H2c/6c/2d/6d), 7.38 - 7.47 (m, 1H, H6e), 7.57 (t, J = 1.8 Hz, 1H, H2e).

**<sup>13</sup>C NMR (101 MHz, CDCl<sub>3</sub>):**  $\delta$  55.2 (s, OCH<sub>3</sub>), 108.6 (s, C4b), 113.5 (s, C3b), 113.9 (s), 121.9 (s, C6e), 123.7 (s, C2e), 127.4 (s, C4e), 129.0 (s, C5e), 129.1 (s), 129.9 (s, C1e), 131.5 (s, C3e), 131.7 (s, C5a), 134.7 (s, C2a), 137.7 (s, C4a), 145.1 (s, C2b), 152.1 (s, C5b), 159.0 (s, C4c/4d).

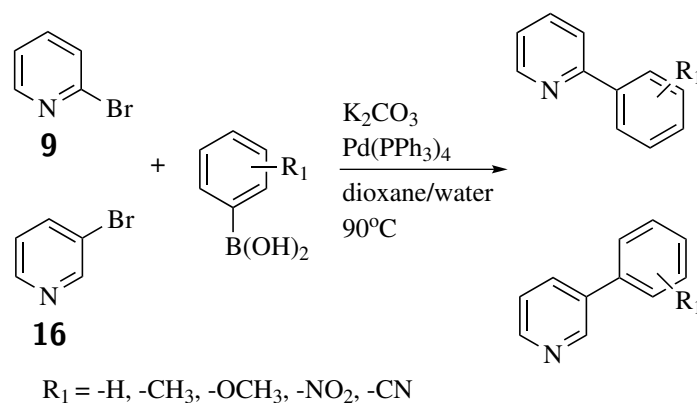
**<sup>1</sup>H NMR (400 MHz, DMSO-d<sub>6</sub>):**  $\delta$  3.76 (s, 3H, OCH<sub>3</sub>), 3.82 (s, 3H, OCH<sub>3</sub>), 6.89 (d, J = 8.9 Hz, 2H, H3b/4b), 7.02 - 7.06 (m, 3H, H3c/5c/3d), 7.25 (d, J = 3.5 Hz, 1H, H5d), 7.35 - 7.51 (m, 6H, H2c/6c/2d/6d/4e/5e), 7.86 (d, J = 8.3 Hz, 1H, H6e), 8.00 (m, 1H, H2e), 12.80 (s, 1H, NH).

**<sup>13</sup>C NMR (101 MHz, DMSO-d<sub>6</sub>):**  $\delta$  55.5 (s, OCH<sub>3</sub>), 55.7 (s, OCH<sub>3</sub>), 109.4 (s, C4b), 109.9 (s, C3c/5c), 114.1 (s, C3b), 114.6 (s, C3d/5d), 122.7 (s, C6e), 123.5 (s, C2e), 123.7 (s, C1d), 127.3 (s, C4e), 127.7 (s, C5e), 127.9 (s, C1c), 128.6 (s, C2c/6c), 130.4 (s, C2d/6d), 131.2 (s, C1e), 132.4 (s, C3e), 134.3 (s, C5a), 137.2 (s, C2a), 137.9 (s, C4a), 146.4 (s, C2b), 151.3 (s, C5b), 158.5 (s, C4c), 159.4 (s, C4d).

### 3.3 Flow Synthesis of 2-arylpyridine and 3-arylpyridine derivatives and subsequent ortho-arylation towards their 2-phenylpyridine derivatives



#### 3.3.1 Synthesis of 2-arylpyridine and 3-arylpyridine derivatives [1]



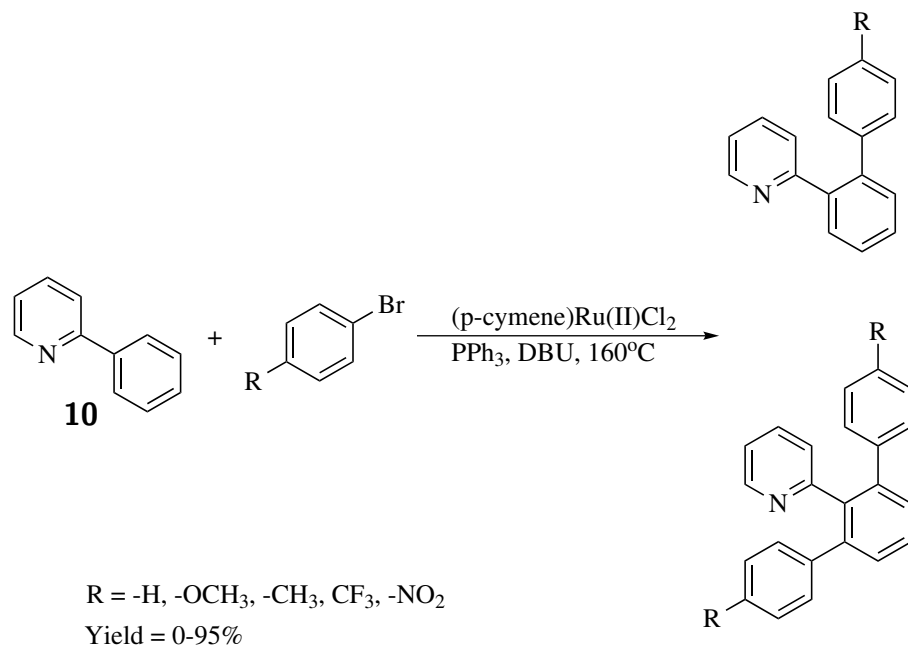
Scheme 27: General Procedure **1A**.

The appropriate amount of 2-bromo or 3-bromo pyridine (**9** or **16**) (1 eq., 1 mmol), the appropriate substituted boronic acid **47**, **48**, **49**, **50**, **51** or **52** (1.2 eq., 1.2 mmol or 3eq., 3 mmol for the synthesis of products: **18**, **19**, **20**, **21**, **22**), K<sub>2</sub>CO<sub>3</sub> (2 eq., 276mg, 2 mmol) and 2.1 mol% of Pd(PPh<sub>3</sub>)<sub>4</sub> (2.1 mol%, 24mg, 0.021 mmol), and dioxane/water mixture as solvent (1:1, 20 mL) were charged into a round bottomed flask. The mixture was stirred for 5min at room temperature and was then filtered through filter paper,

before being transferred to the syringe pump. The residence time was 23 min and the temperature of the heating plate was set to 90°C. The inner diameter of the capillary material was 1mm. The volume of the reactor (Figure 37) was 16 mL. The flow rate was 0.695 mL/min and the volume of the reactor Figure 37 was 16 mL. After the reaction zone, the product solution was collected. For work-up, diethylether (20 mL) was added and the crude mixture was extracted with 2N solution of hydrochloric acid (3 x 20 mL). The aqueous layer was basified using 2N solution of sodium hydroxide and then extracted with diethylether (3 x 100 mL). The organic layer was washed with brine, dried over sodium sulfate and evaporated under vacuum. In most of the cases the pure product was obtained without further purification. However in the cases that impurities were still present, purification via column chromatography on silica gel (P.E:EtOAc= 10:1) was performed.



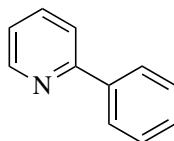
## 3.3.2 Synthesis of ortho-arylated 2-phenylpyridine derivatives [1]

Scheme 28: General Procedure **1B**.

The appropriate amount of 2-phenylpyridine derivative **10** (1 eq., 0.25 mmol), the appropriate bromobenzene derivative **41**, **53**, **54**, **55** or **56** (3 eq., 0.75 mmol), DBU (4 eq., 152 mg, 1 mmol), PPh<sub>3</sub> (10 mol%, 6.5 mg, 0.025 mmol), dichloro(p-cymene)ruthenium(II)dimer (5 mol%, 7.6 mg, 0.0125 mmol) (with the exception of the synthesis of **30**, in which 7.5mol% of dichloro(p-cymene)ruthenium(II)dimer was used (7.5 mol%, 11.5 mg, 0.01875 mmol)) and NMP as solvent (1 mL) were charged into a round bottomed flask. The mixture was stirred at room temperature until complete dissolution of all reagents. Then this solution was transferred to the syringe pump system. The flow rate was set to 0.533 mL/min which corresponded to a residence time of 30 min and the temperature of the heating plate was set to 160°C. After pumping through the reaction mixture, 20mL pure solvent was pumped through the coil in order to flush the system. The inner diameter of the capillary was 1 mm. The volume of the reactor (Figure 37) was 16 mL. After the reaction zone, the product solution was collected. For work-up, ethyl acetate (60 mL) was added to the reaction solution. Afterwards it was extracted three times with a saturated solution of ammonium chloride (3 x 100 mL). The combined aqueous phases were ex-

tracted once again with ethyl acetate (30 mL). The combined organic phases were washed three times with brine (3 x 100 mL). The organic phase was dried with sodium sulfate, filtered and the solvent evaporated. The crude products were purified via preparative HPLC using a Phenomenex Luna C18(2) column and the flow rate was 20 mL/min for both following methods. The method which has been employed for products **23** and **24** was the following: 10 min 70% CH<sub>3</sub>OH/30% H<sub>2</sub>O, 10-30 min 70% CH<sub>3</sub>OH/30% H<sub>2</sub>O → 90% CH<sub>3</sub>OH/10% H<sub>2</sub>O, 30-31 min 90% CH<sub>3</sub>OH/10% H<sub>2</sub>O → 100% CH<sub>3</sub>OH/0% H<sub>2</sub>O, 31-50 min 100% CH<sub>3</sub>OH/0% H<sub>2</sub>O. The method which has been employed for products **25**, **26**, **27**, **28**, and **29** was the following: 10 min 70% CH<sub>3</sub>OH/30% H<sub>2</sub>O, 10-40 min 70% CH<sub>3</sub>OH/30% H<sub>2</sub>O → 90% CH<sub>3</sub>OH/10% H<sub>2</sub>O, 40-41 min 90% CH<sub>3</sub>OH/10% H<sub>2</sub>O → 100% CH<sub>3</sub>OH/0% H<sub>2</sub>O, 41-50 min 100% CH<sub>3</sub>OH/0% H<sub>2</sub>O.

### 3.3.3 Synthesis of 2-phenylpyridine (10)



**C<sub>11</sub>H<sub>9</sub>N**  
**M = 155.07**

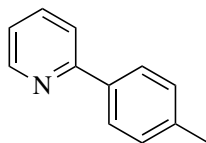
This derivative [142] was synthesized according to general procedure **1A** using 2-bromopyridine **9** (158 mg, 1 mmol) and phenylboronic acid **47** (146 mg, 1.2 mmol).

- Yield: 93% (144 mg, 0.93 mmol)
- Appearance: yellow oil
- TLC: R<sub>f</sub> = 0.65 (P.E: EtOAc= 3:1)

**<sup>1</sup>H NMR (200 MHz, CDCl<sub>3</sub>):** δ 7.18 - 7.35 (m, 1H, H3a), 7.34 - 7.59 (m, 3H, H5a/H3b/H5b), 7.68 - 7.89 (m, 2H, H4a/H4b), 7.92 - 8.09 (m, 2H, H2b/H6b), 8.72 (dt, 1H, J = 5.0, 1.1 Hz, H6a).

**<sup>13</sup>C NMR (50 MHz, CDCl<sub>3</sub>):** δ 120.6 (s, C3a), 122.1 (s, C5a), 126.9 (s, C2b/6b), 128.7 (s, C3b/5b), 128.9 (d, C4b), 136.7 (s, C4a), 139.3 (s, C1b), 149.6 (s, C2a), 157.4 (s, C6a).

### 3.3.4 Synthesis of 2-(p-tolyl)pyridine (11)



**C<sub>12</sub>H<sub>11</sub>N**  
**M = 169.09**

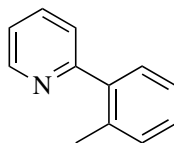
This derivative [143] was synthesized according to general procedure **1A** using 2-bromopyridine **9** (158 mg, 1 mmol) and p-tolylboronic acid **48** (163 mg, 1.2 mmol).

- Yield: 61% (103 mg, 0.61 mmol)
- Appearance: yellow oil
- TLC: R<sub>f</sub> = 0.8 (P.E: EtOAc= 3:1)

**<sup>1</sup>H NMR (200 MHz, CDCl<sub>3</sub>):** δ 2.41 (s, 3H, CH<sub>3</sub>), 7.16 - 7.25 (m, 1H, H5a), 7.29 (d, 2H, J = 8.4 Hz, H3b/H5b), 7.66 - 7.80 (m, 2H, H3a/4a), 7.90 (d, 2H, J = 8.2 Hz, H2b/H6b), 8.64 - 8.73 (m, 1H, H6a).

**<sup>13</sup>C NMR (50 MHz, CDCl<sub>3</sub>):** δ 20.9 (s, CH<sub>3</sub>), 119.9 (s, C3a), 121.5 (s, C5a), 126.5 (s, C2b/6b), 129.s (d, C3b/5b), 136.3 (s, C4b), 136.4 (d, C4a), 138.6 (s, C1b), 149.3 (s, C2a), 157.2 (s, C6a).

### 3.3.5 Synthesis of 2-(*o*-tolyl)pyridine (**12**)



**C<sub>12</sub>H<sub>11</sub>N**  
**M = 169.09**

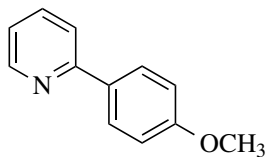
This derivative [144] was synthesized according to general procedure **1A** using 2-bromopyridine **9** (158 mg, 1 mmol) and *o*-tolylboronic acid **49** (163 mg, 1.2 mmol).

- Yield: 91% (153 mg, 0.91 mmol)
- Appearance: yellow oil
- TLC: R<sub>f</sub> = 0.57 (P.E: EtOAc= 3:1)

**<sup>1</sup>H NMR (200 MHz, CDCl<sub>3</sub>):** δ 2.36 (s, 3H, CH<sub>3</sub>), 7.17 - 7.49 (m, 5H, H3a/4a/5a/4b/5b), 7.74 (td, 1H, J = 7.7, 1.9 Hz, H3b), 8.70 (ddd, 1H, J = 4.9, 1.9, 1.0 Hz, H6a).

**<sup>13</sup>C NMR (50 MHz, CDCl<sub>3</sub>):** δ 20.3 (s, CH<sub>3</sub>), 121.6 (s, C3a), 124.1 (s, C5a), 125.9 (s, 6b), 128.3 (s, C3b), 129.6 (s, C5b), 130.7 (s, C4b), 135.7 (s, C4a), 136.1 (s, C1b), 140.3 (s, C2b), 149.1 (s, C2a), 159.9 (s, C6a).

### 3.3.6 Synthesis of 2-(4-methoxyphenyl)pyridine (13)



**C<sub>12</sub>H<sub>11</sub>NO**  
**M = 185.08**

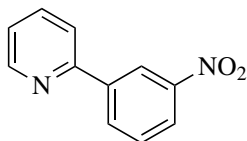
This derivative [145] was synthesized according to general procedure **1A** using 2-bromopyridine **9** (158 mg, 1 mmol) and (4-methoxyphenyl)boronic acid **50** (182 mg, 1.2 mmol).

- Yield: 89% (164 mg, 0.89 mmol)
- Appearance: colorless solid
- M.p: 53-55°C
- TLC: R<sub>f</sub> = 0.48 (P.E: EtOAc= 3:1)

**<sup>1</sup>H NMR (200 MHz, CDCl<sub>3</sub>):** δ 3.86 (s, 3H, CH<sub>3</sub>), 6.91 - 7.09 (d, 2H, H3b/5b), 7.05 - 7.24 (m, 1H, H5a), 7.58 - 7.81 (m, 2H, H3a/4a), 7.82 - 8.04 (d, 2H, H2b/6b), 8.58 - 8.72 (m, 1H, H6a).

**<sup>13</sup>C NMR (50 MHz, CDCl<sub>3</sub>):** δ 55.7 (s, CH<sub>3</sub>), 114.3 (s, C3b/5b), 120 (s, C3a), 121.7 (s, C5a), 128.5 (s, C2b/6b), 132.3 (s, C4a), 136.9 (s, C1b), 149.7 (s, C4b), 157.3 (s, C2a), 160.8 (s, C6a).

### 3.3.7 Synthesis of 2-(3-nitrophenyl)pyridine (14)



**C<sub>11</sub>H<sub>8</sub>N<sub>2</sub>O<sub>2</sub>**  
**M = 200.06**

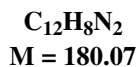
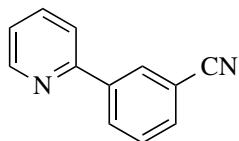
This derivative [146] was synthesized according to general procedure **1A** using 2-bromopyridine **9** (158 mg, 1 mmol) and (3-nitrophenyl)boronic acid **51** (200 mg, 1.2 mmol).

- Yield: 51% (102 mg, 0.51 mmol)
- Appearance: yellow solid
- M.p: 72-73°C
- TLC: R<sub>f</sub> = 0.45 (P.E: EtOAc= 3:1)

**<sup>1</sup>H NMR (200 MHz, CDCl<sub>3</sub>):** δ 7.42 (dd, 1H, J = 7.9, 4.8 Hz, H5a), 7.53 - 7.91 (m, 5H, H3a/4a/4b/5b/6b) 8.60 - 8.73 (m, 1H, H6a), 8.83 (d, 1H, J = 2.0 Hz, H2b).

**<sup>13</sup>C NMR (50 MHz, CDCl<sub>3</sub>):** δ 113.4 (s, C3a), 118.3 (s, C5a), 123.8 (s, C4b), 129.9 (s, C2b), 130.7 (d, C4a/5b), 134.4 (d, C6b), 134.5 (s, C3b), 139.1 (s, C1b), 148.1 (s, C2a), 149.5 (s, C6a).

### 3.3.8 Synthesis of 3-(pyridine-2-yl)benzonitrile (15)



This derivative [147] was synthesized according to general procedure **1A** using 2-bromopyridine **9** (158 mg, 1 mmol) and (3-cyanophenyl)boronic acid **52** (176 mg, 1.2 mmol).

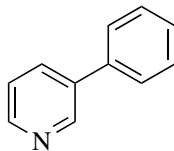
- Yield: 45% (81 mg, 0.45 mmol)
- Appearance: yellow oil
- TLC: R<sub>f</sub> = 0.42 (P.E: EtOAc= 3:1)

**<sup>1</sup>H NMR (200 MHz, CDCl<sub>3</sub>):** δ 7.21 - 7.41 (m, 1H, H5a), 7.59 (t, 1H, J = 7.7 Hz, H3b), 7.62 - 7.92 (m, 3H, H3a/4a/4b), 8.16 - 8.38 (m, 2H, H2b/6b), 8.73 (dt, 1H, J = 4.9, 1.0 Hz, H6a).

**<sup>13</sup>C NMR (50 MHz, CDCl<sub>3</sub>):** δ 113.0 (s, C3b), 120.5 (s, CN), 123.2 (s, C5a), 129.6 (s, C6b), 130.6 (s, C2b), 131.0 (s, C5b), 132.2 (s, C4b), 137.2 (s, C8b), 140.4 (s, C1b), 149.9 (s, C2a), 154.9 (s, C6a).



### 3.3.9 Synthesis of 3-phenylpyridine (17)



**C<sub>11</sub>H<sub>9</sub>N**  
**M = 155.07**

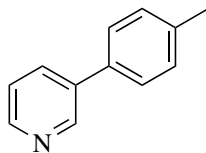
This derivative [148] was synthesized according to general procedure **1A** using 3-bromopyridine **16** (158 mg, 1 mmol) and phenylboronic acid **47** (146 mg, 1.2 mmol).

- Yield: 80% (124 mg, 0.8 mmol)
- Appearance: yellow oil
- TLC: R<sub>f</sub> = 0.32 (P.E: EtOAc= 3:1)

**<sup>1</sup>H NMR (200 MHz, CDCl<sub>3</sub>):** δ 7.31 - 7.61 (m, 6H, H4a/2b/3b/4b/5b/6b), 7.86 (dt, 1H, J = 7.9, 2.0 Hz, H5a), 8.58 (dd, 1H, J = 4.8, 1.6 Hz, H2a), 8.85 (d, 1H, J = 2.4 Hz, H6a).

**<sup>13</sup>C NMR (50 MHz, CDCl<sub>3</sub>):** δ 123.5 (s, C3a), 127.1 (s, C2b/6b), 128.1 (s, C4b), 129.1 (s, C3b/5b), 134.4 (s, C4a), 136.6 (s, C3a), 137.8 (s, C1b), 148.3 (s, C2a), 148.4 (s, C6a).

### 3.3.10 Synthesis of 3-(p-tolyl)pyridine (18)



**C<sub>12</sub>H<sub>11</sub>N**  
**M = 169.09**

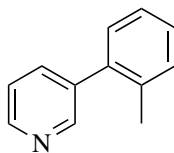
This derivative [149] was synthesized according to general procedure **1A** using 3-bromopyridine **16** (158 mg, 1 mmol) and p-tolylboronic acid **48** (408 mg, 3 mmol).

- Yield: 87% (147 mg, 0.87 mmol)
- Appearance: yellow oil
- TLC: R<sub>f</sub> = 0.75 (P.E: EtOAc= 3:1)

**<sup>1</sup>H NMR (200 MHz, CDCl<sub>3</sub>):** δ 2.33 (s, 3H, CH<sub>3</sub>), 7.34 - 7.26 (m, 2H, H3b/5b), 7.30 - 7.38 (m, 1H, H5a), 7.42 (d, 2H, J = 8.2 Hz, H2b/6b), 7.80 (ddd, 1H, J = 7.9, 2.4, 1.6 Hz, H4a), 8.50 (dd, 1H, J = 4.8, 1.6 Hz, H2a), 8.76 (d, 1H, J = 1.5 Hz, H6a).

**<sup>13</sup>C NMR (50 MHz, CDCl<sub>3</sub>):** δ 21.2 (s, CH<sub>3</sub>), 123.6 (s, C5a), 127.1 (s, C2b/6b), 129.9(s, C3b/5b), 134.2 (s, C4a), 135.0 (s, C1b), 136.7 (s, C4b), 138.1 (s, C3a), 148.2 (s, C2a/6a).

### 3.3.11 Synthesis of 3-(*o*-tolyl)pyridine (**19**)



**C<sub>12</sub>H<sub>11</sub>N**  
**M = 169.09**

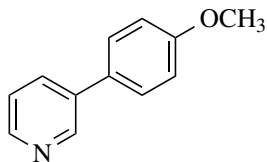
This derivative [150] was synthesized according to general procedure **1A** using 3-bromopyridine **16** (158 mg, 1 mmol) and *o*-tolylboronic acid **49** (408 mg, 3 mmol).

- Yield: 75% (126 mg, 0.75 mmol)
- Appearance: yellow oil
- TLC: R<sub>f</sub> = 0.45 (P.E: EtOAc= 3:1)

<sup>1</sup>H NMR (200 MHz, CDCl<sub>3</sub>): δ 2.28 (s, 3H, CH<sub>3</sub>), 7.06 - 7.40 (m, 5H, H<sub>4a</sub>/5a/3b/4b/5b), 7.62 (dt, 1H, J = 7.9, 2.0 Hz, H<sub>6b</sub>), 8.46 - 8.60 (m, 2H, H<sub>2a</sub>/6a).

<sup>13</sup>C NMR (50 MHz, CDCl<sub>3</sub>): δ 20.1 (s, CH<sub>3</sub>), 122.8 (s, C<sub>5a</sub>), 125.9 (s, C<sub>3b</sub>), 127.9 (s, C<sub>2b</sub>), 129.6 (s, C<sub>4b</sub>), 130.3 (s, C<sub>4a</sub>), 135.4 (s, C<sub>5b</sub>), 136.3 (s, C<sub>3a</sub>), 137.2 (s, C<sub>6b</sub>), 137.9 (s, C<sub>1b</sub>), 147.9 (s, C<sub>6a</sub>), 149.7 (s, C<sub>2a</sub>).

### 3.3.12 Synthesis of 3-(4-methoxyphenyl)pyridine (**20**)



**C<sub>12</sub>H<sub>11</sub>NO**  
**M = 185.08**

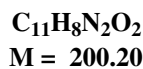
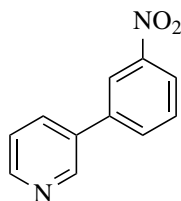
This derivative was synthesized according to general procedure **1A** using 3-bromopyridine **16** (158 mg, 1 mmol) and (4-methoxyphenyl)boronic acid **50** (456 mg, 3 mmol).

- Yield: 58% (107 mg, 0.58 mmol)
- Appearance: yellow solid
- M.p: 58-60°C
- TLC: R<sub>f</sub> = 0.25 (P.E: EtOAc= 3:1)

**<sup>1</sup>H NMR (200 MHz, CDCl<sub>3</sub>):** δ 3.86 (s, 3H, CH<sub>3</sub>), 6.95 - 7.06 (m, 2H, H3b/5b), 7.35 (dd, 1H, J = 7.9, 4.8 Hz, H5a), 7.48 - 7.57 (m, 2H, H2b/6b), 7.85 (dt, 1H, J = 8.0, 2.1 Hz, H4a), 8.50-8.59 (m, 1H, H2a), 8.82 (d, 1H, J = 1.8 Hz, H6a).

**<sup>13</sup>C NMR (50 MHz, CDCl<sub>3</sub>):** δ 55.3 (s, CH<sub>3</sub>), 114.5 (s, C3a/5b), 123.4 (s, C5a), 128.1 (s, C2b/6b), 130.1 (s, C1b), 133.8 (s, C4a), 136.2 (s, C3a), 147.7 (s, C6a), 147.9 (s, C2a), 159.6 (s, C4b).

### 3.3.13 Synthesis of 2-(3-nitrophenyl)pyridine (21)



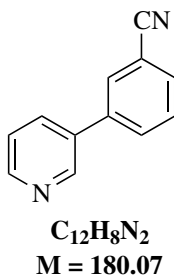
This derivative [151] was synthesized according to general procedure **1A** using 3-bromopyridine **16** (158 mg, 1 mmol) and 2-(3-nitrophenyl)boronic acid **51** (501mg, 3 mmol).

- Yield: 58% (116 mg, 0.58 mmol)
- Appearance: yellow solid
- M.p: 93-95°C
- TLC: R<sub>f</sub> = 0.12 (P.E: EtOAc= 3:1)

**<sup>1</sup>H NMR (200 MHz, CDCl<sub>3</sub>):** δ 7.45 (ddd, 1H, J = 7.9, 4.9, 0.9 Hz, H5b), 7.67 (t, 1H, J = 8.0 Hz, H5a), 7.85 - 8.02 (m, 2H, H4a/6b), 8.27 (ddd, 1H, J = 8.2, 2.3, 1.1 Hz, H4b), 8.45 (t, 1H, J = 2.0 Hz, H2b), 8.68 (dd, 1H, J = 4.9, 1.6 Hz, H2a), 8.89 (d, 1H, J = 2.4 Hz, H6a).

**<sup>13</sup>C NMR (50 MHz, CDCl<sub>3</sub>):** δ 122.0 (s, C4b), 122.9 (s, C2b), 123.9 (s, C5a/5b), 130.2 (s, C6b), 133.0 (s, C3a), 134.3 (s, C4a), 134.5 (s, C2a), 139.4 (s, C1b), 148.1 (s, C6a), 149.6 (s, C3b).

### 3.3.14 Synthesis of 3-(pyridine-3-yl)benzonitrile (**22**)



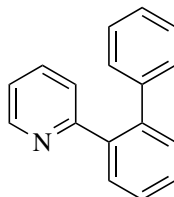
This derivative [152] was synthesized according to general procedure **1A** using 3-bromopyridine **16** (158 mg, 1 mmol) and (3-cyanophenyl)boronic acid **52** (441 mg, 3 mmol).

- Yield: 56% (100 mg, 0.56 mmol)
- Appearance: colorless solid
- M.p: 87-88°C
- TLC: R<sub>f</sub> = 0.41 (P.E: EtOAc= 3:1)

**<sup>1</sup>H NMR (200 MHz, CDCl<sub>3</sub>):** δ 7.40 (dd, 1H, J = 7.9, 4.8 Hz, H6b), 7.53 - 7.72 (m, 2H, H5a/4b), 7.77 (s, 1H, H4a), 7.82 (d, 2H, J = 1.8 Hz, H2b/5b), 8.60-8.68 (dd, 1H, J = 4.8, 1.6 Hz, H2a), 8.81 (d, 1H, J = 2.1 Hz, H6a).

**<sup>13</sup>C NMR (50 MHz, CDCl<sub>3</sub>):** δ 113.3 (s, C3b), 118.4 (s, CN), 123.7 (s, C5a), 129.9 (s, C2b), 130.6 (s, C5b), 131.4 (s, C6b), 131.5 (s, C4b), 134.3 (s, C4a), 134.4 (d, C3a), 139.1 (s, C1b), 148.0 (s, C2a), 149.5 (s, C6a).

### 3.3.15 Synthesis of 2-([1,1'-biphenyl]-2'-yl)pyridine (**23**)



**C<sub>17</sub>H<sub>13</sub>N**  
**M = 231.30**

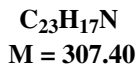
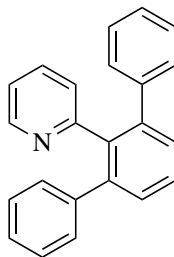
This derivative [135] was synthesized according to general procedure **1B** using 2-phenylpyridine **10** (39 mg, 0.25 mmol) and bromobenzene **41** (118 mg, 0.75 mmol). It was isolated along with the **24** from the same reaction mixture.

- Yield: 26% (15 mg, 0.064 mmol)
- Appearance: colorless solid
- M.p: 87-89°C
- TLC: R<sub>f</sub> = 0.64 (P.E: EtOAc= 3:1)

**<sup>1</sup>H NMR (200 MHz, CDCl<sub>3</sub>):** δ 6.88 (dt, 1H, J = 7.9, 1.1 Hz, H5a), 7.00 - 7.34 (m, 5H, H3a/4a/4b/5b/4c), 7.27 - 7.56 (m, 4H, H2c/3c/5c/6c), 7.61 - 7.78 (m, 1H, H6b), 8.63 (ddd, 2H, J = 4.9, 1.9, 1.0 Hz, H6a/3b).

**<sup>13</sup>C NMR (50 MHz, CDCl<sub>3</sub>):** δ 121.4 (s, C5a), 125.5 (s, C3a), 126.8 (s, C4b), 127.7 (s, C4c), 128.2 (s, C2c/6c), 128.6 (s, C3b/6b), 129.8 (s, C3c/5c), 130.6 (s, C5b/6c), 135.3 (s, C2b), 139.6 (s, C1c), 140.7 (s, C4a), 141.4 (s, C1b), 149.6 (s, C6a), 159.4 (s, C2a).

### 3.3.16 Synthesis of 2-([1,1':3',1''-terphenyl]-2'-yl)pyridine (**24**)



This derivative [138] was synthesized according to general procedure **1B** using 2-phenylpyridine **10** (39 mg, 0.25 mmol) and bromobenzene **41** (118 mg, 0.75 mmol). It was isolated along with **23** from the same reaction mixture.

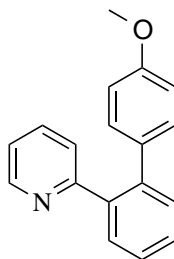
- Yield: 69% (39 mg, 0.13 mmol)
- Appearance: colorless solid
- M.p: 129-131°C
- TLC: R<sub>f</sub> = 0.64 (P.E: EtOAc= 3:1)

**<sup>1</sup>H NMR (200 MHz, CDCl<sub>3</sub>):** δ 6.83 - 6.96 (m, 2H, H<sub>4a</sub>/5<sub>a</sub>), 7.03 - 7.21 (m, 10H, H<sub>2c</sub>/3<sub>c</sub>/4<sub>c</sub>/5<sub>c</sub>/6<sub>c</sub>/2<sub>d</sub>/3<sub>d</sub>/4<sub>d</sub>/5<sub>d</sub>/6<sub>d</sub>), 7.26 - 7.36 (m, 1H, H<sub>3a</sub>), 7.49 (q, 3H, J = 5.4 Hz, H<sub>4b</sub>/5<sub>b</sub>/6<sub>b</sub>), 8.31 (dt, 1H, J = 4.9, 1.4 Hz, H<sub>6a</sub>).

**<sup>13</sup>C NMR (50 MHz, CDCl<sub>3</sub>):** δ 121.5 (s, C<sub>3a</sub>/5<sub>a</sub>), 126.9(s), 127.4 (s, C<sub>3c</sub>/4<sub>d</sub>), 128.2 (s), 128.8 (s, C<sub>2b</sub>), 130.1 (s, C<sub>5b</sub>), 130.2 (s, C<sub>1b</sub>), 135.5 (s, C<sub>3b</sub>), 139.1 (s, C<sub>6c</sub>), 142.2 (s, C<sub>1d</sub>), 142.4 (s, C<sub>4a</sub>), 149.1 (s, C<sub>6a</sub>), 159.5 (s, C<sub>2a</sub>).



### 3.3.17 Synthesis of 2-(4'-methoxy-[1,1'-biphenyl]-2'-yl)pyridine (**25**)



**C<sub>18</sub>H<sub>15</sub>NO**  
**M = 261.32**

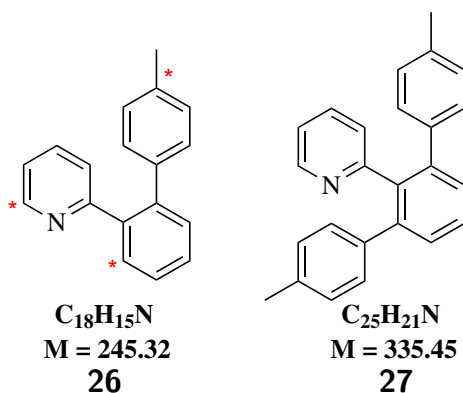
This derivative [135] was synthesized according to general procedure **1B** using 2-phenylpyridine **10** (39 mg, 0.25 mmol) and 1-bromo-4-methoxybenzene **53** (140 mg, 0.75 mmol).

- Yield: 59% (38 mg, 0.14 mmol)
- Appearance: colorless solid
- M.p: 68-70°C
- TLC: R<sub>f</sub> = 0.12 (P.E: EtOAc= 10:1)

**<sup>1</sup>H NMR (200 MHz, CDCl<sub>3</sub>):** δ 3.78 (s, 3H, CH<sub>3</sub>), 6.69 - 6.86 (m, 2H, H3a/5a), 6.90 (d, 1H, J = 7.9 Hz, H4b), 6.98 - 7.19 (m, 3H, H4a/3c/5c), 7.31 - 7.54 (m, 4H, H5b/6b/2c/6c), 7.58 - 7.76 (m, 1H, H3b), 8.64 (ddd, 1H, J = 4.9, 1.8, 1.0 Hz, H6a).

**<sup>13</sup>C NMR (50 MHz, CDCl<sub>3</sub>):** δ 56.4 (s, CH<sub>3</sub>), 114.7 (s, C3c/5c), 122.5 (s, C5a), 126.6 (s, C3a), 128.5 (s, C4b), 129.7 (s, C6b), 131.6 (s, C3b), 131.7 (s, C5b), 131.9 (s, C2c/6c), 134.9 (s, C2b), 136.4 (s, C1c), 140.5 (s, C4a), 141.4 (s, C1b), 150.6 (s, C6a), 159.7 (s, C2a), 160.6 (s, C4c).

### 3.3.18 Synthesis of 2-(4'-methyl-[1,1'-biphenyl]-2-yl)pyridine (**26**) + 2-(4,4''-dimethyl-[1,1':3,1''-terphenyl]-2'-yl)pyridine (**27**)



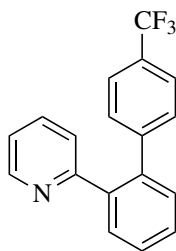
Derivatives **26** [153] and **27** [153] were synthesized according to general procedure **1B** using 2-phenylpyridine **10** (39 mg, 0.25 mmol) and 1-bromo-4-methylbenzene **54** (128 mg, 0.75 mmol).

- Yield: 51% (combined yield) (31 mg, ratio 1:2 of **26** : **27**)
- Appearance: colorless solid
- TLC:  $R_f = 0.18$  (P.E: EtOAc= 10:1)

**26** and **27** were isolated as mixture since they were inseparable (TLC and preparative HPLC). Consequently also the NMR represents this mixture. Quantification can be done according to signals of H6a, H6b, CH<sub>3</sub> which, for the monoarylated compound were marked with an asterisk and correlates to  $\delta$ : 2.32 (s, 3H),  $\delta$ : 7.69 (tt,  $J = 4.2, 2.2$  Hz, 1H)  $\delta$ : 8.65 (ddd,  $J = 4.9, 1.7, 0.9$  Hz, 1H), respectively. Regarding the bis-arylated compound **27** the chemical shifts corresponding to H6a and CH<sub>3</sub> are the following  $\delta$ : 2.27 (s, 12H) and  $\delta$ : 8.34 (ddd,  $J = 4.8, 1.7, 1.0$  Hz, 2H). In the <sup>13</sup>C NMR, the carbons belonging to **27** are distinguished from the carbons of **26** using the symbol '. Additionally, for the pre-mentioned reasons, a melting point for this mixture is not provided.

**<sup>1</sup>H NMR (200 MHz, CDCl<sub>3</sub>):**  $\delta$  2.27 (s, 12H, H6a), 2.32 (s, 3H, \*CH<sub>3</sub>), 6.85 - 7.58 (m, 42H, H3a/4a/5a/4b/5b/6b/2c/3c/5c/6c/2d/3d/5d/6d), 7.69 (tt, 1H,  $J = 4.2, 2.2$  Hz, H3b), 8.34 (ddd, 2H,  $J = 4.8, 1.7, 1.0$  Hz, H6a), 8.65 (ddd, 1H,  $J = 4.9, 1.7, 0.9$  Hz, \*H6a).

$^{13}\text{C}$  NMR (50 MHz,  $\text{CDCl}_3$ ):  $\delta$  21.2 (d,  $^*\text{CH}_3$ ,  $\text{CH}_3$ ,  $\text{CH}_3$ ), 120.9 (s, C3a/ $^*5\text{a}/5\text{a}'$ ), 128.5 (d), 128.9 (s, C2c/6c), 129.6 (t), 130.6 (d, C4b'/6b') 135.0 (s, C1c/1c'/1d), 135.9 (s), 138.8 (s, C4a/1b'/3b'), 141.8 (s, C1b/2a'), 148.6 (s, C2a/ $^*6\text{a}/6\text{a}'$ ).

**3.3.19 Synthesis of 2-(4'-trifluoromethyl-[1,1'-biphenyl]-2-yl)pyridine (28)**

**C<sub>18</sub>H<sub>12</sub>F<sub>3</sub>N**  
**M = 299.30**

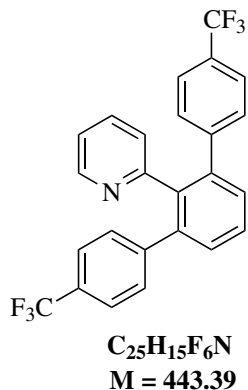
This derivative [154] was synthesized according to general procedure **1B** using 2-phenylpyridine **10** (39 mg, 0.25 mmol) and 1-bromo-4-(trifluoromethyl)benzene **55** (225 mg, 0.75 mmol). It was isolated along with **29** from the same reaction mixture.

- Yield: 3% (2 mg, 0.006 mmol)
- Appearance: colorless solid
- M.p: 88-90°C
- TLC: R<sub>f</sub> = 0.11 (P.E: EtOAc= 10:1)

**<sup>1</sup>H NMR (200 MHz, CDCl<sub>3</sub>):** δ 6.90 (dt, 1H, J = 7.9, 1.2 Hz, H3a), 7.02 - 7.31 (m, 3H, H5a/2c/6c), 7.27 - 7.59 (m, 6H, H4a/4b/5b/6b/3c/5c), 7.57 - 7.76 (m, 1H, H6b), 8.58 (ddd, 1H, J = 4.9, 1.8, 1.0 Hz, H6a)

**<sup>13</sup>C NMR (50 MHz, CDCl<sub>3</sub>):** δ 121.6 (s, C5a), 121.8 (s), 124.8 (d, C3a), 124.9 (d, C4b), 125.1 (q, J = 4.2 Hz, C5c), 126.9 (s), 128.4 (q, J = 273 Hz, CF<sub>3</sub>), 128.7 (q, J = 33 Hz, C4c), 129.2 (s, C2c/6c), 130.4 (s, C3b/6b), 130.6 (s, C5b), 130.7 (s), 135.6 (s, C1b), 139.2 (s, C1c), 139.6 (s, C4a), 145.1 (s, C2b), 149.5 (s, C6a), 158.8 (s, C2a).

### 3.3.20 Synthesis of 2-(4,4''-bis(trifluoromethyl)-[1,1':3',1''-terphenyl]-2'-yl)pyridine (29)



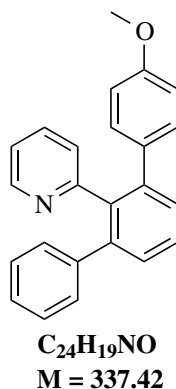
This derivative [155] was synthesized according to general procedure **1B** using 2-phenylpyridine derivative **10** (39 mg, 0.25 mmol) and (1-bromo-4(trifluoromethyl)benzene **55** (225 mg, 0.75 mmol). It was isolated along with **28** from the same reaction mixture.

- Yield: 24% (20 mg, 0.045 mmol)
- Appearance: colorless
- M.p: 138-140°C
- TLC: R<sub>f</sub> =0.37 (P.E: EtOAc= 10:1)

**<sup>1</sup>H NMR (200 MHz, CDCl<sub>3</sub>):** δ 6.86 (dt, 1H, J = 7.8, 1.2 Hz, H4a), 6.98 (ddd, 1H, J = 7.6, 4.9, 1.1 Hz, H5a), 7.22 (d, 4H, J = 8.1 Hz, H3a/5b/2c/6c), 7.32 - 7.52 (m, 7H, H6d/2d/4b/6b/3c/5c/5d), 7.53 - 7.65 (m, 1H, H3d), 8.33 (dt, 1H, J = 4.9, 1.3 Hz, H6a).

**<sup>13</sup>C NMR (50 MHz, CDCl<sub>3</sub>):** δ 121.3 (s, C3a), 124.3 (q, J = 4.1 Hz, C5c), 124.4 (q, J = 3.9 Hz, C5d), 124.5 (s), 126.4 (s), 126.6 (s), 127.4(s), 128.0 (q, J = 262 Hz, CF<sub>3</sub>), 128.4 (q, J = 261 Hz, CF<sub>3</sub>), 128.7 (q, J = 34 Hz, C4c), 129.6 (q, J = 34 Hz, C4d), 129.8 (s, C5b), 135.1 (s, C1b), 138.2 (s, C3b), 140.4 (s, C6c), 144.7 (s, C1d), 144.8 (s), 148.7 (s, C4a), 157.6 (s, C2a/6a).

### 3.3.21 Synthesis of 2-(4-methoxy-[1,1':3',1''-terphenyl]-2'-yl)pyridine (**30**)



This derivative [156] was synthesized according to general procedure **1B** using 2-(4'-methoxy-[1,1'-biphenyl]-2-yl)pyridine **25** (65 mg, 0.25 mmol), bromobenzene **41** (118 mg, 0.75 mmol) and 7.5mol% of dichloro(p-cymene)ruthenium(II)dimer (7.5 mol%, 11.5 mg, 0.01875 mmol).

- Yield: 24% (20 mg, 0.06 mmol)
- Appearance: colorless solid
- M.p: 132-134°C
- TLC: R<sub>f</sub> = 0.18 (P.E: EtOAc= 10:1)

**<sup>1</sup>H NMR (200 MHz, CDCl<sub>3</sub>):** δ 3.75 (s, 3H, CH<sub>3</sub>), 6.63 - 6.78 (m, 2H, H<sub>3c</sub>/5c), 6.82 - 6.97 (m, 2H, H<sub>3d</sub>/5d), 6.97 - 7.20 (m, 7H, H<sub>3a</sub>/4a/5a/5b/2c/6c/4d), 7.23 - 7.60 (m, 4H, H<sub>4b</sub>/6b/6d/2d), 8.34 (dt, 1H, J = 4.9, 1.3, H<sub>6a</sub>)

**<sup>13</sup>C NMR (50 MHz, CDCl<sub>3</sub>):** δ 54.8 (s, CH<sub>3</sub>), 112.18 (s, C<sub>3c</sub>/5c), 120.6 (s, C<sub>5a</sub>), 125.9 (s, C<sub>3a</sub>), 126.5 (s, C<sub>4a</sub>/4d), 127.3 (s, C<sub>3d</sub>/5d), 127.9 (s, C<sub>2d</sub>/6d), 128.9 (s, C<sub>5b</sub>), 129.2 (d, C<sub>2b</sub>), 129.3 (s, C<sub>6b</sub>), 130.4 (s, C<sub>4b</sub>), 133.6 (s, C<sub>2c</sub>), 134.7 (s, C<sub>6c</sub>), 138.1 (s, C<sub>1c</sub>), 141.1 (t, C<sub>1b</sub>), 141.3 (s, C<sub>3b</sub>), 141.5 (s, C<sub>1d</sub>). 148.2 (s, C<sub>6a</sub>), 157.8 (s, C<sub>2a</sub>), 158.8 (s, C<sub>4c</sub>).

## A Appendix

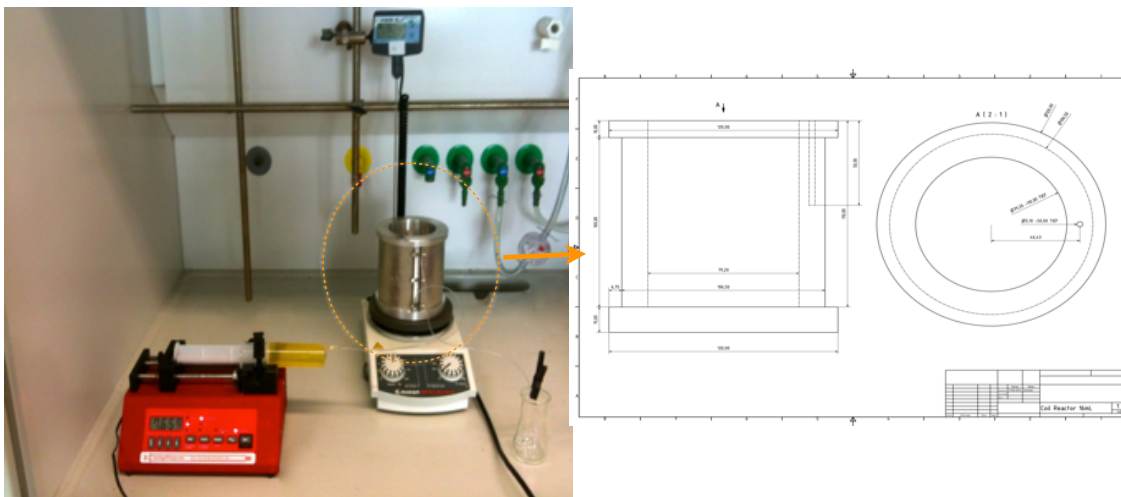


Figure 37: In-house developed continuous-flow reactor system and technical drawing of the aluminium reactor.



Figure 38: X-Cube.



Figure 39: AFRICA.

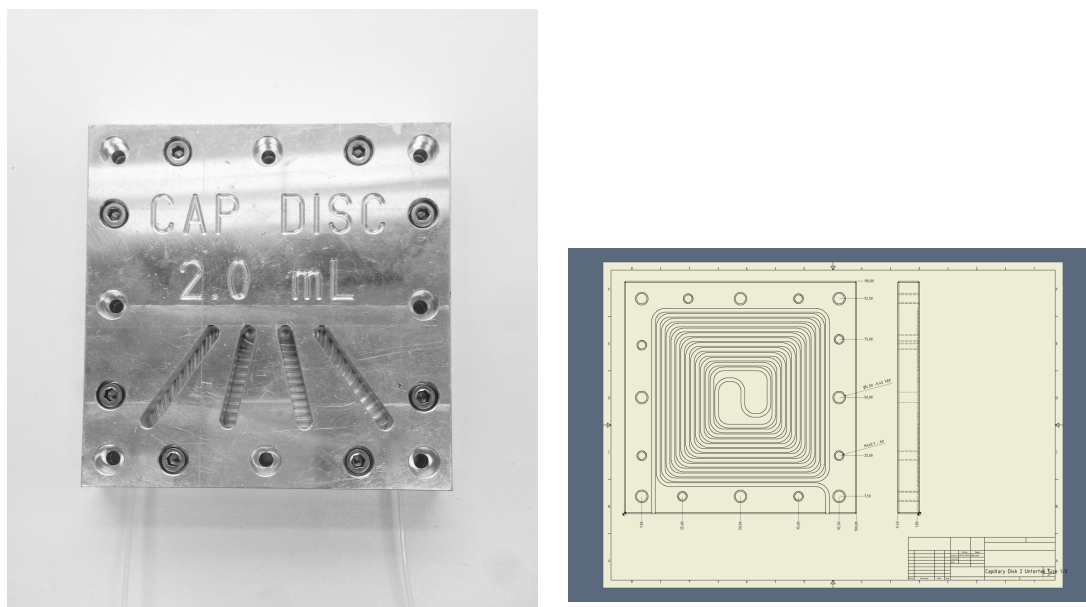


Figure 40: Cap disk.



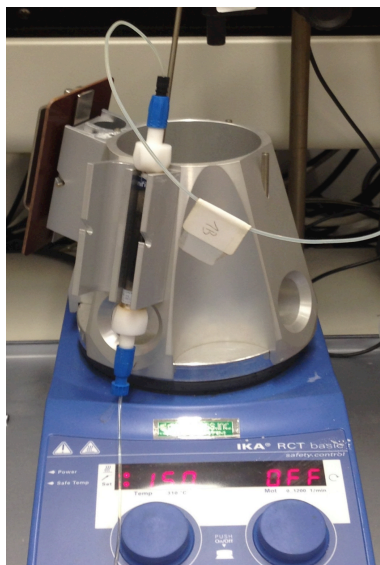


Figure 41: Reactor from Syrris, which allows the use of a glass column for encapsulation of heterogeneous additives.

## B Bibliography

### References

- [1] M. Christakakou, M. Schön, M. Schnürch, and M. D. Mihovilovic *Synlett* **24** no. 18, (2013) 2411–2418.
- [2] L. Vaccaro, D. Lanari, A. Marrocchi, and G. Strappaveccia *Green Chemistry* **16** no. 8, (2014) 3680–3704.
- [3] T. N. Glasnov and C. O. Kappe *Advanced Synthesis & Catalysis* **352** no. 17, (2010) 3089–3097.
- [4] I. R. Baxendale, J. Deeley, C. M. Griffiths-Jones, S. V. Ley, S. Saaby, and G. K. Tranmer *Chemical Communications* no. 24, (2006) 2566–2568.
- [5] J. P. McMullen and K. F. Jensen *Organic Process Research & Development* **14** no. 5, (2010) 1169–1176.
- [6] H. Sahoo, J. G. Kralj, and K. F. Jensen *Angewandte Chemie International Edition* **46** no. 30, (2007) 5704–5708.
- [7] B. Desai, K. Dixon, E. Farrant, Q. Feng, K. R. Gibson, W. P. van Hoorn, J. Mills, T. Morgan, D. M. Parry, M. K. Ramjee, C. N. Selway, G. J. Tarver, G. Whitlock, and A. G. Wright *Journal of Medicinal Chemistry* **56** no. 7, (2013) 3033–3047.
- [8] Z. Yu, Y. Lv, C. Yu, and W. Su *Organic Process Research & Development* **17** no. 3, (2013) 438–442.
- [9] G. Gasparini, I. Archer, E. Jones, and R. Ashe *Organic Process Research & Development* **16** no. 5, (2012) 1013–1016.
- [10] A. Polyzos, M. O'Brien, T. P. Petersen, I. R. Baxendale, and S. V. Ley *Angewandte Chemie International Edition* **50** no. 5, (2011) 1190–1193.
- [11] X. Ye, M. D. Johnson, T. Diao, M. H. Yates, and S. S. Stahl *Green Chemistry* **12** no. 7, (2010) 1180–1186.

- [12] F. Lévesque and P. H. Seeberger *Organic Letters* **13** no. 19, (2011) 5008–5011.
- [13] D. Šterk, M. Jukič, and Z. Časar *Organic Process Research & Development* **17** no. 1, (2012) 145–151.
- [14] S. A. May, M. D. Johnson, T. M. Braden, J. R. Calvin, B. D. Haeberle, A. R. Jines, R. D. Miller, E. F. Plocharczyk, G. A. Renner, R. N. Richey, C. R. Schmid, R. K. Vaid, and H. Yu *Organic Process Research & Development* **16** no. 5, (2012) 982–1002.
- [15] D. Barrow, *Properties and Use of Microreactors*, pp. 43–57. Wiley-VCH Verlag GmbH & Co. KGaA, 2008.
- [16] M. Irfan, T. N. Glasnov, and C. O. Kappe *ChemSusChem* **4** no. 3, (2011) 300–316.
- [17] M. Colombo and I. Peretto *Drug Discovery Today* **13** no. 15-16, (2008) 677–684.
- [18] H. Oyamada, T. Naito, and S. Kobayashi *Beilstein Journal of Organic Chemistry* **7** (2011) 735–739.
- [19] B. Desai and C. O. Kappe *Journal of Combinatorial Chemistry* **7** no. 5, (2005) 641–643.
- [20] S. Saaby, K. R. Knudsen, M. Ladlow, and S. V. Ley *Chemical Communications* no. 23, (2005) 2909–2911.
- [21] B. J. Deadman, C. Battilocchio, E. Sliwinski, and S. V. Ley *Green Chemistry* **15** no. 8, (2013) 2050–2055.
- [22] X. Y. Mak, P. Laurino, and P. H. Seeberger *Beilstein Journal of Organic Chemistry* **5** (2009) 19.
- [23] J. Wegner, S. Ceylan, and A. Kirschning *Chemical Communications* **47** no. 16, (2011) 4583–4592.
- [24] H. Li, C. C. C. Johansson Seechurn, and T. J. Colacot *ACS Catalysis* **2** no. 6, (2012) 1147–1164.

- [25] C. C. C. Johansson Seechurn, M. O. Kitching, T. J. Colacot, and V. Snieckus *Angewandte Chemie International Edition* **51** no. 21, (2012) 5062–5085.
- [26] J. D. Sellars and P. G. Steel *Chemical Society Reviews* **40** no. 10, (2011) 5170–5180.
- [27] R. Jana, T. P. Pathak, and M. S. Sigman *Chemical Reviews* **111** no. 3, (2011) 1417–1492.
- [28] G. P. McGlacken and I. J. S. Fairlamb *European Journal of Organic Chemistry* **2009** no. 24, (2009) 4011–4029.
- [29] R. F. Heck and J. P. Nolley *The Journal of Organic Chemistry* **37** no. 14, (1972) 2320–2322.
- [30] K. Sonogashira, Y. Tohda, and N. Hagihara *Tetrahedron Letters* **16** no. 50, (1975) 4467 – 4470.
- [31] N. Miyaura and A. Suzuki *Journal of the Chemical Society, Chemical Communications* no. 19, (1979) 866–867.
- [32] A. O. King, N. Okukado, and E.-i. Negishi *J. Chem. Soc., Chem. Commun.* (1977) 683–684.
- [33] D. Milstein and J. K. Stille *Journal of the American Chemical Society* **100** no. 11, (1978) 3636–3638.
- [34] Y. Hatanaka and T. Hiyama *The Journal of Organic Chemistry* **53** no. 4, (1988) 918–920.
- [35] R. J. P. Corriu and J. P. Masse *J. Chem. Soc., Chem. Commun.* (1972) 144a–144a.
- [36] K. Tamao, K. Sumitani, and M. Kumada *Journal of the American Chemical Society* **94** no. 12, (1972) 4374–4376.
- [37] K. C. Nicolaou, P. G. Bulger, and D. Sarlah *Angewandte Chemie International Edition* **44** no. 29, (2005) 4442–4489.

- [38] A. O. King, E. G. Corley, R. K. Anderson, R. D. Larsen, T. R. Verhoeven, P. J. Reider, Y. B. Xiang, M. Belley, and Y. a. Leblanc *The Journal of Organic Chemistry* **58** no. 14, (1993) 3731–3735.
- [39] M. Labelle, M. Belley, Y. Gareau, J. Gauthier, D. Guay, R. Gordon, S. Grossman, T. Jones, Y. Leblanc, M. McAuliffe, C. McFarlane, P. Masson, K. Metters, N. Ouimet, D. Patrick, H. Piechuta, C. Rochette, N. Sawyer, Y. Xiang, C. Pickett, A. Ford-Hutchinson, R. Zamboni, and R. Young *Bioorganic & Medicinal Chemistry Letters* **5** no. 3, (1995) 283 – 288.
- [40] R. D. Larsen, E. G. Corley, A. O. King, J. D. Carroll, P. Davis, T. R. Verhoeven, P. J. Reider, M. Labelle, J. Y. Gauthier, Y. B. Xiang, and R. J. Zamboni *The Journal of Organic Chemistry* **61** no. 10, (1996) 3398–3405.
- [41] A. M. Echavarren and A. Homs, *Mechanistic Aspects of Metal-Catalyzed C,C- and C,X-Bond Forming Reactions*, pp. 1–64. Wiley-VCH Verlag GmbH & Co. KGaA, 2014.
- [42] K. Köhler, K. Wussow, and A. S. Wirth, *Palladium-Catalyzed Cross-Coupling Reactions - A General Introduction*, pp. 1–30. Wiley-VCH Verlag GmbH & Co. KGaA, 2013.
- [43] N. Miyaura and A. Suzuki *Chemical Reviews* **95** no. 7, (1995) 2457–2483.
- [44] A. Kirschning, W. Solodenko, and K. Mennecke *Chemistry - A European Journal* **12** no. 23, (2006) 5972–5990.
- [45] W. Solodenko, H. Wen, S. Leue, F. Stuhlmann, G. Sourkouni-Argirusi, G. Jas, H. Schönfeld, U. Kunz, and A. Kirschning *European Journal of Organic Chemistry* **2004** no. 17, (2004) 3601–3610.
- [46] P. He, S. J. Haswell, and P. D. I. Fletcher *Applied Catalysis A: General* **274** no. 1-2, (2004) 111–114.
- [47] I. R. Baxendale, C. M. Griffiths-Jones, S. V. Ley, and G. K. Tranmer *Chemistry - A European Journal* **12** no. 16, (2006) 4407–4416.

- [48] N. S. Wilson, C. R. Sarko, and G. P. Roth *Organic Process Research & Development* **8** no. 3, (2004) 535–538.
- [49] T. Noël and A. J. Musacchio *Org. Lett.* **13** no. 19, (2011) 5180–5183.
- [50] A. Nagaki, A. Kenmoku, Y. Moriwaki, A. Hayashi, and J.-i. Yoshida *Angewandte Chemie International Edition* **49** no. 41, (2010) 7543–7547.
- [51] M. Baumann, I. R. Baxendale, S. V. Ley, and N. Nikbin *Beilstein Journal of Organic Chemistry* **7** (2011) 442–495.
- [52] M. Elbing and G. C. Bazan *Angewandte Chemie International Edition* **47** no. 5, (2008) 834–838.
- [53] D. Bellus *Lect. Heterocycl. Chem.* **9** (1987) 65.
- [54] S. C. Rasmussen, R. L. Schwiderski, and M. E. Mulholland *Chemical Communications* **47** no. 41, (2011) 11394–11410.
- [55] K. E. Maly *Journal of Materials Chemistry* **19** no. 13, (2009) 1781–1787.
- [56] A. F. Pozharskii, A. T. Soldatenkov, and A. R. Katritzky, *Index*, pp. 371–382. John Wiley & Sons, Ltd, 2011.
- [57] T. Muller and S. Bräse *Angewandte Chemie International Edition* **50** no. 50, (2011) 11844–11845.
- [58] M. Schnürch, R. Flasik, A. F. Khan, M. Spina, M. D. Mihovilovic, and P. Stanetty *European Journal of Organic Chemistry* **2006** no. 15, (2006) 3283–3307.
- [59] S. Schröter, C. Stock, and T. Bach *Tetrahedron* **61** no. 9, (2005) 2245–2267.
- [60] J.-R. Wang and K. Manabe *Synthesis* **2009** no. 09, (2009) 1405–1427.
- [61] V. F. Slagt, A. H. M. de Vries, J. G. de Vries, and R. M. Kellogg *Organic Process Research & Development* **14** no. 1, (2009) 30–47.
- [62] J. Magano and J. R. Dunetz *Chemical Reviews* **111** no. 3, (2011) 2177–2250.

- [63] L. Djakovitch, N. Batail, and M. Genelot *Molecules* **16** no. 6, (2011) 5241–5267.
- [64] I. J. S. Fairlamb *Chemical Society Reviews* **36** no. 7, (2007) 1036–1045.
- [65] M. G. Banwell, T. E. Goodwin, S. Ng, J. A. Smith, and D. J. Wong *European Journal of Organic Chemistry* **2006** no. 14, (2006) 3043–3060.
- [66] A. Suzuki *Journal of Organometallic Chemistry* **576** no. 1-2, (1999) 147–168.
- [67] S. Kotha, K. Lahiri, and D. Kashinath *Tetrahedron* **58** no. 48, (2002) 9633–9695.
- [68] D. G. Hall, *Structure, Properties, and Preparation of Boronic Acid Derivatives. Overview of Their Reactions and Applications*, pp. 1–99. Wiley-VCH Verlag GmbH & Co. KGaA, 2006.
- [69] E. M. Suh and Y. Kishi *Journal of the American Chemical Society* **116** no. 24, (1994) 11205–11206.
- [70] T. Noël and S. L. Buchwald *Chemical Society Reviews* **40** no. 10, (2011) 5010–5029.
- [71] N. Marion and S. P. Nolan *Accounts of Chemical Research* **41** no. 11, (2008) 1440–1449.
- [72] D. S. Surry and S. L. Buchwald *Angewandte Chemie International Edition* **47** no. 34, (2008) 6338–6361.
- [73] D. S. Surry and S. L. Buchwald *Chemical Science* **2** no. 1, (2011) 27–50.
- [74] S. Würtz and F. Glorius *Accounts of Chemical Research* **41** no. 11, (2008) 1523–1533.
- [75] R. Martin and S. L. Buchwald *Accounts of Chemical Research* **41** no. 11, (2008) 1461–1473.
- [76] W. R. Reynolds and C. G. Frost, *Coupling Reactions in Continuous-Flow Systems*, pp. 409–443. Wiley-VCH Verlag GmbH & Co. KGaA, 2013.

- [77] N. Dastbaravardeh, M. Christakakou, M. Haider, and M. Schnürch *Synthesis* **46** no. 11, (2014) 1421–1439.
- [78] C. K. Y. Lee, A. B. Holmes, S. V. Ley, I. F. McConvey, B. Al-Duri, G. A. Leeke, R. C. D. Santos, and J. P. K. Seville *Chem. Commun.* (2005) 2175–2177.
- [79] C. G. Frost and L. Mutton *Green Chemistry* **12** no. 10, (2010) 1687–1703.
- [80] Y. Uozumi, Y. M. A. Yamada, T. Beppu, N. Fukuyama, M. Ueno, and T. Kitamori *Journal of the American Chemical Society* **128** no. 50, (2006) 15994–15995.
- [81] S. Ceylan, C. Friese, C. Lammel, K. Mazac, and A. Kirschning *Angewandte Chemie International Edition* **47** no. 46, (2008) 8950–8953.
- [82] G. Shore, S. Morin, and M. G. Organ *Angewandte Chemie International Edition* **45** no. 17, (2006) 2761–2766.
- [83] J. Wegner, S. Ceylan, and A. Kirschning *Advanced Synthesis & Catalysis* **354** no. 1, (2012) 17–57.
- [84] T. Noël, S. Kuhn, A. J. Musacchio, K. F. Jensen, and S. L. Buchwald *Angewandte Chemie International Edition* **50** no. 26, (2011) 5943–5946.
- [85] D. Balcells, E. Clot, and O. Eisenstein *Chemical Reviews* **110** no. 2, (2010) 749–823.
- [86] V. S. Thirunavukkarasu, S. I. Kozhushkov, and L. Ackermann *Chemical Communications* **50** no. 1, (2014) 29–39.
- [87] J. Wencel-Delord and F. Glorius *Nat Chem* **5** no. 5, (2013) 369–375.
- [88] G. Rouquet and N. Chatani *Angewandte Chemie International Edition* **52** no. 45, (2013) 11726–11743.
- [89] K. M. Engle and J.-Q. Yu *The Journal of Organic Chemistry* **78** no. 18, (2013) 8927–8955.
- [90] B. Li and P. H. Dixneuf *Chemical Society Reviews* **42** no. 13, (2013) 5744–5767.



- [91] J. J. Mousseau and A. B. Charette *Accounts of Chemical Research* **46** no. 2, (2012) 412–424.
- [92] S. R. Neufeldt and M. S. Sanford *Acc. Chem. Res.* **45** (2012) 936–946.
- [93] O. Daugulis, H.-Q. Do, and D. Shabashov *Acc. Chem. Res.* **42** (2009) 1074–1086.
- [94] T. A. Ramirez, B. Zhao, and Y. Shi *Chemical Society Reviews* **41** no. 2, (2012) 931–942.
- [95] I. Özdemir, S. Demir, B. Çetinkaya, C. Gourlaouen, F. Maseras, C. Bruneau, and P. H. Dixneuf *Journal of the American Chemical Society* **130** no. 4, (2008) 1156–1157.
- [96] B. Liégault, I. Petrov, S. I. Gorelsky, and K. Fagnou *The Journal of Organic Chemistry* **75** no. 4, (2010) 1047–1060.
- [97] J. Wencel-Delord, T. Droge, F. Liu, and F. Glorius *Chemical Society Reviews* **40** no. 9, (2011) 4740–4761.
- [98] J. A. Labinger and J. E. Bercaw *Nature* **417** no. 6888, (2002) 507–514.
- [99] L. Zhang, M. Geng, P. Teng, D. Zhao, X. Lu, and J.-X. Li *Ultrasonics Sonochemistry* **19** no. 2, (2012) 250–256.
- [100] P. Bruice, *Organic chemistry*. Prentice Hall, 2010.
- [101] A. Kirschning and G. Jas, *Applications of Immobilized Catalysts in Continuous Flow Processes*, vol. 242 of *Topics in Current Chemistry*, ch. 6, pp. 209–239. Springer Berlin Heidelberg, 2004.
- [102] L. Rycek, R. Puthenkalam, M. Schnürch, M. Ernst, and M. D. Mihovilovic *Bioorganic & Medicinal Chemistry Letters* **25** no. 2, (2015) 400–403.
- [103] W. Sieghart, *Subunit Composition and Structure of GABAA-Receptor Subtypes*, pp. 69–86. Humana Press, 2007.
- [104] G. Johnston *Pharmacology & Therapeutics* **69** no. 3, (1996) 173.

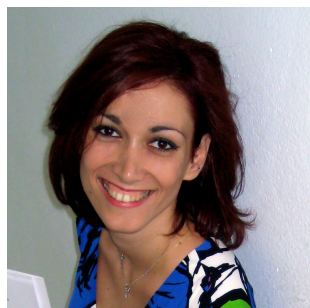
- [105] Y.-J. Lee, Y. M. Lee, C.-K. Lee, J. K. Jung, S. B. Han, and J. T. Hong *Pharmacology & Therapeutics* **130** no. 2, (2011) 157–176.
- [106] L. Ma, J. Chen, X. Wang, X. Liang, Y. Luo, W. Zhu, T. Wang, M. Peng, S. Li, S. Jie, A. Peng, Y. Wei, and L. Chen *Journal of Medicinal Chemistry* **54** no. 19, (2011) 6469–6481.
- [107] C. R. Chen, R. Tan, W. M. Qu, Z. Wu, Y. Wang, Y. Urade, and Z. L. Huang *British Journal of Pharmacology* **164** no. 5, (2011) 1534–1546.
- [108] S. Tripathi, M.-H. Chan, and C. Chen *Bioorganic & Medicinal Chemistry Letters* **22** no. 1, (2012) 216–221.
- [109] B. Taferner, W. Schuehly, A. Huefner, I. Baburin, K. Wiesner, G. F. Ecker, and S. Hering *Journal of Medicinal Chemistry* **54** no. 15, (2011) 5349–5361.
- [110] B. Johns and J. Shotwell, *Therapeutic Compounds*. Google Patents, 2011.
- [111] G.-H. Kim, D. Halder, J. Park, W. Namkung, and I. Shin *Angewandte Chemie International Edition* **53** no. 35, (2014) 9271–9274.
- [112] S. D. Schwartz, C. D. Regillo, B. L. Lam, D. Elliott, P. J. Rosenfeld, N. Z. Gregori, J.-P. Hubschman, J. L. Davis, G. Heilwell, M. Spirn, J. Maguire, R. Gay, J. Bateman, R. M. Ostrick, D. Morris, M. Vincent, E. Anglade, L. V. Del Priore, and R. Lanza *The Lancet* **385** (2014) 509 – 516.
- [113] H. Wichterle, I. Lieberam, J. A. Porter, and T. M. Jessell *Cell* **110** no. 3, 385–397.
- [114] D. R. Williams, M.-R. Lee, Y.-A. Song, S.-K. Ko, G.-H. Kim, and I. Shin *Journal of the American Chemical Society* **129** no. 30, (2007) 9258–9259.
- [115] M. Warashina, K. H. Min, T. Kuwabara, A. Huynh, F. H. Gage, P. G. Schultz, and S. Ding *Angewandte Chemie* **118** no. 4, (2006) 605–607.
- [116] L. Anastasia, M. Sampaolesi, N. Papini, D. Oleari, G. Lamorte, C. Tringali, E. Monti, D. Galli, G. Tettamanti, G. Cossu, and B. Venerando *Cell Death Differ* **13** no. 12, (2006) 2042–2051.

- [117] L.-M. Recnik, M. Abd El Hameid, M. Haider, M. Schnürch, and M. D. Mihovilovic *Synthesis* **45** no. 10, (2013) 1387–1405.
- [118] Z. Wang, *Radziszewski Reaction*. John Wiley & Sons, Inc., 2010.
- [119] E. B. Anderson and T. E. Long *Polymer* **51** no. 12, (2010) 2447–2454.
- [120] T. Dao-Huy, M. Haider, F. Glatz, M. Schnürch, and M. D. Mihovilovic *European Journal of Organic Chemistry* (2014) 8119 – 8125.
- [121] B. Liégault, D. Lapointe, L. Caron, A. Vlassova, and K. Fagnou *The Journal of Organic Chemistry* **74** no. 5, (2009) 1826–1834.
- [122] A. Battace, M. Lemhadri, T. Zair, H. Doucet, and M. Santelli *Organometallics* **26** no. 3, (2006) 472–474.
- [123] S. F. Vasilevsky, S. Klyatskaya, E. V. Tretyakov, and J. Elguero *Heterocycles* **60** (2003) 879–886.
- [124] D. Niculescu-Duvaz, I. Niculescu-Duvaz, B. M. J. M. Suijkerbuijk, D. Ménard, A. Zambon, A. Nourry, L. Davies, H. A. Manne, F. Friedlos, L. Ogilvie, D. Hedley, A. K. Takle, D. M. Wilson, J.-F. Pons, T. Coulter, R. Kirk, N. Cantarino, S. Whittaker, R. Marais, and C. J. Springer *Bioorganic & Medicinal Chemistry* **18** no. 18, (2010) 6934–6952.
- [125] L. L. Chng, N. Erathodiyil, and J. Y. Ying *Accounts of Chemical Research* **46** no. 8, (2013) 1825–1837.
- [126] R. J. Sundberg and H. F. Russell *The Journal of Organic Chemistry* **38** no. 19, (1973) 3324–3330.
- [127] A. Nadin *Angewandte Chemie International Edition* **43** no. 30, (2004) 3876–3877.
- [128] S. Seršen, J. Kljun, F. Požgan, B. Štefane, and I. Turel *Organometallics* **32** no. 2, (2013) 609–616.
- [129] F. Požgan and P. H. Dixneuf *Advanced Synthesis & Catalysis* **351** no. 11-12, (2009) 1737–1743.

- [130] S. Oi, S. Fukita, and Y. Inoue *Chemical Communications* no. 22, (1998) 2439–2440.
- [131] B. Yu, X. Yan, S. Wang, N. Tang, and C. Xi *Organometallics* **29** no. 14, (2010) 3222–3226.
- [132] N. Yoshikai, A. Matsumoto, J. Norinder, and E. Nakamura *Synlett* **2010** no. 02, (2010) 313–316.
- [133] A. Prades, M. Poyatos, and E. Peris *Advanced Synthesis & Catalysis* **352** no. 7, (2010) 1155–1162.
- [134] M. Koley, N. Dastbaravardeh, M. Schnürch, and M. D. Mihovilovic *ChemCatChem* **4** no. 9, (2012) 1345–1352.
- [135] W. Li, Z. Yin, X. Jiang, and P. Sun *The Journal of Organic Chemistry* **76** no. 20, (2011) 8543–8548.
- [136] J.-H. Chu, S.-L. Tsai, and M.-J. Wu *ChemInform* **41** no. 14, (2010) 3757–3764.
- [137] N. Dastbaravardeh, M. Schnürch, and M. D. Mihovilovic *European Journal of Organic Chemistry* **2013** no. 14, (2013) 2878–2890.
- [138] S. Oi, R. Funayama, T. Hattori, and Y. Inoue *Tetrahedron* **64** no. 26, (2008) 6051–6059.
- [139] S. Oi, S. Fukita, N. Hirata, N. Watanuki, S. Miyano, and Y. Inoue *Organic Letters* **3** no. 16, (2001) 2579–2581.
- [140] P. B. Arockiam, C. Bruneau, and P. H. Dixneuf *Chemical Reviews* **112** no. 11, (2012) 5879–5918.
- [141] C. Pérez-Caaveiro, J. Pérez Sestelo, M. M. Martínez, and L. A. Sarandeses *The Journal of Organic Chemistry* **79** no. 20, (2014) 9586–9593.
- [142] D. Srimani and A. Sarkar *Tetrahedron Letters* **49** no. 44, (2008) 6304–6307.
- [143] W.-J. Guo and Z.-X. Wang *The Journal of Organic Chemistry* **78** no. 3, (2013) 1054–1061.

- [144] O. Diebolt, P. Braunstein, S. P. Nolan, and C. S. J. Cazin *Chemical Communications* **8** no. 27, (2008) 3190–3192.
- [145] G. M. Scheuermann, L. Rumi, P. Steurer, W. Bannwarth, and R. Mulhaupt *Journal of the American Chemical Society* **131** no. 23, (2009) 8262–8270.
- [146] J. Wen, S. Qin, L.-F. Ma, L. Dong, J. Zhang, S.-S. Liu, Y.-S. Duan, S.-Y. Chen, C.-W. Hu, and X.-Q. Yu *Organic Letters* **12** no. 12, (2010) 2694–2697.
- [147] M. R. Luzung, J. S. Patel, and J. Yin *The Journal of Organic Chemistry* **75** no. 23, (2010) 8330–8332.
- [148] L. Wu, Z.-W. Li, F. Zhang, Y.-M. He, and Q.-H. Fan *Advanced Synthesis & Catalysis* **350** no. 6, (2008) 846–862.
- [149] M. J. Iglesias, A. Prieto, and M. C. Nicasio *Organic Letters* **14** no. 17, (2012) 4318–4321.
- [150] J.-B. Liu, H. Yan, H.-X. Chen, Y. Luo, J. Weng, and G. Lu *Chemical Communications* **49** no. 46, (2013) 5268–5270.
- [151] V. K. R. Kumar, S. Krishnakumar, and K. R. Gopidas *European Journal of Organic Chemistry* **2012** no. 18, (2012) 3447–3458.
- [152] G. A. Molander, S. L. J. Trice, and S. M. Kennedy *The Journal of Organic Chemistry* **77** no. 19, (2012) 8678–8688.
- [153] N. Luo and Z. Yu *Chemistry - A European Journal* **16** no. 3, (2010) 787–791.
- [154] P. B. Arockiam, C. Fischmeister, C. Bruneau, and P. H. Dixneuf *Green Chemistry* **15** no. 1, (2013) 67–71.
- [155] J. Zhang, Q. Yang, Z. Zhu, M. L. Yuan, H. Y. Fu, X. L. Zheng, H. Chen, and R. X. Li *European Journal of Organic Chemistry* **2012** no. 34, (2012) 6702–6706.
- [156] B. Li, Z.-H. Wu, Y.-F. Gu, C.-L. Sun, B.-Q. Wang, and Z.-J. Shi *Angewandte Chemie International Edition* **50** no. 5, (2011) 1109–1113.

## C Curriculum Vitae



### PERSONAL

- Name: Maria Christakakou
- Born: 10/08/1982, Athens-Greece
- Nationality: Greek
- Address: Wiedner Hauptstrasse 118/31, Vienna 1050, Austria
- Email: mchrist@ioc.tuwien.ac.at

### EDUCATION

- Vienna University of Technology  
PhD Program Technical Natural Sciences, present  
Research topic: “Exploration of procedures translating batch synthesis into flow for the synthesis of bioactive small molecules”  
Supervised by Prof. Marko D. Mihovilovic
- University of Reading -UK, Department of Chemistry  
Master of Science in Chemical Research, 2010  
Research topic: “Investigation of the use of thiomorpholinone templates in peptide synthesis”  
Supervised by Prof. Laurence M. Harwood

- Aristotle University of Thessaloniki-Greece, Department of Chemistry  
Bachelor of Science in Chemistry, 2009

## PAPERS

- N. Dastbaravardeh, M. Christakakou, M. Haider, M. Schnürch: “Recent Advances in Palladium-Catalyzed C(sp<sup>3</sup>)-H Activation for the Formation of Carbon-Carbon and Carbon-Heteroatom Bonds”, *Synthesis* 2014, 46, (11):1421-1439.
- M. Christakakou, M. Schnürch, M. Schön, M.D. Mihovilovic: “Arylation of pyridines via Suzuki-Miyaura cross-coupling and pyridine directed C-H activation using a continuous-flow approach”, *Synlett* 2013, 24, (18):2411-2418.

## CONFERENCES/CONTRIBUTIONS

- Poster contribution Austrian Chemistry Days Graz 2013; 23-27th September 2013 “Exploration of Metal Catalyzed C-C bond forming reactions in a Continuous Flow System”.
- 14th Tetrahedron Symposium Vienna 2013; 25 – 28th June, 2013 (local organizing committee and participation).
- Poster contribution XXVth European Colloquium on Heterocyclic Chemistry Reading 2012; 13-17th August 2012 “Arylation of Heterocycles via Suzuki-Miyaura Cross-Coupling using a Continuous Flow Approach”.
- Participation at the seminar: “Chemistry and Physics in the education of mankind”, organised by the Union of Greece & Cyprus Physicists, Corfu, March 2007.
- Trainee chemist, at “NIKAS” Food Industries, 2004.

## AWARDS

- Elected best pupil for the year in the county sponsored educational trip to Cyprus.
- Awarded School Prize for excellence.

## ADDITIONAL SKILLS

- English (Good):
  - First Certificate in English, University of Cambridge.
  - I.E.L.T.S
- German (Good): Zertificat Deutsch
- Italian (Fair)
- ECDL Certificate: Modules, Databases, Concepts of IT, Word Processing, Presentations, Information and Communication, Spreadsheets, Using the Computer and Managing Files.
- Experienced in the use of various analytical techniques in organic chemistry. Extensive knowledge of chemistry specific databases, search and analysis programs (Scifinder, Beilstein Commander, ChemOffice, Topspin, e.g.).
- Piano studies, grade 5
- Driving licence

## INTERESTS AND ACTIVITIES

Close up magic (Performing card magic, coin magic); Dancing (Argentine Tango); Jewel design and creation; Running (Half Marathon); Ashtanga Yoga; Swimming; Tennis; Reading; Traveling; Photography; Playing Piano; Nutrition; Cooking.